REPORT NO.
UCB/EERC-80/10
MAY 1980

EARTHQUAKE ENGINEERING RESEARCH CENTER

GENERAL APPLICABILITY OF A NONLINEAR MODEL OF A ONE STORY STEEL FRAME

by
BJORN INGI SVEINSSON
and
HUGH D. McNIVEN

Report to
National Science Foundation

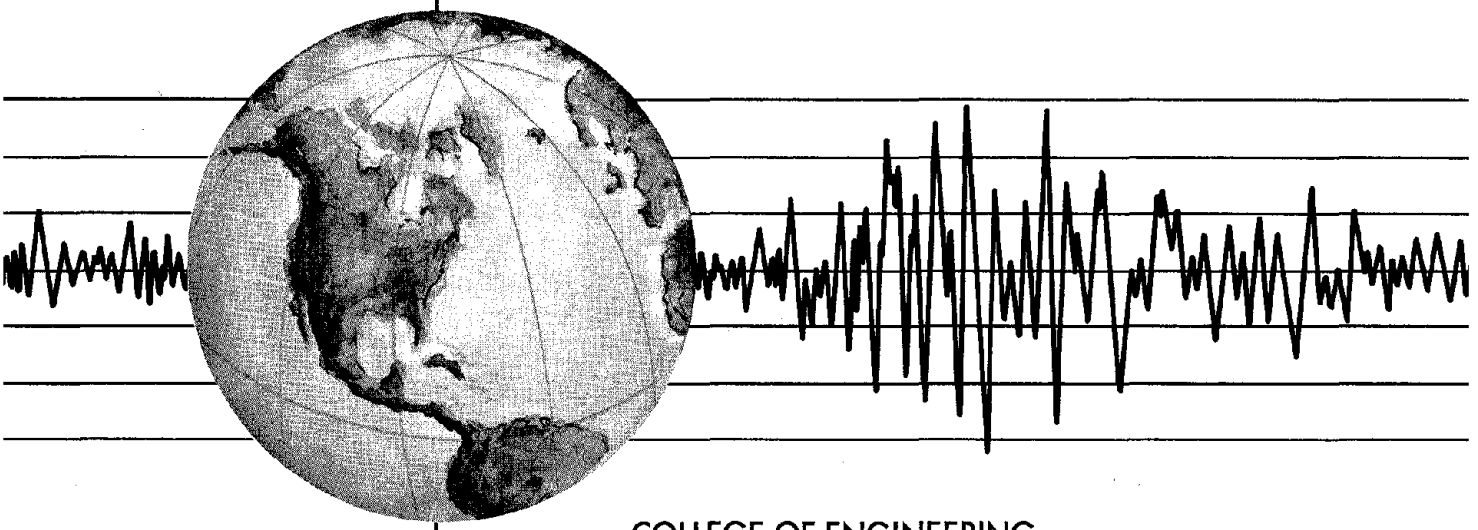

COLLEGE OF ENGINEERING

UNIVERSITY OF CALIFORNIA · Berkeley, California

50272-101

REPORT DOCUMENTATION PAGE	1. REPORT NO. NSF/RA-800196	2.	3. Recipient's Accession No. PB81 124877
4. Title and Subtitle: General Applicability of a Nonlinear Model of a One Story Steel Frame			5. Report Date: May 1980 6.
7. Author(s): Bjorn Ingi Sveinsson and Hugh D. McNiven			8. Performing Organization Rept. No. UCB/EERC-80/10
9. Performing Organization Name and Address: Earthquake Engineering Research Center, University of California, Richmond Field Station, 47th and Hoffman Blvd., Richmond, California 94804			10. Project/Task/Work Unit No. 11. Contract(C) or Grant(G) No. (C) (G) PFR79-08257
12. Sponsoring Organization Name and Address: National Science Foundation, 1800 G Street, N.W., Washington, D. C. 20550			13. Type of Report & Period Covered 14.

15. Supplementary Notes

16. Abstract (Limit: 200 words)

This report deals with the question of whether a nonlinear mathematical model of a structure constructed using system identification and the nonlinear structural response to one particular earthquake excitation, can satisfactorily predict the nonlinear responses of the same structure to other earthquake excitations.

The structure is a single story steel frame, and the study consists of both experimental and analytical parts. The physical structure is subjected to four historical strong motion earthquake acceleration time histories by means of the shaking table at the Earthquake Engineering Research Center of the University of California, Berkeley, California.

The analytical part consists of constructing a mathematical model of the structure. The form of the model is the same as that adopted by Matzen and McNiven. It accommodates viscous damping and nonlinear material behavior by means of the Ramberg-Osgood equations. The parameters in the model (there are four) are established from the responses to the El Centro earthquake. With the mathematical model complete, responses to the El Centro, Pacoima, Taft and Parkfield Earthquakes are predicted using the model. These responses are compared to the corresponding responses from the experimental program.

The significant finding from the study is that the mathematical model, constructed using response data from the El Centro earthquake, predicts responses to the other three earthquakes as accurately at it does to the El Centro.

The shortcoming of the model, equally evident in its prediction of all four earthquakes, is its inability to predict displacement time histories, following the first major excursion into the plastic deformation domain. We indulge in the luxury of accounting for the weakness and suggesting ways for overcoming it, with the price attached.

18. Availability Statement: Release Unlimited	19. Security Class (This Report)	21. No. of Pages 114
	20. Security Class (This Page)	22. Price

GENERAL APPLICABILITY OF A NONLINEAR MODEL OF A ONE STORY STEEL FRAME

By

Bjorn Ingi Sveinsson
Assistant Specialist
University of California, Berkeley

and

Hugh D. McNiven
Professor of Engineering Science
University of California, Berkeley

Report to

National Science Foundation

Report No. UBC/EERC-80/10
Earthquake Engineering Research Center
College of Engineering
University of California
Berkeley, California

May 1980

ABSTRACT

This report deals with the question of whether a nonlinear mathematical model of a structure constructed using system identification and the nonlinear structural response to one particular earthquake excitation, can satisfactorily predict the nonlinear responses of the same structure to other earthquake excitations.

The structure is a single story steel frame, and the study consists of both experimental and analytical parts. The physical structure is subjected to four historical strong motion earthquake acceleration time histories by means of the shaking table at the Earthquake Engineering Research Center of the University of California, Berkeley, California.

The analytical part consists of constructing a mathematical model of the structure. The form of the model is the same as that adopted by Matzen and McNiven. It accommodates viscous damping and nonlinear material behavior by means of the Ramberg-Osgood equations. The parameters in the model (there are four) are established from the responses to the El Centro earthquake. With the mathematical model complete, responses to the El Centro, Pacoima, Taft and Parkfield Earthquakes are predicted using the model. These responses are compared to the corresponding responses from the experimental program.

The significant finding from the study is that the mathematical model, constructed using response data from the El Centro earthquake, predicts responses to the other three earthquakes as accurately at it does to the El Centro.

The shortcoming of the model, equally evident in its prediction of all four earthquakes, is its inability to predict displacement time histories, following the first major excursion into the plastic

deformation domain. We indulge in the luxury of accounting for the weakness and suggesting ways for overcoming it, with the price attached.

ACKNOWLEDGMENTS

This investigation was sponsored by the National Science Foundation under Grant No.79-08257. The support is gratefully acknowledged.

The authors greatly appreciate the many suggestions made by Professor R.W. Clough who reviewed the manuscript.

Thanks are due to Messrs. David Steere, Ivo Van Asten, Derald Clearwater, John McNab and Steve Miller of the Earthquake Engineering Research Center for their electronic and machine shop work. The computing and plotting facilities to reduce and plot the test data were provided by the Computer Center at the University of California, Berkeley.

The typing was done by Ms. Toni Avery and Ms. Ruth Horning and the drafting by Ms. Gail Feazell.

TABLE OF CONTENTS

LIST OF TABLES

LIST OF FIGURES

1. INTRODUCTION

One of the first mathematical models, if not the first, constructed using system identification to predict the nonlinear response of a structure to earthquake excitation, was the one formulated by Matzen and McNiven [1]. It is a model of a one-story steel frame. The model has been well received and the study has helped to encourage the use of system identification in earthquake engineering. There has been however, a persistent point of skepticism related to the model's ability to predict the structure's response to a variety of excitations.

The mathematical model of the paper was constructed using experimental response data for the frame from shaking table excitations that matched the El Centro earthquake of 1940. When displaying the ability of the model to predict the frame responses, those generated using the model were compared to the experimental, but both for the El Centro earthquake. Because a mathematical model is useful only if it can predict responses to a variety of earthquake excitations, the skepticism is understandable.

It is true that in the paper [1] response to the Taft earthquake was compared to that predicted by the model and the results were impressive. The caution remained, however, because the Taft excitation caused responses in the frame that were only mildly nonlinear.

The purpose of this study is to explore this unanswered question; whether the model derived from response to one earthquake can simulate response to a different input. As the columns of the frame are slightly different from those used by Matzen and McNiven, we construct our own mathematical model for the frame again using system identification, and again using responses to the El Centro earthquake. The experimental

program in the study involved the measurement of nonlinear responses not only to the El Centro earthquake, but to the significantly nonlinear responses to three other historical earthquakes. These are the Pacoima, the Taft and the Parkfield earthquakes. To ensure valid comparisons, the columns which yield, causing the nonlinear responses, were all fabricated from the same piece of steel.

The significant finding of the study is that the model, constructed using data from the El Centro earthquake, predicts the frame's responses to the other three earthquakes as well as it does to that from the El Centro.

In addition to establishing the general predictive ability of the mathematical model, the study produces a side benefit that we feel is also important. To understand this finding, we return to the study of Matzen and McNiven. The model they constructed predicts the nonlinear acceleration time history of the response almost exactly, but predicts accurately the displacement time history only until the first major excursion of the strain into the plastic zone. Following this large plastic deformation the predicted displacement response is offset from the experimental by a small amount which remains essentially constant for the remainder of the excitation. We have found in this study the same accuracy and inaccuracy of the model revealed in comparison of the time histories of the accelerations and displacements, respectively, for all four excitations.

As a result of this study we are confident that we have pinpointed the major causes leading to the flaw in the mathematical model's ability to predict the displacement for the full duration of excitation.

We feel there are two reasons. The first is due to the peculiar stress-strain behavior of mild steel. The second can be laid to the

inability of the Ramberg-Osgood equations to reproduce elastic-plastic material behavior. These two arguments will be expanded on in some detail in the last chapter of this report.

The second chapter is devoted to a description of the experimental program. The test structure, its instrumentation and the different earthquake excitations are all described.

In the third chapter we construct the mathematical model using system identification. The form of the model, the criterion function and the optimization algorithm are outlined rather briefly. Any problems that were encountered pertinent to the results are described.

Assessment of the model is made in the fourth chapter. The model is subjected to the three additional forcing functions. The solutions are established giving the time histories of the responses and these, in turn, are compared to the experimental responses.

In the final chapter we outline what we feel are the significant findings emerging from the study.

2. TESTS

To accomplish the objectives of this research, a single-story steel structure was subjected to a variety of earthquake excitations on the shaking table at the Earthquake Engineering Research Center (EERC), of the University of California at Berkeley.

2.1 Test Structure

The primary requirements for the design of the test structure were that it have essentially a single-degree-of-freedom and that it exhibit a very simple hysteretic energy absorbing behavior. Such a structure was at hand, having been built and tested at EERC by Rea, Clough, and Bouwkamp (1969)[2] and tested again by Matzen and McNiven (1976)[1]. The detailed structure used for this work, shown in Figs. 2.1 and 2.2,is similar to Matzen's and McNiven's.

A complete description of the test structure is given by Rea, et al. (1969)[2]. Briefly, the structure consists of a heavy steel platform supported by four columns; two fixed to the table and pinned at the top, and two pinned at both the top and bottom. The platform, which is rigid compared to the columns, has overall plan dimensions of 10 ft by 7 ft. The cantilever columns, fabricated from WF 4 x 13 lb mild steel, are 66.5 in. in overall length and are installed so that they bend about their weak axes. Parabolic straps are added to strengthen the base of the fixed-ended columns.

Two identical pairs of cantilever columns are used. Each pair can be used twice as virgin columns by rotating them top to bottom after the completion of a test involving a major excitation. All four columns were fabricated from the same piece of steel.

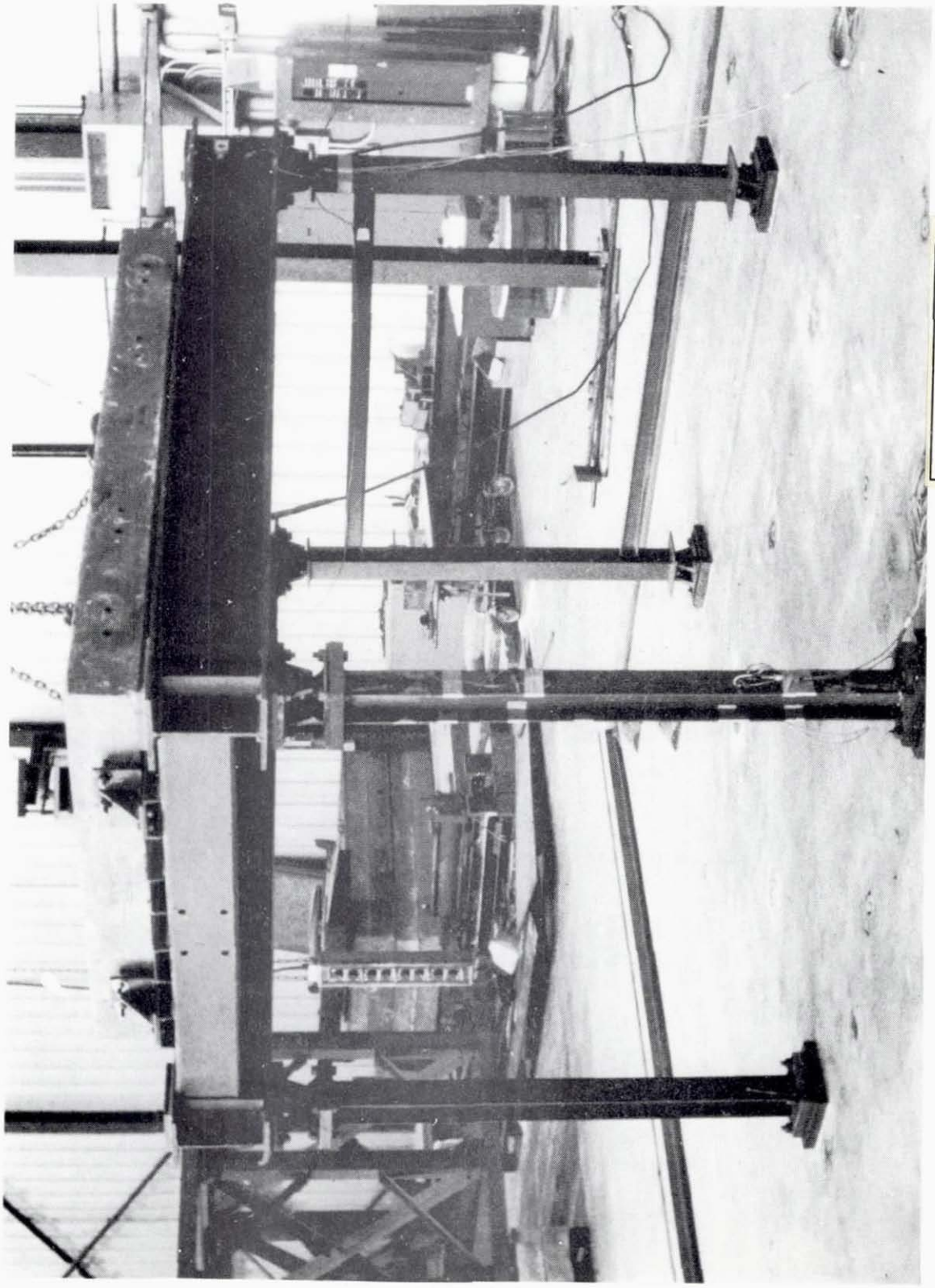

FIG. 2.1. TEST STRUCTURE ON SHAKING TABLE

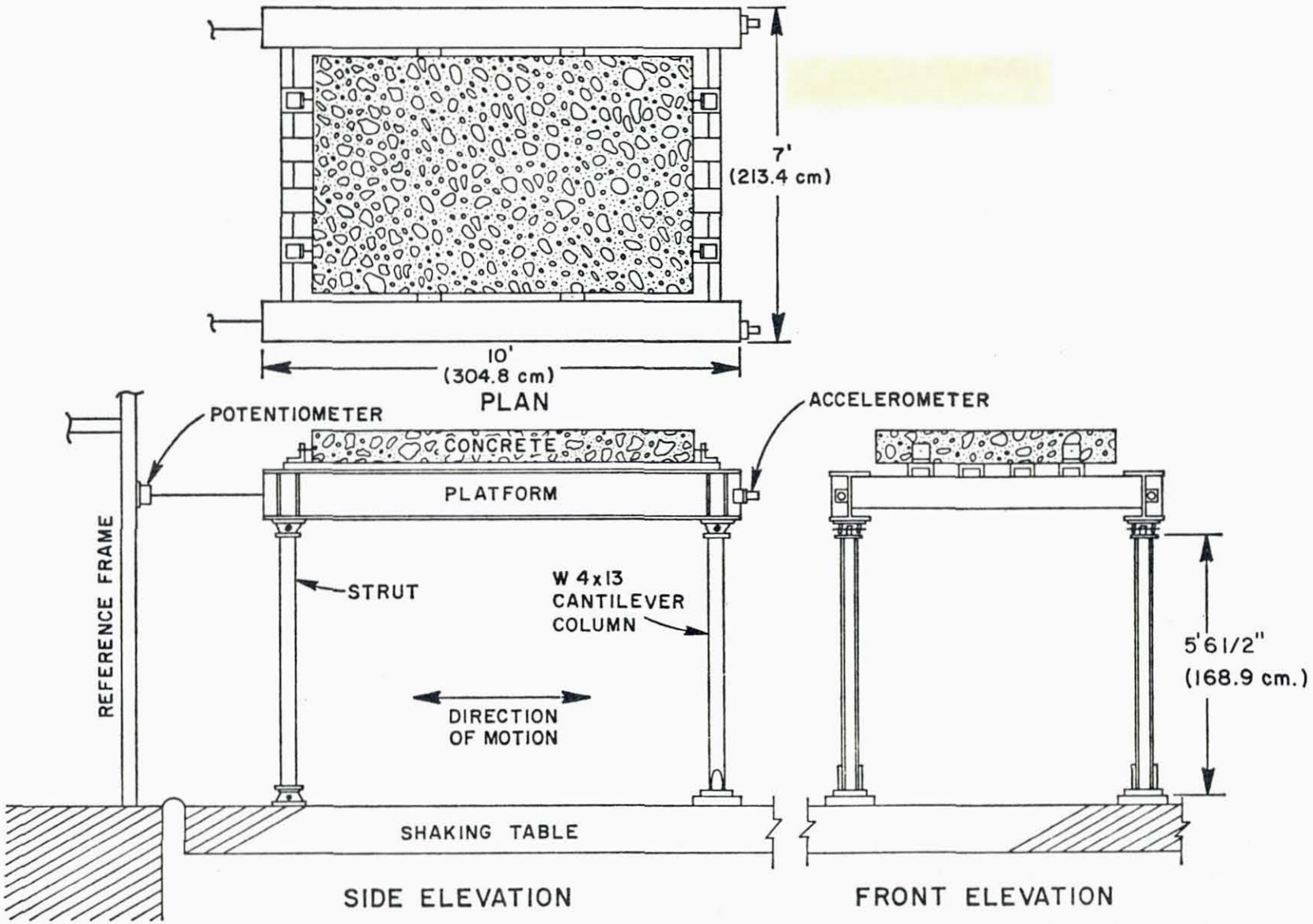

FIG. 2.2. PLAN AND ELEVATION VIEWS OF TEST STRUCTURE

2.2 Shaking Table Facility

The shaking table is 20 ft by 20 ft and is capable of moving in the vertical direction and one horizontal direction in such a way that good replicas of strong-motion earthquakes can be obtained. In the tests conducted for this work, only the horizontal motion was used. The maximum displacement and velocity that can be achieved by the table in the horizontal direction are 5 in. and 25 in./sec., respectively. The shaking table may be used to subject a structure weighing up to 100 kips to a table acceleration of 1 g in the horizontal direction and, simultaneously, 1/2 g in the vertical direction. The useful frequency range is 0 to 20 Hz.

The earthquake motions, which are in the form of digitized acceleration time histories, cannot be used directly to excite the shaking table, since the table input requires displacement time histories. Acceleration is converted to analog form using a digital to analog converter and then changed to displacement by integrating twice using an electronic analog integrator. The amplitude scaling of the displacement record during a test is controlled by a "span" setting. A span of 1000 will, typically, give a displacement time history that has a nominal peak value of 5 in., the capacity of the table. The table facility is described in full by Rea and Penzien (1973)[3].

2.3 Instrumentation

Accelerometers are mounted on both sides of the platform of the structure recording the acceleration of each side. The acceleration of the table is recorded by 3 built-in accelerometers - one in the middle of the table and one on each side. The table acceleration is taken as the average of the three. The total displacement of the platform is

found using potentiometers which measure the displacement of each side of the structure relative to a reference frame remote from the table. The table displacement is measured in the same manner as the table accelerations. The accelerations and displacements of both sides of the platform are then averaged and the average is used to represent the response of the structure in all subsequent calculations.

The rather high scanning rate used for the tests is 100 samples per second, which is about twice the rate normally used with the table.

The accuracy of the recorded data cannot, of course, be precisely determined since it depends on the accuracy of calibration for each test. However, the overall accuracy of the data acquisition system is thought to be within about 0.1%.

2.4 Tests

The procedure for each set of tests is similar:

a. Install a new pair of columns.

b. Conduct preliminary tests to determine the properties of the structure.

c. Subject the structure to a low intensity excitation to establish the linear response.

d. Subject the structure to a high intensity excitation to establish the nonlinear response.

e. Repeat the preliminary tests to see what changes in the initial properties, if any, have occurred.

2.4.1 Preliminary Tests

The preliminary low-amplitude pull-back and free vibration tests are carried out on the structure for each new pair of columns. The tests are performed twice, as mentioned above,to determine if a

significant change has occurred in any of the structural properties, particularly the damping. The table is locked in place and the structure pulled back with an assembly consisting of a chain and steel cable attached to the platform, a short length of small diameter rod, a winch, and a force transducer which is attached to the floor. The pull-back force used is 1,000 and 1,500 lb and the corresponding displacement is recorded using the data acquisition system. The rod is then cut and the structure allowed to vibrate freely while the acceleration and displacement time histories are recorded on magnetic tape and on an oscillograph. The structure is then excited manually and allowed to vibrate freely during which time the acceleration and displacement time histories are again recorded. The free vibration time history is then run through a Fast Fourier Transform program available within the data acquisition system, and from the spectral analysis the fundamental frequency of the structure is determined accurately.

2.4.2 Shaking Table Tests

The objectives of this research require a variety of excitations that are severe enough to cause significant inelastic deformations. To meet this requirement, four series of tests are performed using four identical pairs of columns. The typical procedure for each series of tests consists of calibrating the transducers, making one or more low intensity runs to produce an elastic response and to ensure that the table and data acquisition are functioning properly, and then performing one or two high intensity runs.

Some results from the shaking table tests are available immediately after a test has been made, and these results are used to select the intensity of the following tests. A program written for the NOVA computer

is able to give, for each channel, both positive and negative extreme values and the time at which they occur, as well as the offset before the excitation is started. The accelerometers and potentiometers at the top of the structure, as well as the table motion, are monitored using the oscillograph.

The following describe the four series:

A. The El Centro, 1940 N-S component was used for this series. The initial run was using Span 350 and had a maximum table acceleration of 0.215 g. Then the high intensity run was selected using a span of 950, or table acceleration of 0.692 g.

B. The Pacoima record of the S16E component of the San Fernando earthquake of 1971 was used for this series. The initial runs used Spans of 150 and 200 with maximum table accelerations of 0.186 g and 0.232 g, respectively. The high intensity run was selected using Span 750 with a maximum table acceleration of 1.032 g. The span was limited by the maximum allowable table displacement.

C. The N69W component of the Taft 1952 record was used in this series. The initial run used Span 350 with a maximum table acceleration of 0.198 g. The high intensity runs were then selected using Spans 950 and 800 with maximum table accelerations of 0.609 g and 0.479 g, respectively.

D. The final series used the N65E component of the Parkfield earthquake of 1966 as recorded at Cholame, Shandon California. The initial run used Span 450 with a maximum table acceleration of 0.199 g. The high intensity run was then selected using Span 1000 with a maximum table acceleration of 0.467 g.

2.5 Data Reduction

Typically from 20 to 30 second of data were recorded for each test depending on the test series (or excitation), accomodating a few seconds both before and after the excitation signal. The quiesent period before the test was subsequently used to make possible corrections for initial offsets.

The digital data collected during the shaking table tests, in the form of 16-Bit words are stored temporarily on a magnetic disk and then, at the conclusion of each test, transferred to a 9-tract magnetic tape. In this form the data cannot be directly used with the CDC Computer, which requires 7-track tapes and 60-Bit words. Conversions to rectify this mismatch are made using existing programs. The final step, after rearranging the data as the time-history of each channel, is to convert both the absolute acceleration at the top of the structure and the relative displacement of the top of the structure, with respect to the reference frame, to quantities relative to the table motions. These two response quantities, along with the table accelerations, are then stored on another magnetic tape for use in the identification program.

2.6 Test Results

The data employed in this work are the following:

a. The preliminary tests of all series A, B, C and D, both before and after the high intensity run.

b. El Centro Span 950.

c. Pacoima Span 750.

d. Taft Span 950.

e. Parkfield Span 1000.

2.6.1 Preliminary Tests

The preliminary tests are performed as described in Section 2.4.1 and the main results are contained as follows in Tables 2.1 to 2.4:

Column 1: The force used to pull back the structure after correcting for the angle.

Column 2: The displacement corresponding to the force in Column 1 - average of both sides.

Column 3: The corresponding stiffness - [(1)/(2)].

Column 4: The stiffness obtained from the beam formula for a cantilevered member with a transverse load at its end. (The effect of the parabolic strap was ignored in this calculation.)

Column 5: The frequency of the structure as obtained from a Fourier analysis of the free vibration response.

Column 6: The damping as a fraction of critical damping computed directly from the oscillograph recording. The damping ratio is evaluated from:

$$\xi = \frac{1}{2m\pi} \ln\left(\frac{V_n}{V_{n+m}}\right)$$

where V_n and V_{n+m} are the peak displacements in the n^{th} and $n+m^{th}$ cycles, and $\ln\left(\frac{V_n}{V_{n+m}}\right)$ is the logarithmic decrement. The damping is assumed to be so small that the ratio of undamped to damped frequency is nearly one.

Column 7: The viscous damping coefficient, C, calculated from the equation defining ξ,

$$\xi = \frac{C}{2M\omega}$$

or

$$C = 2M\xi\omega = \frac{K\xi}{\pi f}$$

Column 8: The effective weight of the structure calculated as:

$$W = \frac{K \cdot g}{(2\pi f)^2}$$

Column 9: The average of all the values in columns 8 of all four tables, because the mass is the same for all four series.

Column 10: The weight as obtained by weighing the platform and adding 1/3 of the column weights. (Appendix C).

The rows of the tables are defined as follows:

Rows 1 and 2: Preliminary tests performed before the high intensity run.

Row 2: Free vibration by exciting the structure by hand.

Rows 3 and 4: Preliminary tests performed after the high intensity run.

Row 4: Free vibration by exciting the structure by hand.

TABLE 2.1

TEST SERIES A

P (lb) (1)	Δ (in) (2)	(1)/(2) K (#/in) (3)	$2\left(\frac{3EI}{L^3}\right)^+$ (#/in) (4)	f (Hz) (5)	ξ (6)	$C = \frac{\xi K}{\pi f}$ (#-sec/in) (7)	$W = Kg/(2\pi f)^2$ (lb) (8)	$\bar{W}$ (lb) (9)	W weighed (lb) (10)
963	0.469	2054	2225	1.84	0.0112	3.980	5938	5933	5978
963	0.469	2054	2225	1.85	0.0093	3.287	5874	5933	5978
963	0.461	2089	2225	1.83	0.0132	4.796	6105	5933	5978
963	0.461	2089	2225	1.82	0.0141	5.152	6173	5933	5978

TABLE 2.2

TEST SERIES B

P (lb) (1)	A (in) (2)	(1)/(2) K (#/in) (3)	$2\left(\frac{3EI}{L^3}\right)^+$ (#/in) (4)	f (Hz) (5)	ξ (6)	$C = \frac{\xi K}{\pi f}$ (#-sec/in) (7)	$W = Kg/(2\pi f)^2$ (lb) (8)	$\bar{W}$ (lb) (9)	W Weighed (lb) (10)
1444	0.781	1850	2225	1.76	0.0092	3.078	5846	5933	5978
1444	0.781	1850	2225	1.76	0.0096	3.212	5846	5933	5978
1467	0.819	1792	2225	1.72	0.0128	4.245	5929	5933	5978
1467	0.819	1792	2225	1.72	0.0132	4.378	5929	5933	5978

+ Using Values from the AISC Manual.

TABLE 2.3

TEST SERIES C

P (lb) (1)	Δ (in) (2)	K (#/in) (3)	$2\left(\frac{3EI}{L^3}\right)$+ (#/in) (4)	f (Hz) (5)	ξ (6)	$C = \frac{\xi K}{\pi f}$ (#-sec/in) (7)	$W = Kg/(2\pi f)^2$ (lb) (8)	$\overline{W}$ (lb) (9)	W weighed (lb) (10)
1444	0.747	1932	2225	1.77	0.0085	2.953	6036	5933	5978
1444	0.747	1932	2225	1.76	0.0081	2.830	6105	5933	5978
1444	0.772	1871	2225	1.77	0.0122	4.105	5845	5933	5978
1444	0.772	1871	2225	1.75	0.0121	4.118	5980	5933	5978

TABLE 2.4

TEST SERIES D

P (lb) (1)	Δ (in) (2)	K (#/in) (3)	$2\left(\frac{3EI}{L^3}\right)$+ (#/in) (4)	f (Hz) (5)	ξ (6)	$C = \frac{\xi K}{\pi f}$ (#-sec/in) (7)	$W = Kg/(2\pi f)^2$ (lb) (8)	$\overline{W}$ (lb) (9)	W weighed (lb) (10)
1444	0.777	1858	2225	1.77	0.0083	2.773	5805	5933	5978
1444	0.777	1858	2225	1.76	0.0078	2.722	5871	5933	5978
1444	0.793	1821	2225	1.75	0.0129	4.273	5820	5933	5978
1444	0.793	1821	2225	1.75	0.0122	4.041	5820	5933	5978

+ Using Values from the AISC Manual.

From the tables we can deduce the following:

a. The stiffness changes somewhat when the structure experiences inelastic strains - strain hardening has the effect of increasing the stiffness. Deterioration of the welds at the base of the columns and possibly local buckling effects of the flanges on the other hand, would cause the stiffness to decrease. From the measure of the frequency (obtained by Fourier analysis), which is a more accurate way of establishing the stiffness with a fixed mass, we see that in general, the stiffness decreases in all test series A, B, C and D.

b. Comparing the values of the damping coefficient obtained from the free vibration tests both before and after the high intensity excitation, we see that by yielding the structure increases its damping properties by about 50%. This appears to be a result of the plastic straining of the structure as the free vibration amplitudes of both tests were approximately the same. Matzen and McNiven[1], on the other hand, found the damping to be amplitude dependent for this type of structure and this type of tests.

2.6.2 Test Series A - El Centro Span 950

After the test data had been reduced, the most important response quantities were plotted with the CALCOMP plotter. The measured table acceleration time history is shown in Fig. 2.3. By using the measured acceleration time history on the top of the structure, i.e., the absolute response, and multiplying it by the mass of the structure and changing the sign one can obtain an approximate resisting force time history of the structure. That is

$$M\ddot{v}_t + C\dot{v} + P = 0$$

$$\text{or} \quad -M\ddot{v}_t = P + C\dot{v} \tag{2.1}$$

where $\ddot{v}_t$ is the absolute platform acceleration

$\dot{v}$ is the relative velocity (not measured)

P is the resisting force in the columns.

Obviously this is only accurate at the peak values of the displacement, i.e., at reversal points when the velocity, $\dot{v}$, and hence the damping force, is zero. When this force is plotted against the displacement, it gives one an idea of the shape of the dynamic hysteresis loops, although the true static value appears only at the reversal points. This behavior is referred to here as pseudo-hysteretic and its loops are plotted and presented in Fig. 2.4 for test series A. Furthermore, the measured relative acceleration and displacement time histories of the platform are presented in Figs. 2.5 and 2.6. One can see both from the pseudo-hysteresis loops and the displacement time history that the amount of permanent displacement is about 1.5 in., whereas the maximum relative displacement during the run was 4.75 in. From the shape of the pseudo-hysteresis loops we see that the first major excursion into the inelastic region is essentially elastic-perfectly plastic, whereas all subsequent loops have a smooth transition from elastic to plastic response indicating strain hardening behavior. This "two-phase" cyclic inelastic behavior of mild steel is central to the problem of modeling the behavior of mild steel structures. We will return to it in the context of modeling.

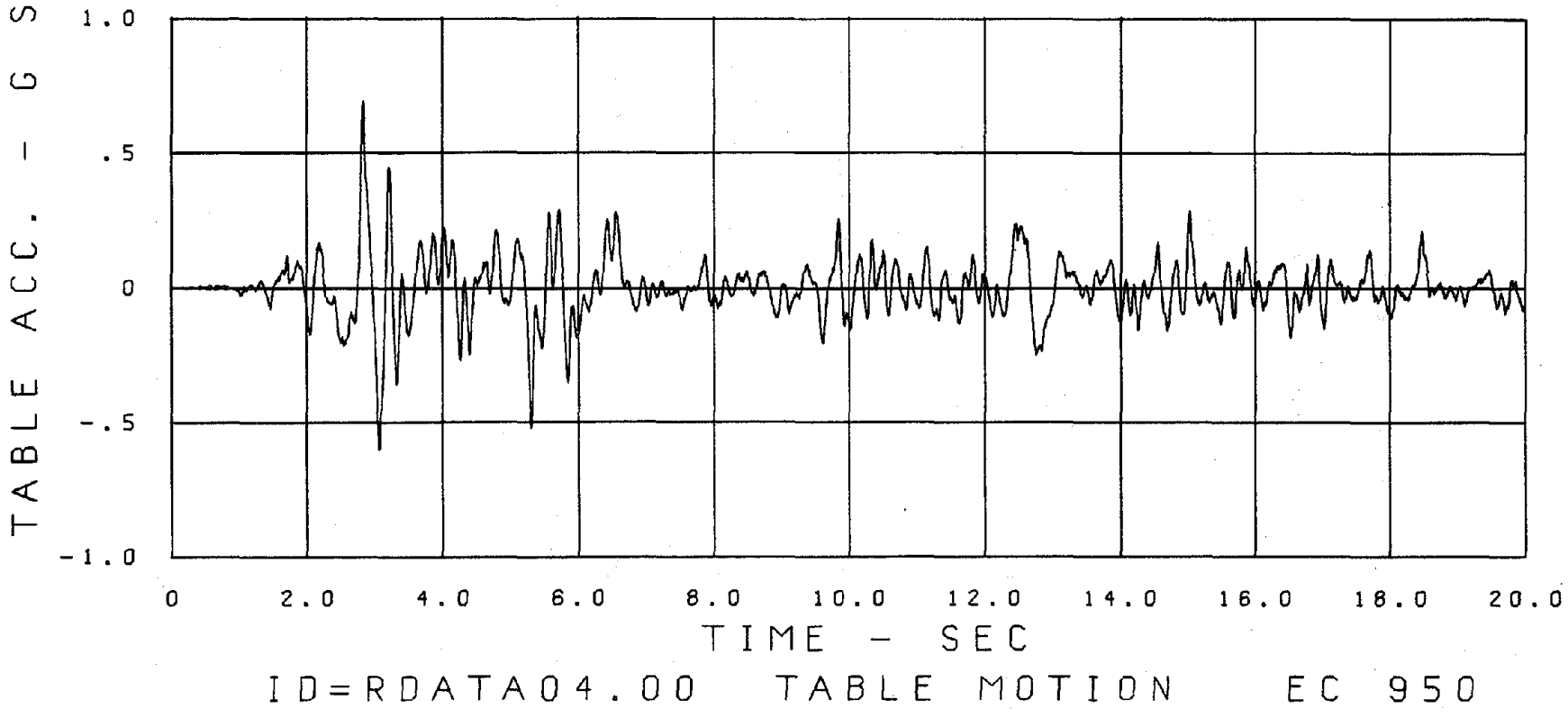

Fig. 2.3. MEASURED TABLE ACCELERATION, EL CENTRO SPAN 950.

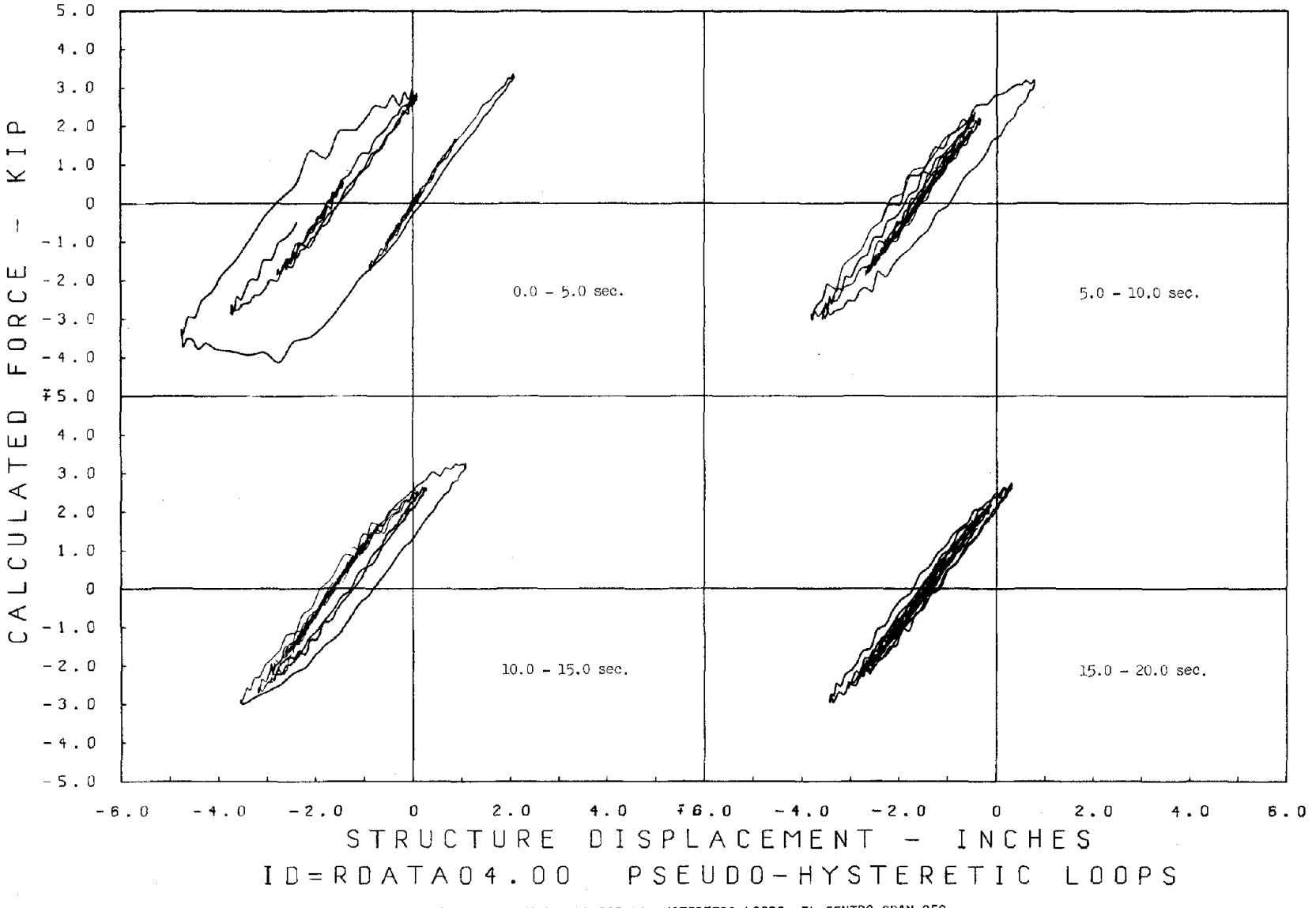

Fig. 2.4. MEASURED PSEUDO HYSTERETIC LOOPS, EL CENTRO SPAN 950.

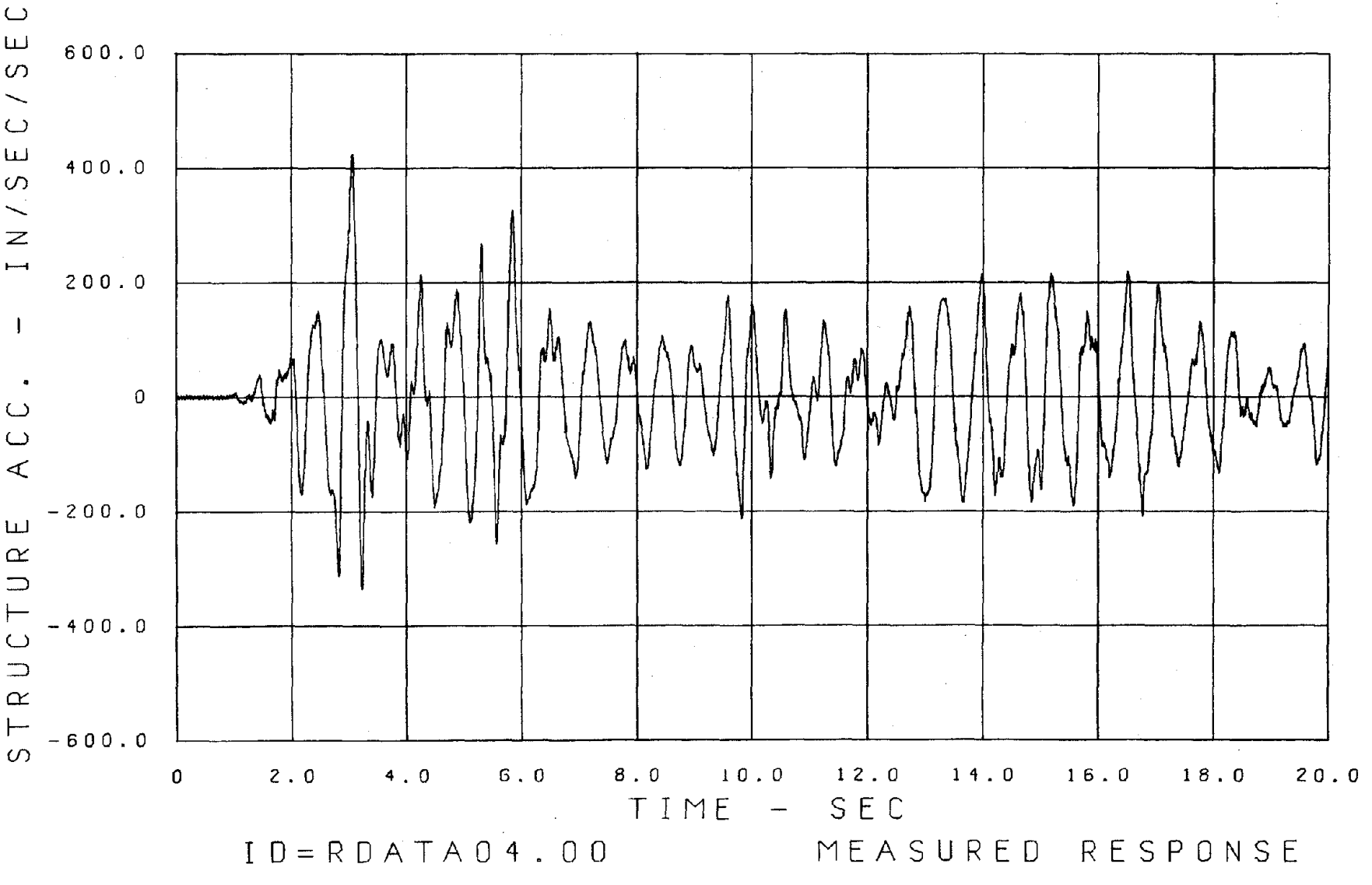

Fig. 2.5. MEASURED ACCELERATION RESPONSE TIME HISTORY, EL CENTRO SPAN 950.

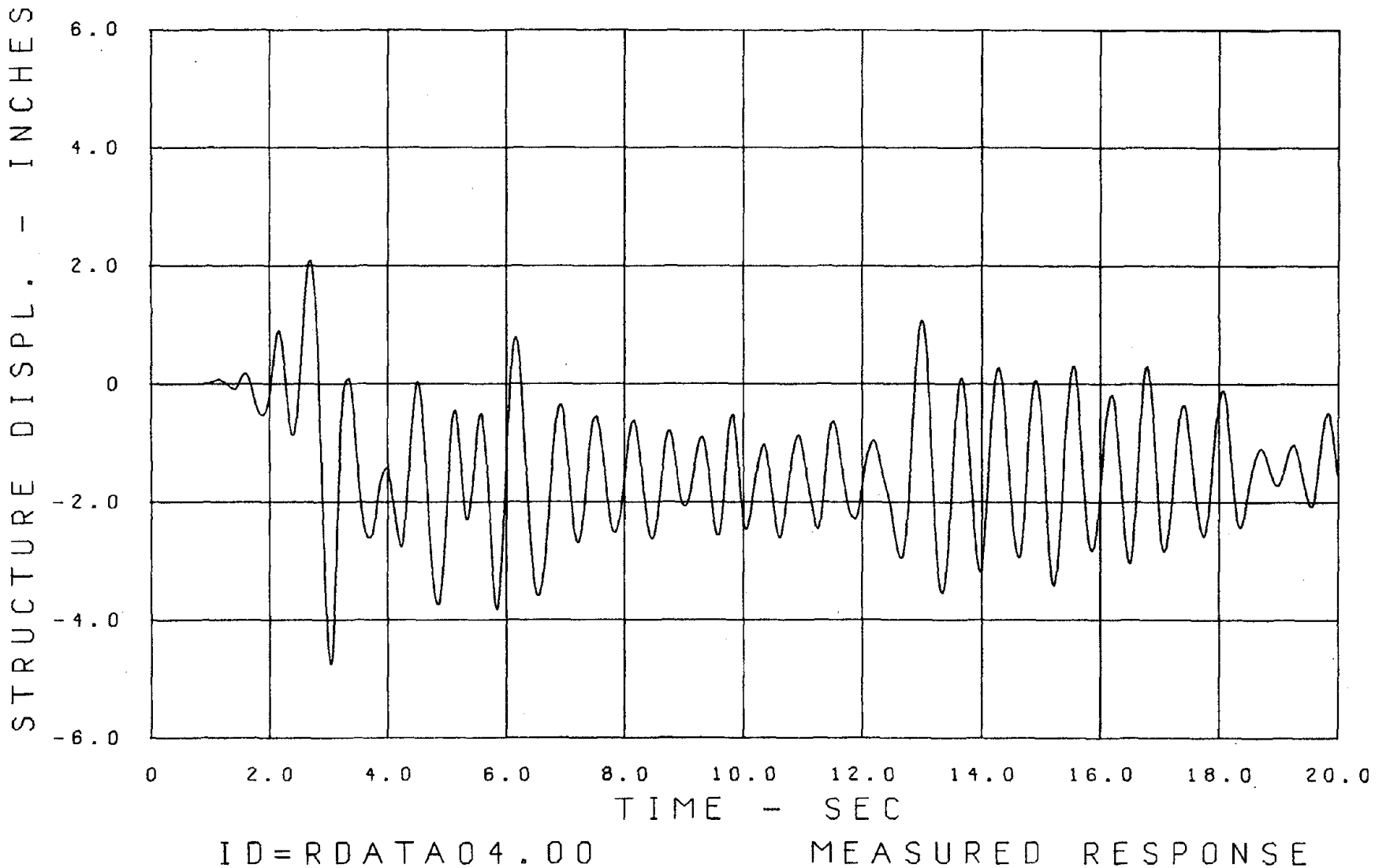

Fig. 2.6. MEASURED DISPLACEMENT RESPONSE TIME HISTORY, EL CENTRO SPAN 950.

2.6.3 Test Series B - Pacoima Span 750

The measured table acceleration and responses of the structure are shown in Figs. 2.7, 2.9 and 2.10. The pseudo-hysteresis loops are shown in Fig. 2.8. They and Fig. 2.10 show a permanent displacement of about 2.0 in., whereas the maximum relative displacement of the platform was 4.85 in. The same elastic-perfectly-plastic behavior during the first major inelastic excursion is observed while all subsequent inelastic excursions have a smooth transition from elastic to plastic response.

2.6.4 Test Series C - Taft Span 950

The measured table acceleration, pseudo-hysteresis loops and response quantities are shown in Figs. 2.11 to 2.14. The pseudo-hysteresis loops and the displacement time history show a permanent displacement of about 0.5 in., whereas the peak relative displacement is 3.40 in. The same difference as before is observed between the first and subsequent hysteresis loops.

2.6.5 Test Series D - Parkfield Span 1000

The measured table acceleration, pseudo-hysteresis loops and response quantities are shown in Figs. 2.15 to 2.18. The pseudo-hysteresis loops and the displacement time history show a permanent displacement of about 0.6 in., whereas the maximum displacement is 4.1 in. The first excursion into the inelastic range is small, but has essentially the elastic-perfectly plastic behavior. The subsequent loops are smooth.

2.6.6 Notes

Few things should be noted about the tests. First, during all of the tests the structure experiences a slight twisting which causes a

minor difference in the response of the two sides of the structure. This has slightly more effect on the peak acceleration response (2%) than it does on the peak displacement (1%). What causes the twist is uncertain, but it may be due to either or both of two reasons;

a. slight difference between the center of mass and the center of stiffness, and

b. a twist of the table during excitation.

The second thing to be noted is a high frequency noise which originates in the servomechanism of the table which is superimposed on the structural response. This noise is partly responsible for the raggedness of the pseudo-hysteresis loops. See also Section 3.4.

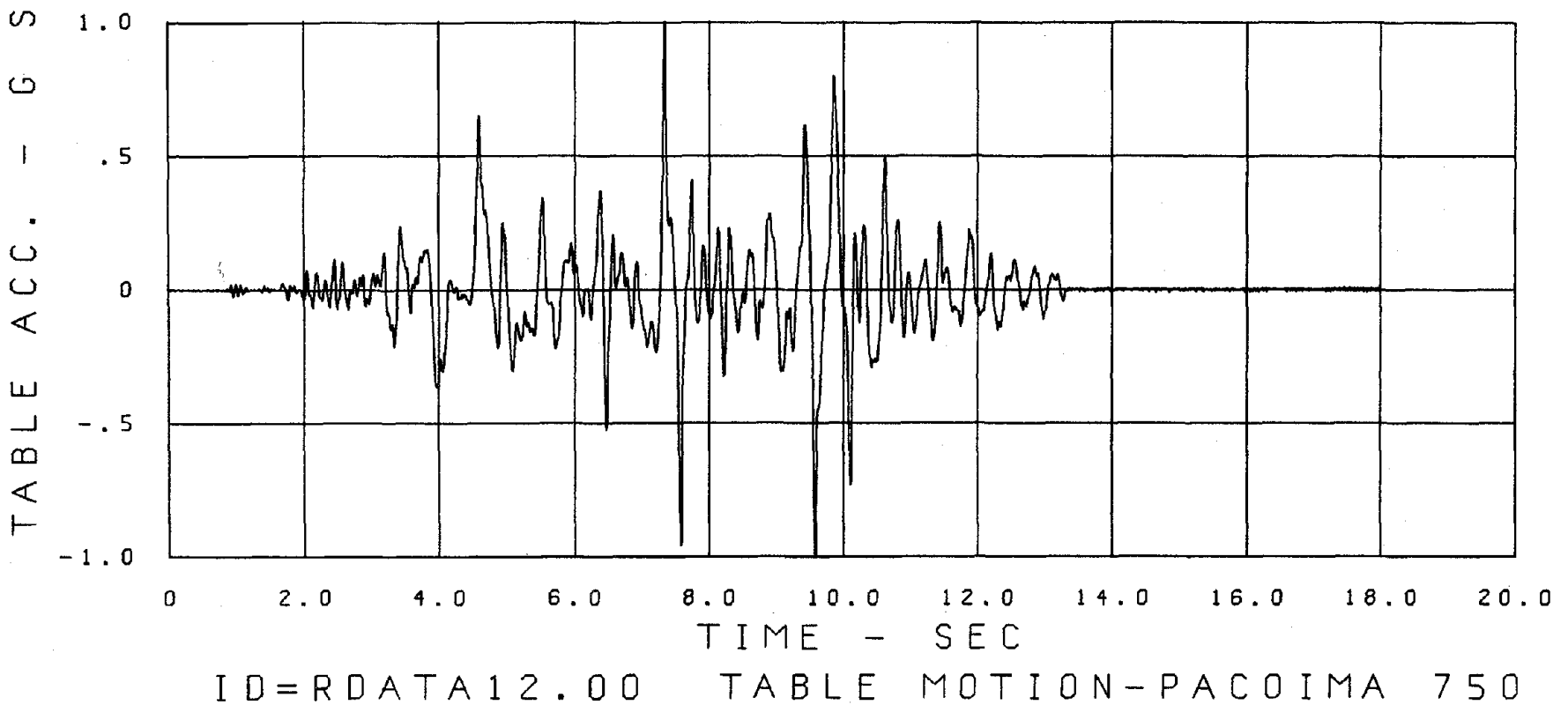

Fig. 2.7. MEASURED TABLE ACCELERATION, PACOIMA SPAN 750.

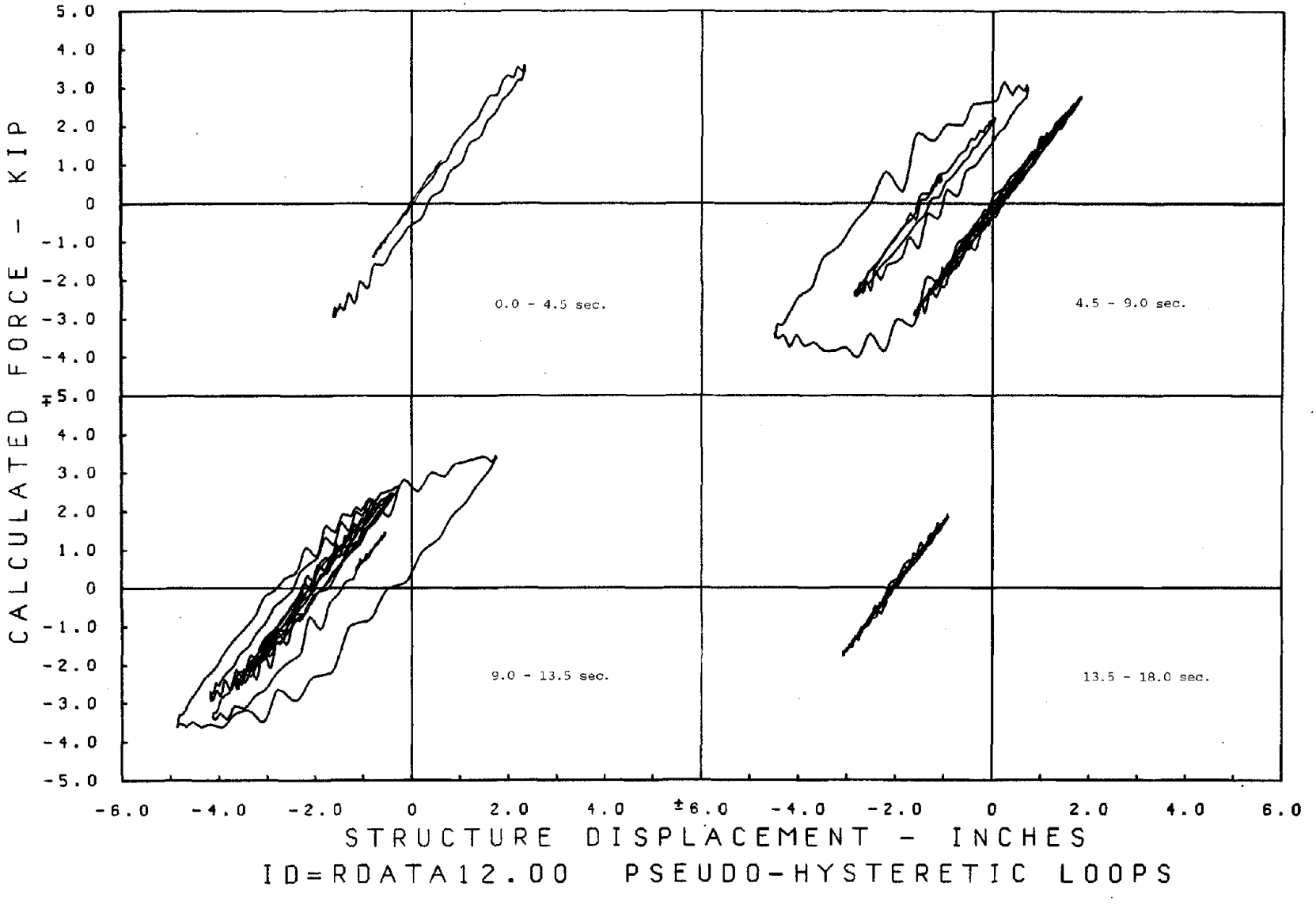

Fig. 2.8. MEASURED PSEUDO HYSTERETIC LOOPS, PACOIMA SPAN 750.

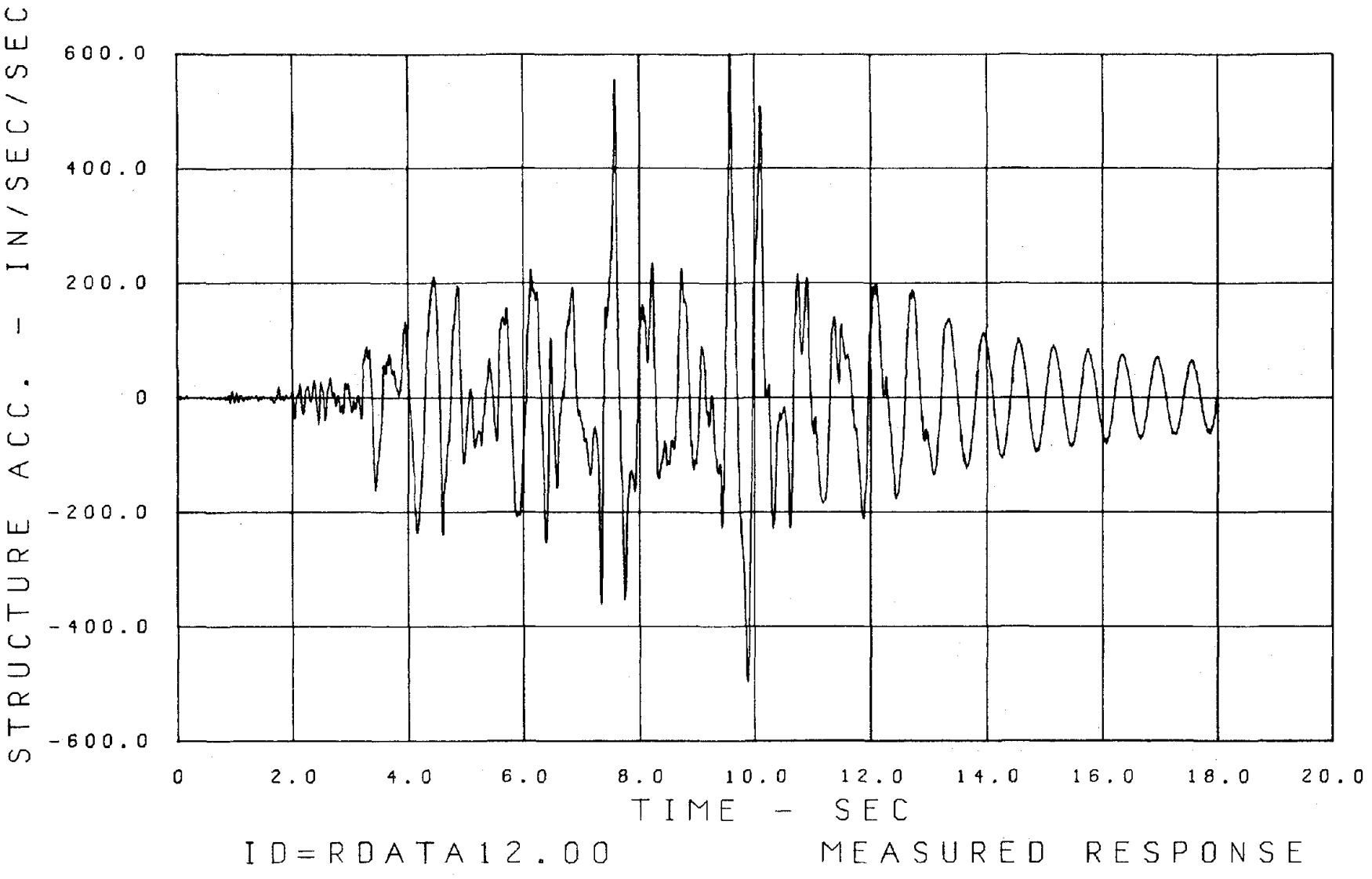

Fig. 2.9. MEASURED ACCELERATION RESPONSE TIME HISTORY, PACOIMA SPAN 750.

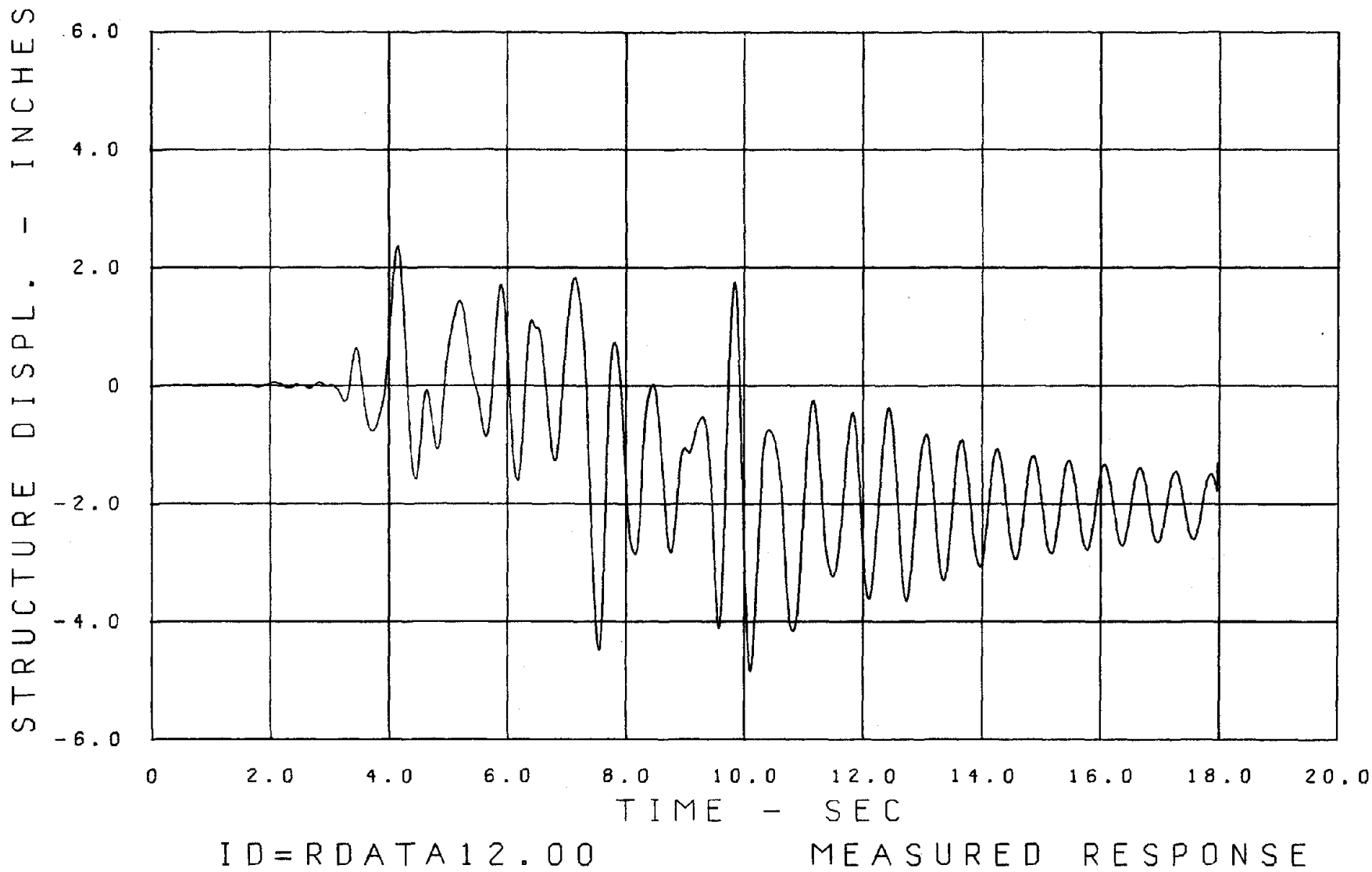

Fig. 2.10. MEASURED DISPLACEMENT RESPONSE TIME HISTORY, PACOIMA SPAN 750.

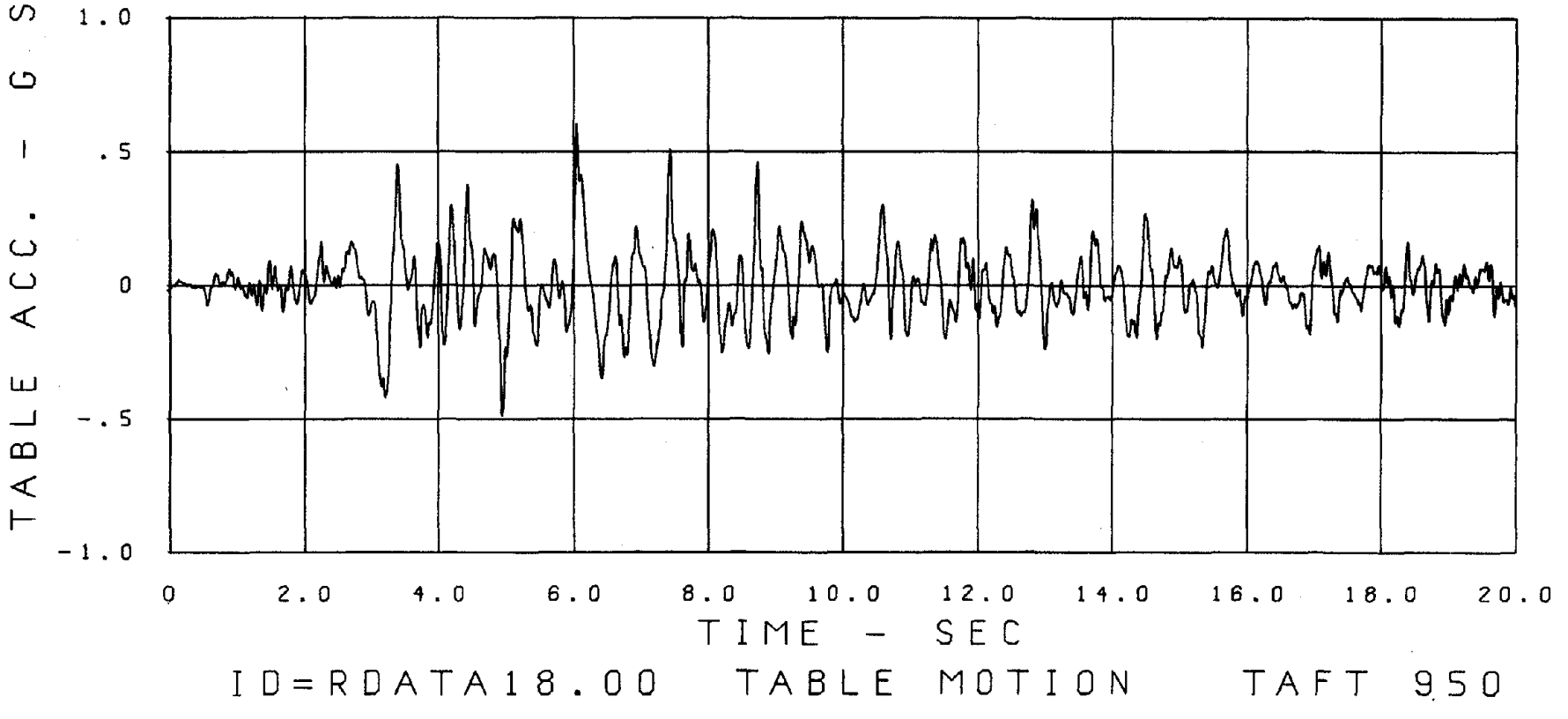

Fig. 2.11. MEASURED TABLE ACCELERATION, TAFT SPAN 950.

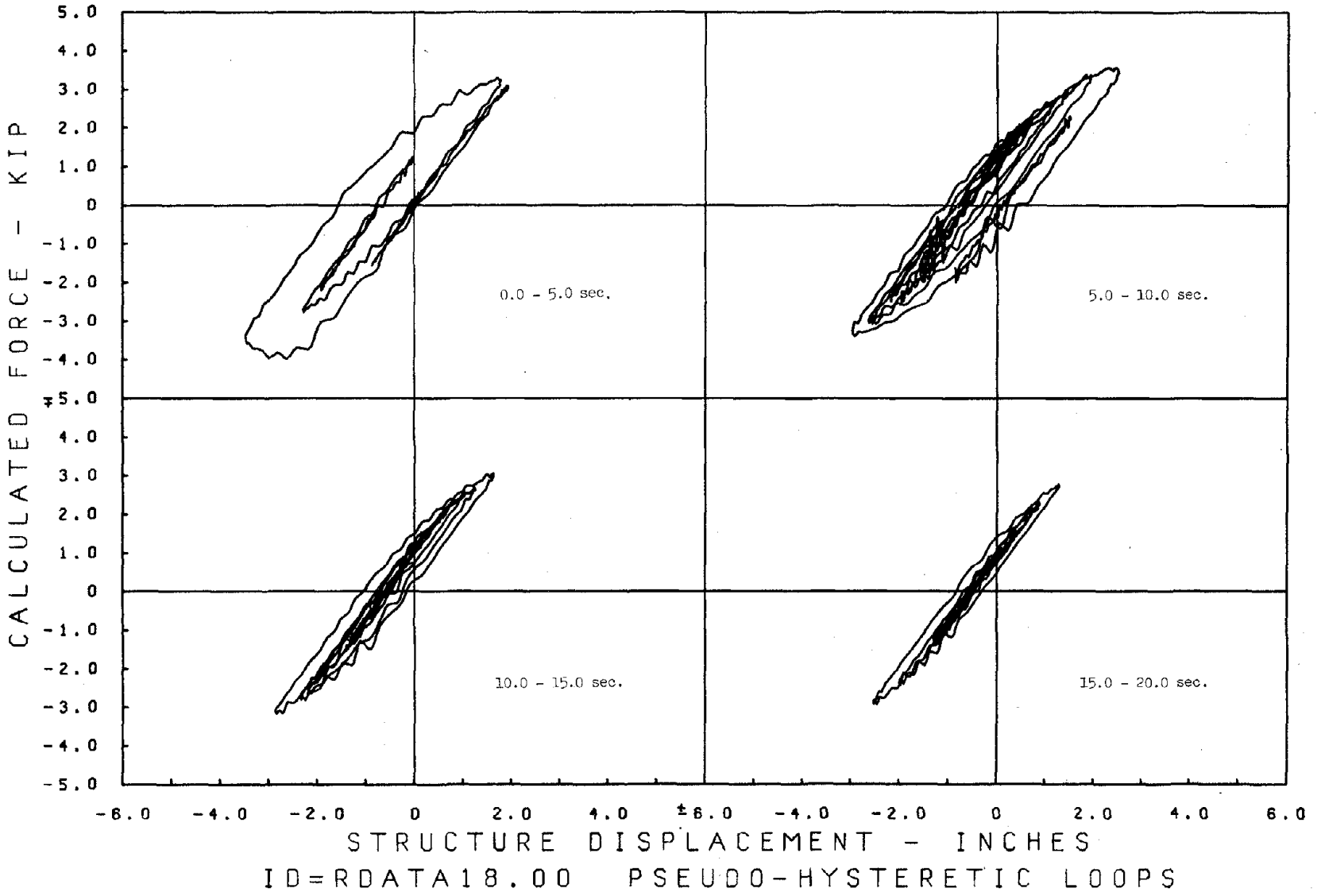

Fig. 2.12. MEASURED PSEUDO HYSTERETIC LOOPS, TAFT SPAN 950.

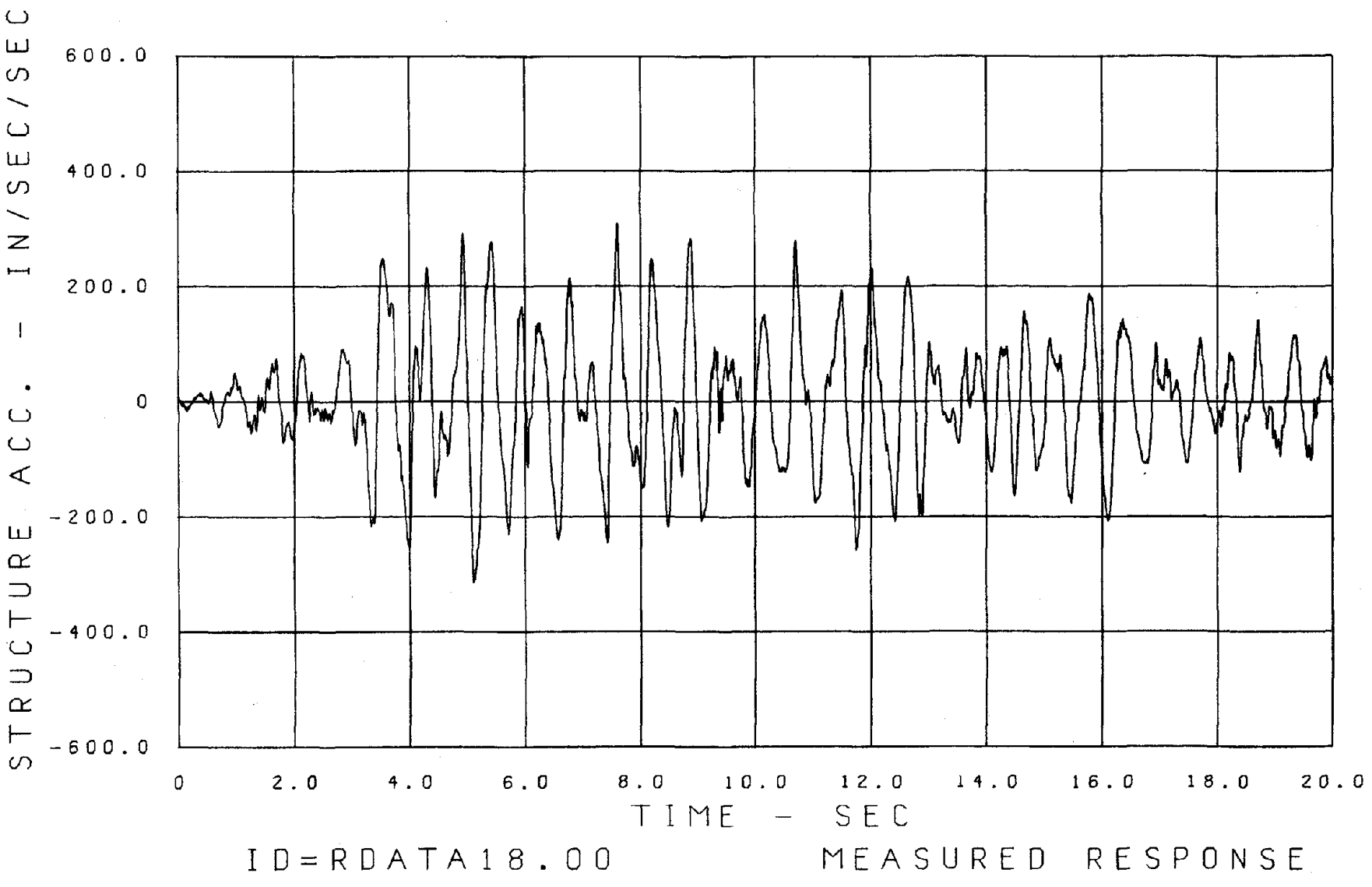

Fig. 2.13. MEASURED ACCELERATION RESPONSE TIME HISTORY, TAFT SPAN 950.

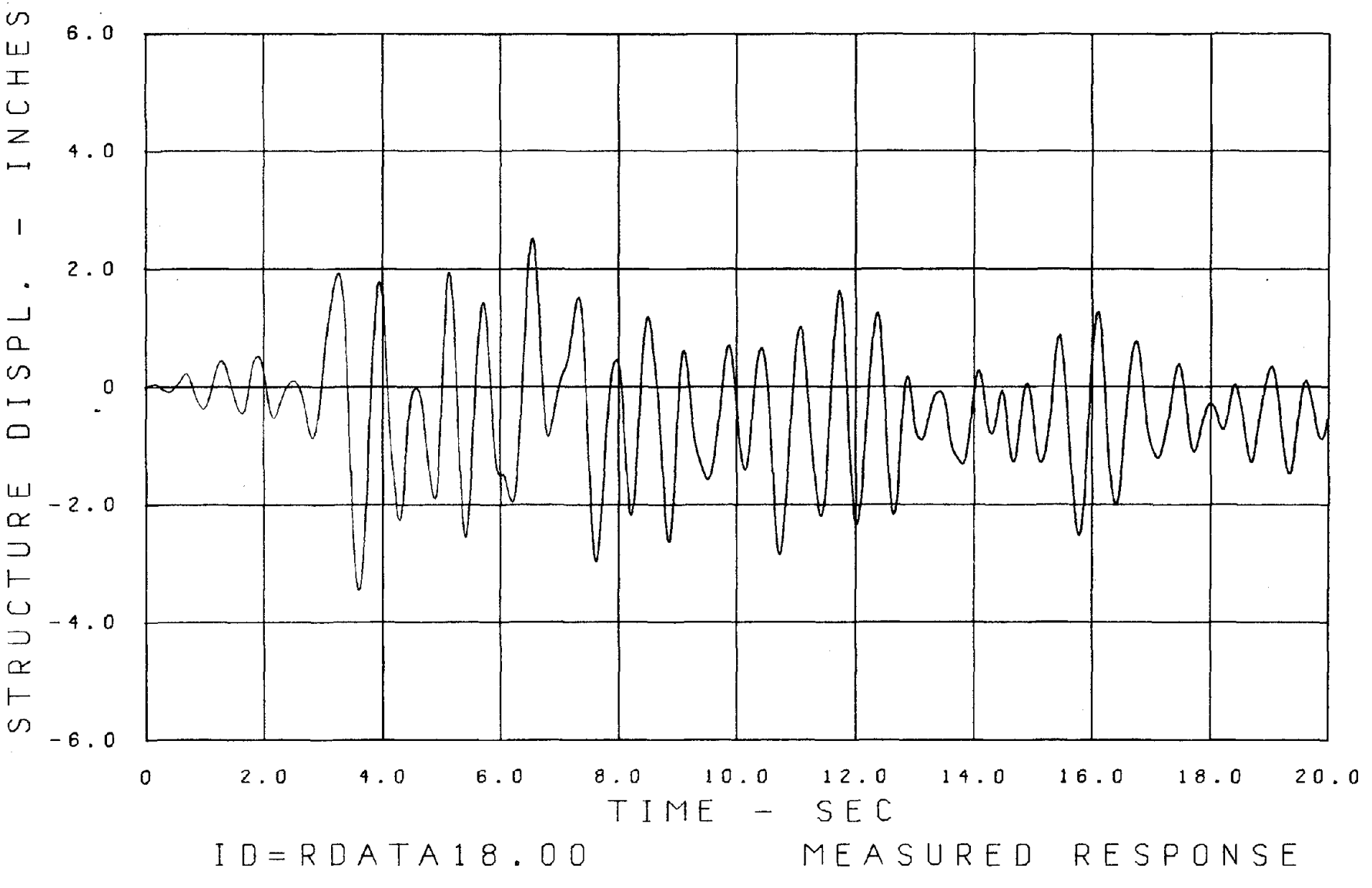

Fig. 2.14. MEASURED DISPLACEMENT RESPONSE TIME HISTORY, TAFT SPAN 950.

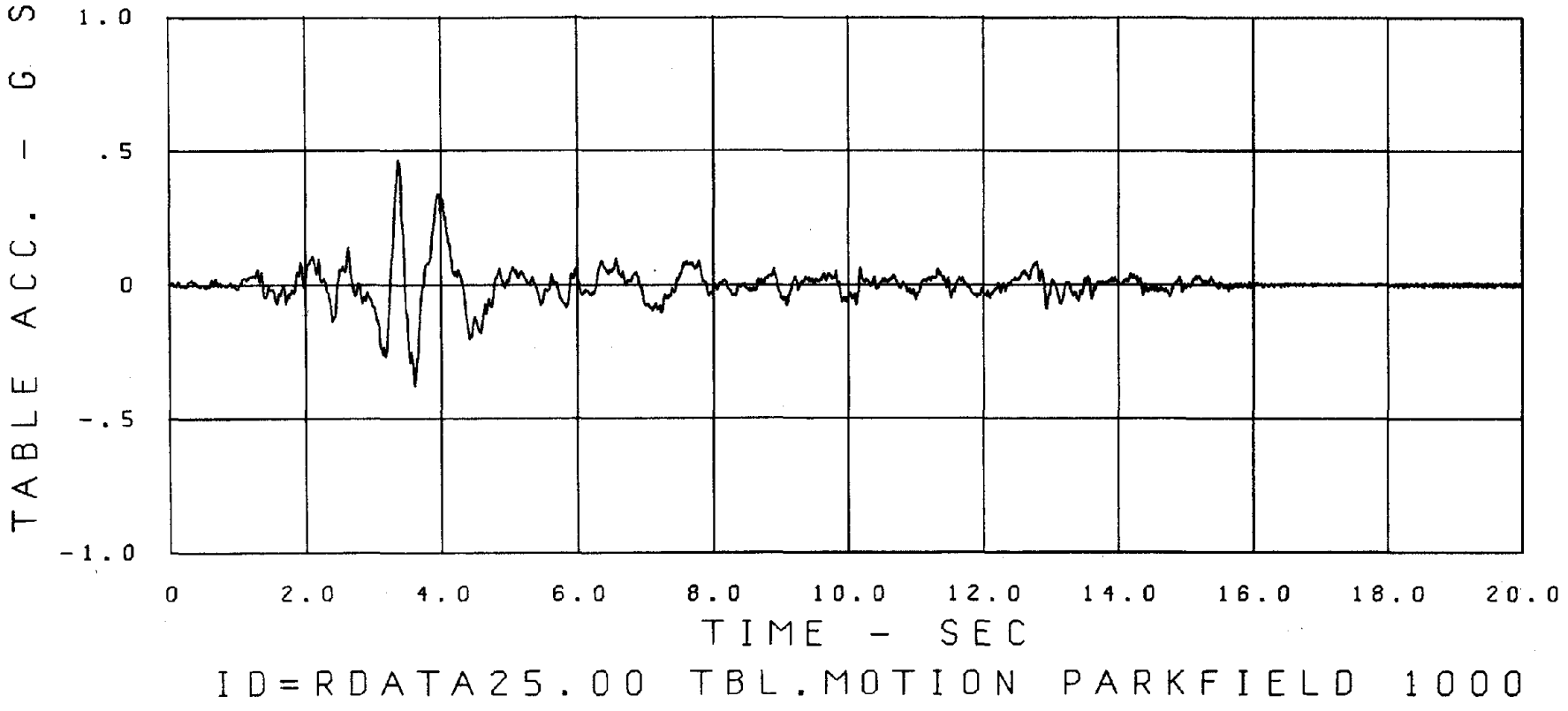

Fig. 2.15. MEASURED TABLE ACCELERATION, PARKFIELD SPAN 1000.

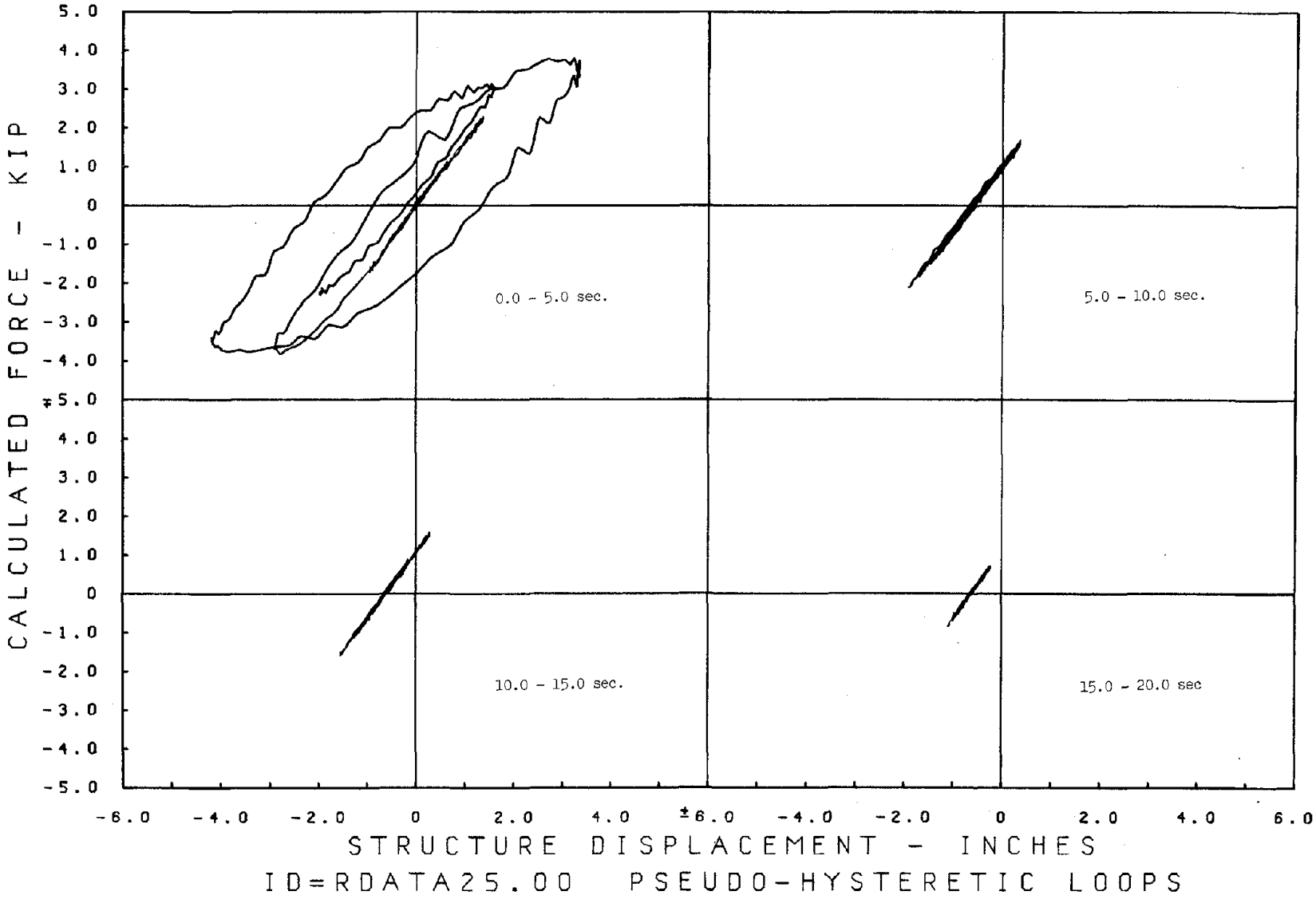

Fig. 2.16. MEASURED PSEUDO HYSTERETIC LOOPS, PARKFIELD SPAN 1000.

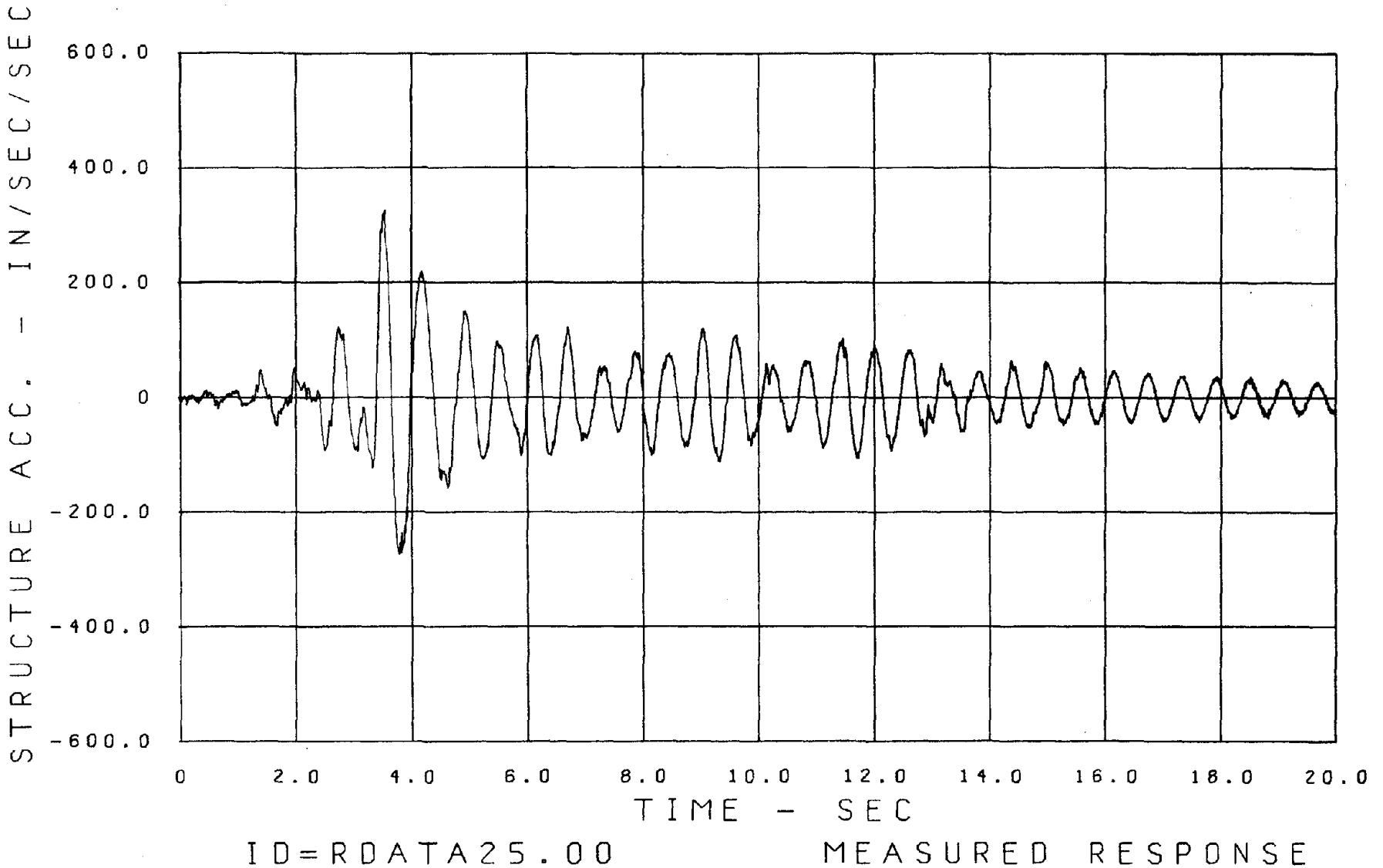

Fig. 2.17. MEASURED ACCELERATION RESPONSE TIME HISTORY, PARKFIELD SPAN 1000.

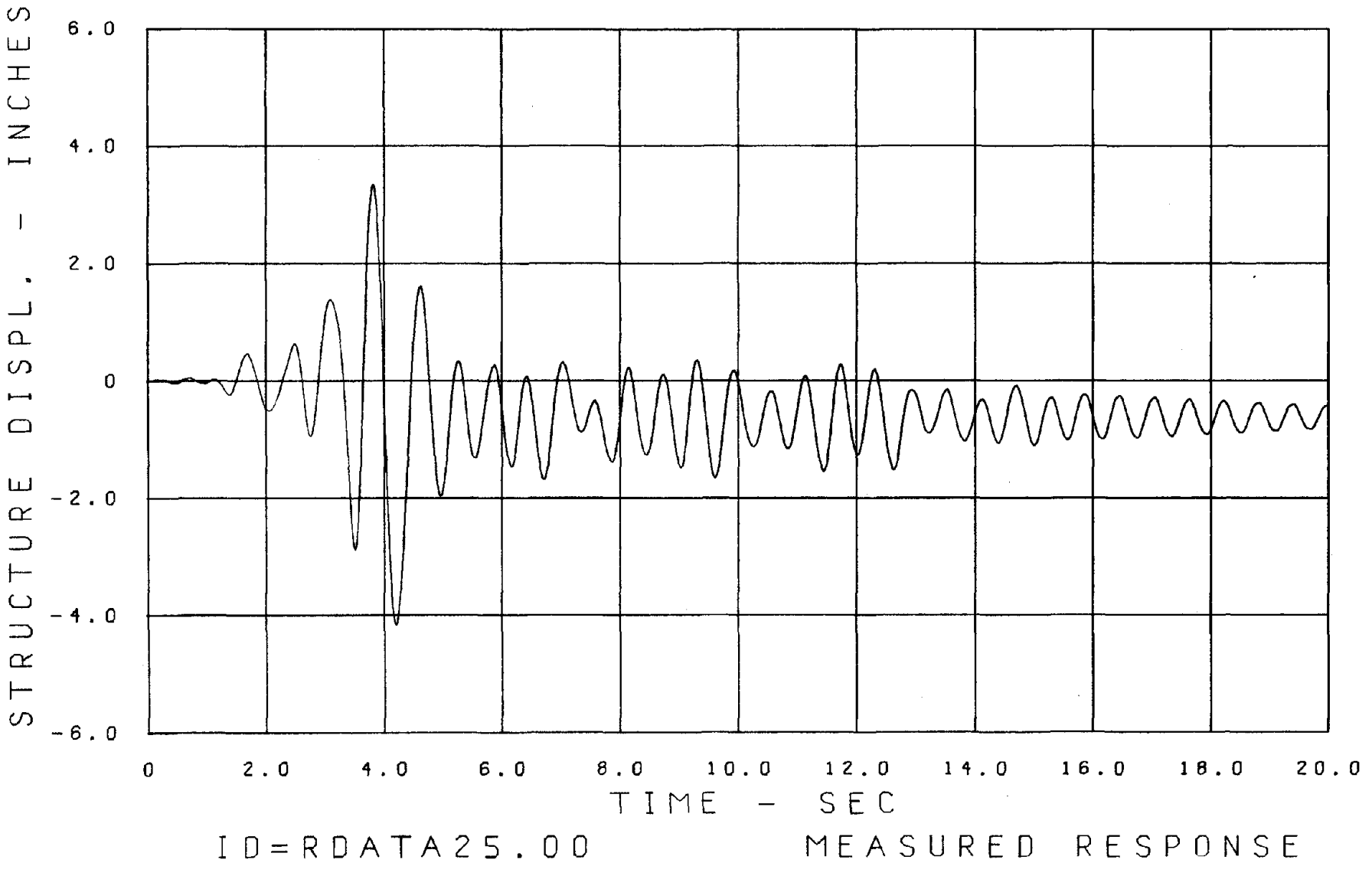

Fig. 2.18. MEASURED DISPLACEMENT RESPONSE TIME HISTORY, PARKFIELD SPAN 1000.

3. CONSTRUCTION OF THE MATHEMATICAL MODEL

Though the frame used in the present test series differs slightly from that used by Matzen and McNiven[1], the model is constructed in the same way. We assume the same form for the model, use a similar criterion function and the same optimization algorithm (the modified Gauss-Newton) to establish the parameters that appear in the differential equation. What is important for this work is that we use the inelastic response quantities from the El Centro test series in the criterion function. Because all three parts of system identification are described in detail in [1], they will be described here only briefly.

3.1 The Model

For a single-degree-of-freedom linear structure subjected to base excitation, the equation of motion is:

$$M\ddot{v}(t) + C\dot{v}(t) + Kv(t) = - M \ddot{v}_g(t) \; ; \; \dot{v}(0) = v(0) = 0 \qquad (3.1)$$

where $v(t)$ is the displacement of the top of the structure relative to the table.

M is the mass

C is the viscous damping coefficient

K is the stiffness

$\ddot{v}_g(t)$ is the table motion (acceleration)

This equation is only good for low intensity excitations or when the response is linear, because K is taken as a constant. The parameters M, C and K can easily be established using low-amplitude pull back tests and free vibration tests. For more general excitations, when the

restoring force is no longer elastic, it is necessary to exchange the elastic force in Eq. (3.1) by a term P(x) representing the hysteretic behavior of the structure. The equation becomes:

$$M\ddot{v}(t) + C\dot{v}(t) + P(x) = - M\ddot{v}_g(t) \; ; \; v(0) = \dot{v}(0) = 0 \qquad (3.2)$$

To complete the form of the model it is necessary to select a proper mathematical model to represent the force P(x). We use a Ramberg-Osgood type of model similar to the one used by Matzen and McNiven (1976)[1]. The equations are:

$$x(P) = \frac{P}{K}\left(1 + A\left|\frac{P}{K}\right|^{R-1}\right) \qquad \text{for the skeletal curve} \qquad (3.3)$$

$$x(P) = x_{re} + \frac{P-P_{re}}{K}\left(1+A\left|\frac{P-P_{re}}{2K}\right|^{R-1}\right) \quad \text{for branch curves.} \qquad (3.4)$$

K, R and A are the three Ramberg-Osgood parameters and (P_{re}, x_{re}) are the coordinates of the most recent velocity reversal. Because the equations give x as a function of P instead of the reverse in Eqs. (3.3) and (3.4), it is necessary to iterate within each time step to minimize the error. Along with these equations there must be rules governing the behavior of the loops resulting from the equations. A complete description of the rules is given in Appendix A, whereas the integration of Eq. (3.2) is described in Appendix B.

3.2 Criterion Function

For the identification we use test series A, El Centro Span 950, and adopt an existing computer program which was written by Matzen and McNiven (1976)[1] and is described in detail in their report. The criterion function we use here has the form

$$CR^T(\bar{\beta},T) = \sum_{i=1}^{n} \{(\ddot{v}_i(\bar{\beta},t) - \ddot{u}_i(t))^2 * WA + (v_i(\bar{\beta},t) - u_i(t))^2 * WD\} \Delta T_i$$

$$= CR^A(\bar{\beta},T) + CR^D(\bar{\beta},T) \tag{3.5}$$

where $\ddot{v}_i(\bar{\beta},t)$ and $v_i(\bar{\beta},t)$ are the response quantities calculated from the model using parameters $\bar{\beta}$ and excitation $\ddot{v}_g(t)$, $\ddot{u}_i(t)$ and $u_i(t)$ are response quantities measured from the actual structure when subjected to the same $\ddot{v}_g(t)$. WA and WD are weighting factors for the squared acceleration and displacement errors, respectively. $\bar{\beta}$ is a vector of the three Ramberg-Osgood parameters and the damping parameter; this is the variable that changes during the minimization of the error. N is the number of time steps used in the identification process. ΔT_i is the time step used in the integration. It is a constant and equal to 0.01 sec.

For this study we choose to minimize the criterion function, Eq. (3.5) by only considering the acceleration response. This is done because we have found that acceleration and displacement are not independent response quantities. We, therefore, use weighting factors WA = 1.0 and WD = 0.0 in Eq. (3.5).

3.3 Optimization of the Criterion Function

We use the Modified Gauss-Newton optimization algorithm as we have found that for the number of parameters involved it is the most powerful. We do not describe it here, but refer for its description to Ref. [1].

After adopting the algorithm, there are two important decisions that have to be made. The first is a set of initial values of the

parameters. Experience has shown that a clever choice of these initial values significantly speeds convergence to the final values. The parameter vector is

$$\beta = \begin{Bmatrix} C \\ K \\ A \\ R \end{Bmatrix}$$

Sensible values of C and K can be derived from the free vibration tests of the frame which are listed in Table 2.1. Initial choices of A and R are more difficult. Here we decide to use the same initial values that Matzen and McNiven[1] used successfully for their optimization with a similar frame. The initial parameter vector accordingly is

$$\bar{\beta} = \begin{Bmatrix} 4.304 \\ 2072 \\ 0.01 \\ 10.0 \end{Bmatrix}$$

The second decision is the value of the upper limit of integration in the criterion function; that is the portion of the duration of excitation response used to obtain the final vector $\bar{\beta}^*$. The general rule is that the larger the T the more accurate is the final vector, but the more expensive is the computer program.

We let economy rule our first decision and let T = 2.75 sec. This will prove to be an unfortunate decision. The program converged in five iterations to the vector

$$\bar{\beta}^* = \begin{Bmatrix} -1.267 \\ 2061.2 \\ 0.1172 \\ 2.633 \end{Bmatrix}$$

This vector won't do as a negative damping coefficient is inadmissible. Thinking that perhaps the fault lies with the initial vector, we chose an arbitrary initial vector

$$\overline{\beta} = \begin{Bmatrix} 4.00 \\ 1945 \\ 0.016 \\ 20.0 \end{Bmatrix}$$

and the same value for T. The algorithm converged to the same final vector, this time in seven iterations.

The fault seems therefore to be not with the initial parameter vector, but with the value of T.

To satisfy our curiosity about the influence of the choice of T, we decided to carry out optimization by increasing T incrementally and to record the resulting final values of the parameter for each value of T. The second initial parameter vector is used in each optimization. The results are recorded in Table 3.1 and are shown graphically in Fig. 3.1.

We study these values in conjunction with the measured displacement time history which is shown in Fig. 2.6. Because T = 2.75 gave an unacceptable vector, we examine Fig. 2.6 and find that the first large deflection, (meaning the first excursion into the plastic zone of the hysteresis loop) occurs at about T = 3.0 sec. We then observe that for T = 3.0 sec. the parameters have acceptable values but they are in a region of T where they are extremely sensitive to changes in T. We also note from Fig. 3.1 that as T approaches the full duration of excitation, i.e., 20 sec., the values level off and become insensitive to changes in T. We reason that the instability of the values of the parameter vector for small T's and the growing stability

TABLE 3.1

T (sec)	E^A_{MIN}	E^D_{MIN}	E^T_{MIN}	E^T_{MIN}/T	No. of Itera-tions	C (#-sec/in)	K (#/in)	A	R
2.75	35	0	35	12.79	7	-1.267	2061.2	0.117	2.634
2.80	36	0	36	12.73	7	-1.074	2054.4	0.112	2.700
2.90	41	0	41	14.21	9	-1.850	2071.2	0.128	2.576
2.95	46	0	46	15.45	7	-1.626	2073.6	0.128	2.461
2.97	63	0	63	21.30	9	-0.566	1989.4	0.0624	3.664
2.98	73	0	73	24.49	7	-0.0123	1962.9	0.0391	4.484
2.99	82	0	82	27.53	5	0.406	1945.2	0.0232	5.409
3.00	90	0	90	30.00	7	0.666	1934.4	0.0140	6.317
3.01	101	0	101	33.58	5	0.863	1925.9	0.00742	7.464
3.02	104	0	104	34.51	4	0.935	1922.7	0.00532	8.071
3.05	123	0	123	40.33	8	1.158	1914.4	0.00148	10.430
3.10	156	0	156	50.40	9	1.948	1904.8	0.000238	13.810
3.20	214	0	214	66.91	9	0.797	1913.2	0.00110	11.707
3.30	234	0	234	70.93	8	0.885	1925.1	0.00479	9.440
3.50	247	0	247	70.57	5	1.036	1926.4	0.00623	9.088
3.75	276	0	276	73.58	6	1.701	1929.6	0.01356	7.859
4.00	323	1	324	81.09	5	2.587	1927.8	0.02413	6.852
4.50	417	2	419	93.07	5	3.965	1897.5	0.02945	6.261
5.00	546	3	548	109.70	5	3.949	1867.3	0.02386	6.339
5.50	705	3	708	128.72	6	4.476	1827.0	0.01694	6.600
6.00	782	4	785	130.89	6	5.204	1804.5	0.01350	6.777
7.00	894	4	898	128.25	7	4.479	1805.3	0.01188	7.198
8.00	1130	4	1134	141.69	7	5.908	1751.8	0.004786	8.641
9.00	1168	4	1172	130.25	5	5.831	1742.1	0.003327	9.270
10.00	1221	5	1226	122.59	5	5.222	1756.5	0.004964	8.721
12.00	1325	8	1333	111.08	6	5.206	1771.5	0.008612	7.889
14.00	1588	12	1600	114.30	4	5.109	1781.0	0.01404	7.066
16.00	2212	20	2232	139.50	5	4.323	1789.1	0.02541	5.848
18.00	2625	25	2650	147.23	4	3.854	1788.8	0.02941	5.475
20.00	2768	28	2796	139.79	4	3.671	1787.7	0.02920	5.462

E^A_{MIN} is minimum squared acceleration error. E^D_{MIN} is minimum squared displacement error. $E^T_{MIN} = E^A_{MIN} + E^D_{MIN}$

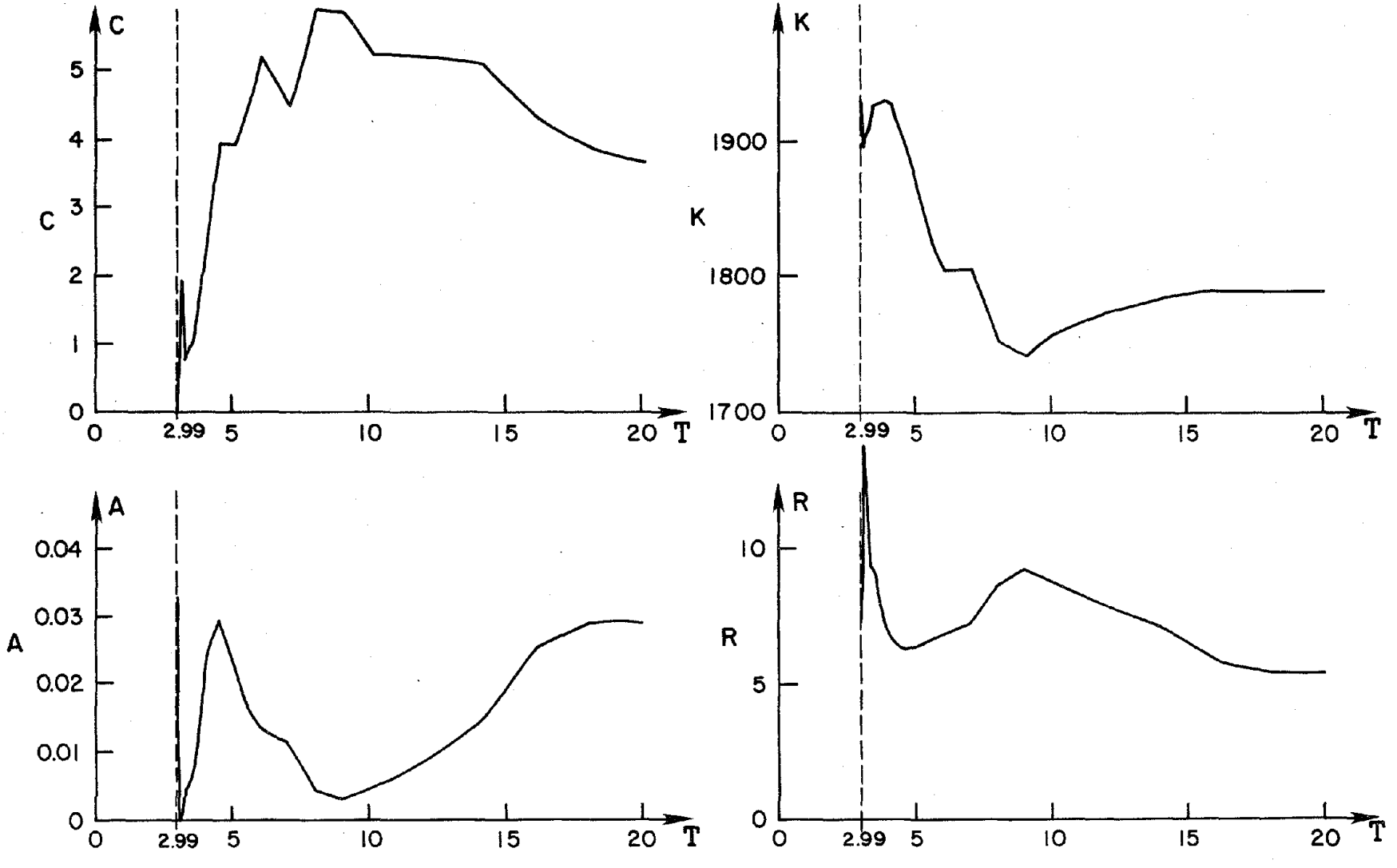

FIG. 3.1 VARIATION OF THE MINIMIZING PARAMETERS WITH T

as T increases is because we are characterizing the hysteretic behavior of mild steel using a single set of parameters. When we examine the pseudo-hysteresis loops in Fig. 2.4 we see that mild steel behaves in this context as if it were two different materials. We see that for the first 10 sec. of shaking we have the first major loop which indicates an elastic-plastic material behavior. This is followed by smaller loops which indicate elastic response. As the response continues we have many extensive loops, most exhibiting plastic behavior, but now the loops are gradually rounded indicating a work hardened material. This large array of later loops all display very much the same kind of hysteretic behavior, each contributing this behavior to the accumulating behavior contributing to the value of $\overline{\beta}^*$ as T increases. By the time we reach the full duration, the latter influence dominates the value of $\overline{\beta}^*$ stabilizing its value. Because we have decided on a single value for $\overline{\beta}^*$, we choose the value from the full duration, which completes the formulation of the model.

We do this however at a price. When we use the completed model to predict the experimental displacement time history, we see the price, the offset between experimental and predicted displacements which grows during the first few large displacements and then remains constant for the duration of the response. This is explained with the aid of Fig. 3.2.

The material model we have chosen is Ramberg-Osgood containing parameters obtained for the full duration of the response resulting in a model that reproduced hysteresis loops exhibiting work hardening behavior. When the response first dictates a displacement beyond yield, the material behavior is elastic-plastic, whereas the model predicts work hardening. At the first major reversal point both loops have the

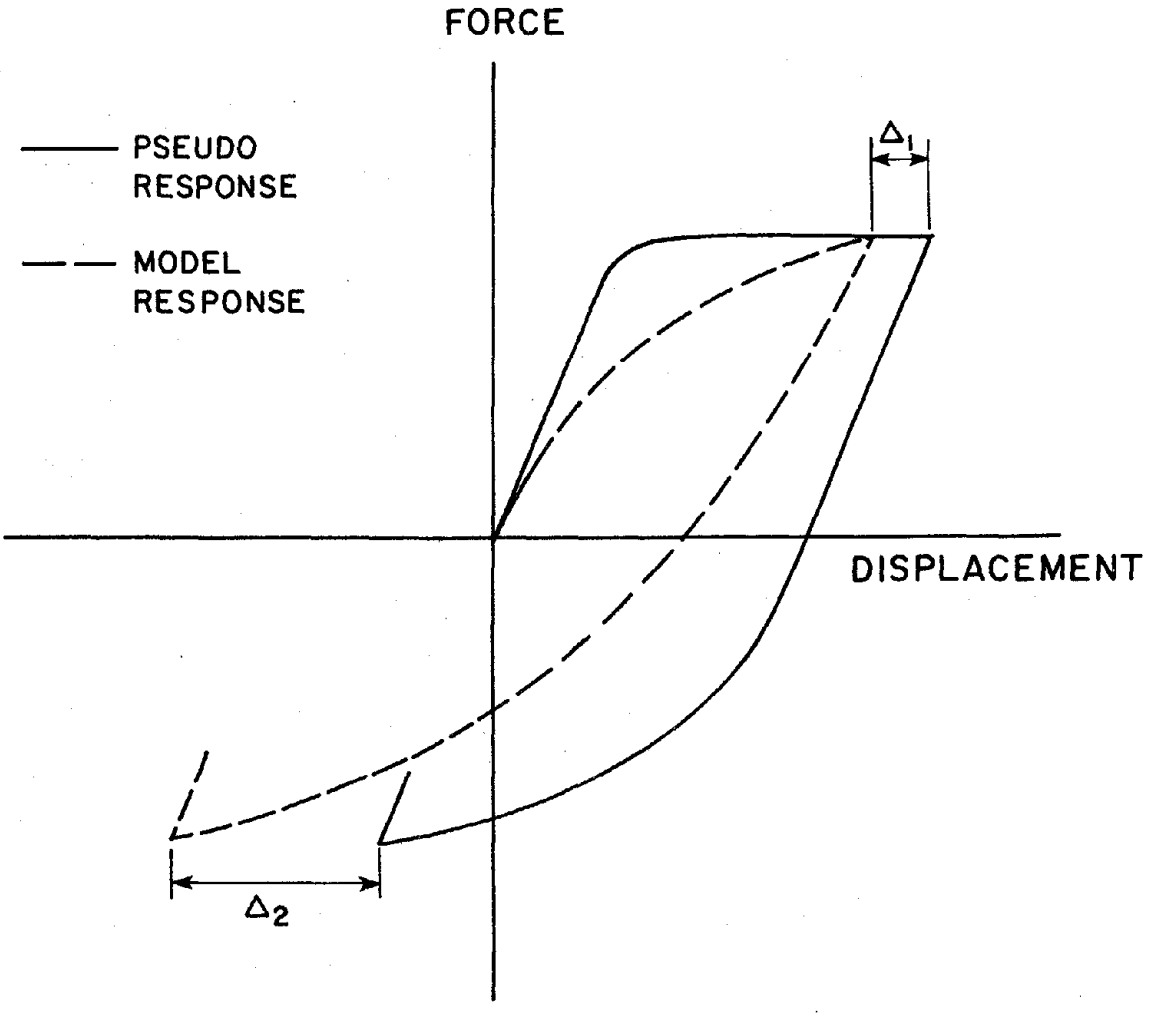

FIG. 3.2 IDEALIZED STRUCTURE AND MODEL RESPONSES EXPLAINING THE OFFSET IN DISPLACEMENT RESPONSE, EL CENTRO SPAN 950

same P but the predicted behavior displays a displacement smaller than the physical. This offset grows when the response changes direction as the structure still shows a little elastic-plastic behavior which is reflected in a slightly higher stiffness than the model. The maximum offset at the next reversal point is identified as Δ_2 in Fig. 3.2. This maximum offset then remains constant so that the subsequent predicted displacement time history matches the experimental except for this constant offset.

The model would be improved if the material were characterized by two sets of parameters, one for the elastic-plastic and one for the work hardening behavior; it is evident that the Ramberg-Osgood material model is incapable of reproducing an elastic-plastic behavior.

In spite of the minor deficiency of the final model, we feel that the improvement which would be realized by using a different material model and two sets of parameters would not be worth the price of the complexity that would accompany it.

3.4 The Model Performance - El Centro Span 950

Because this was the excitation the model was constructed from, it was expected that predictions from it would be accurate - at least for the accelerations and, if ignoring the initial excursion into the inelastic range, also for the displacements. The parameters used were:

$$\left.\begin{array}{ll} M = 15.47 & \dfrac{\#\text{-sec}^2}{\text{in.}} \\ C = 3.671 & \dfrac{\#\text{-sec}}{\text{in.}} \\ K = 1787.7 & \#/\text{in.} \\ A = 0.0292 & \\ R = 5.462 & \end{array}\right] \quad \text{Parameters for T = 20.00 sec.}$$

and were kept constant throughout the excitation. The input signal of El Centro Span 950 is shown in Fig. 2.3 and the resulting calculated and measured (dashed line and solid line, respectively) acceleration and displacement time histories are shown in Figs. 3.3 and 3.4. The calculated hysteresis loops are shown in Fig. 3.5. By looking at Figs. 3.3 and 3.5 we see that the acceleration response is very well predicted by the model and that the main discrepancies occur in the time interval 2.0 - 4.0 sec. or in the same interval that the elastic-plastic behavior is encountered. The displacement, on the other hand, is well matched until the 3 sec. mark where in a matter of four seconds we get a difference between the model and the structure response which from then on seems to remain constant. This, of course, is due to the elastic-plastic behavior of the structure at about the time t = 3.0 sec. which our analysis predicts. To compare the two responses, acceleration and displacement, two error functions are evaluated throughout the time history. They have the forms:

$$E^{A}(\bar{\beta},T_N) = \sum_{i=1}^{N} (\ddot{v}_i(\bar{\beta},t) - \ddot{u}_i(t))^2 \qquad (3.6.a)$$

$$E^{D}(\bar{\beta},T_N) = \sum_{i=1}^{N} (v_i(\bar{\beta},t) - u_i(t))^2 \qquad (3.6.b)$$

for the acceleration and displacement, respectively. The variables are the same as in the criterion function, Eq. (3.5). The acceleration error function, Eq. (3.6.a) is the same as the minimized criterion function, Eq. (3.5). To see how the error functions behave, they are plotted against time and and shown in Figs. 3.6 and 3.7. It is clearly seen that 50% of the acceleration error is accumulated in the time interval 2 to 4 sec. and about 60% in the time interval 2 to 5 sec. The displacement error deviates from zero at about t = 3.0 sec.

and after t = 3.5 sec. it changes linearly with time, meaning that the error remains constant. This means that the displacement pattern is correct, but there is an offset following the 3.5 sec. mark.

The last thing that we compare are the hysteretic behaviors, experimental and predicted. The most obvious difference is that the loops from experimental data (using Eq. (2.1)) are irregular and somewhat jagged, whereas those from the Ramberg-Osgood formulation are, of course, smooth.

Our explanation of the jaggedness of the experimental loops is only tentative. First, these we term pseudo-hysteresis loops in that they reflect not only the material restoring force, which true loops account for, but also the viscous damping which could fluctuate during a reversal causing some roughness. Noise in the data recorded by the accelerometers, which remains unknown, also could, and no doubt does, account for some.

We note, without comment, that most of the raggedness appears to begin with the beginning of work hardening of the material and continues throughout this domain.

The second difference between the two sets of loops is that illustrated by Fig. 3.2 which has been explained already.

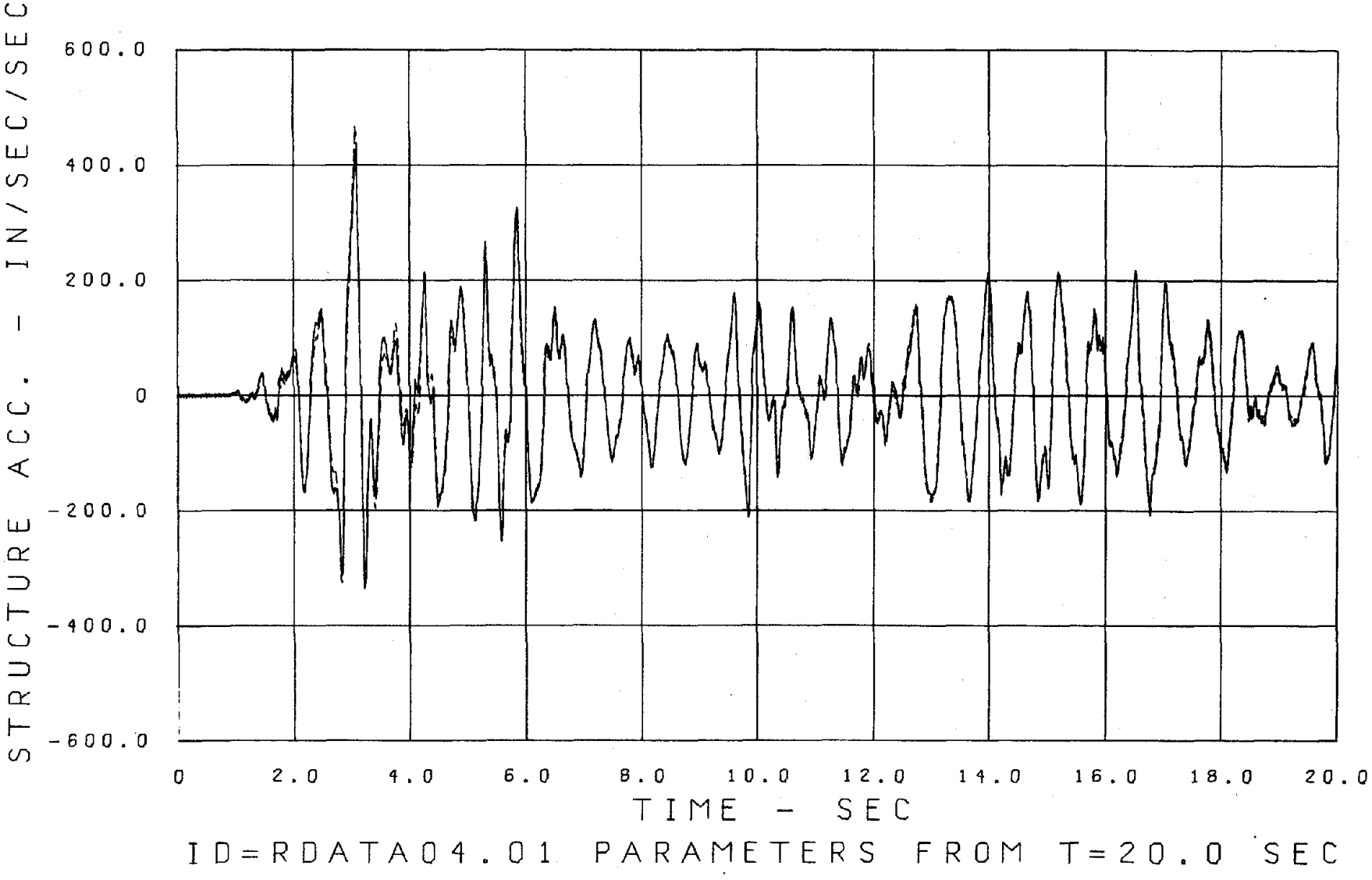

Fig. 3.3. COMPARISON OF MEASURED AND COMPUTED ACCELERATION RESPONSE TIME HISTORIES, EL CENTRO SPAN 950.

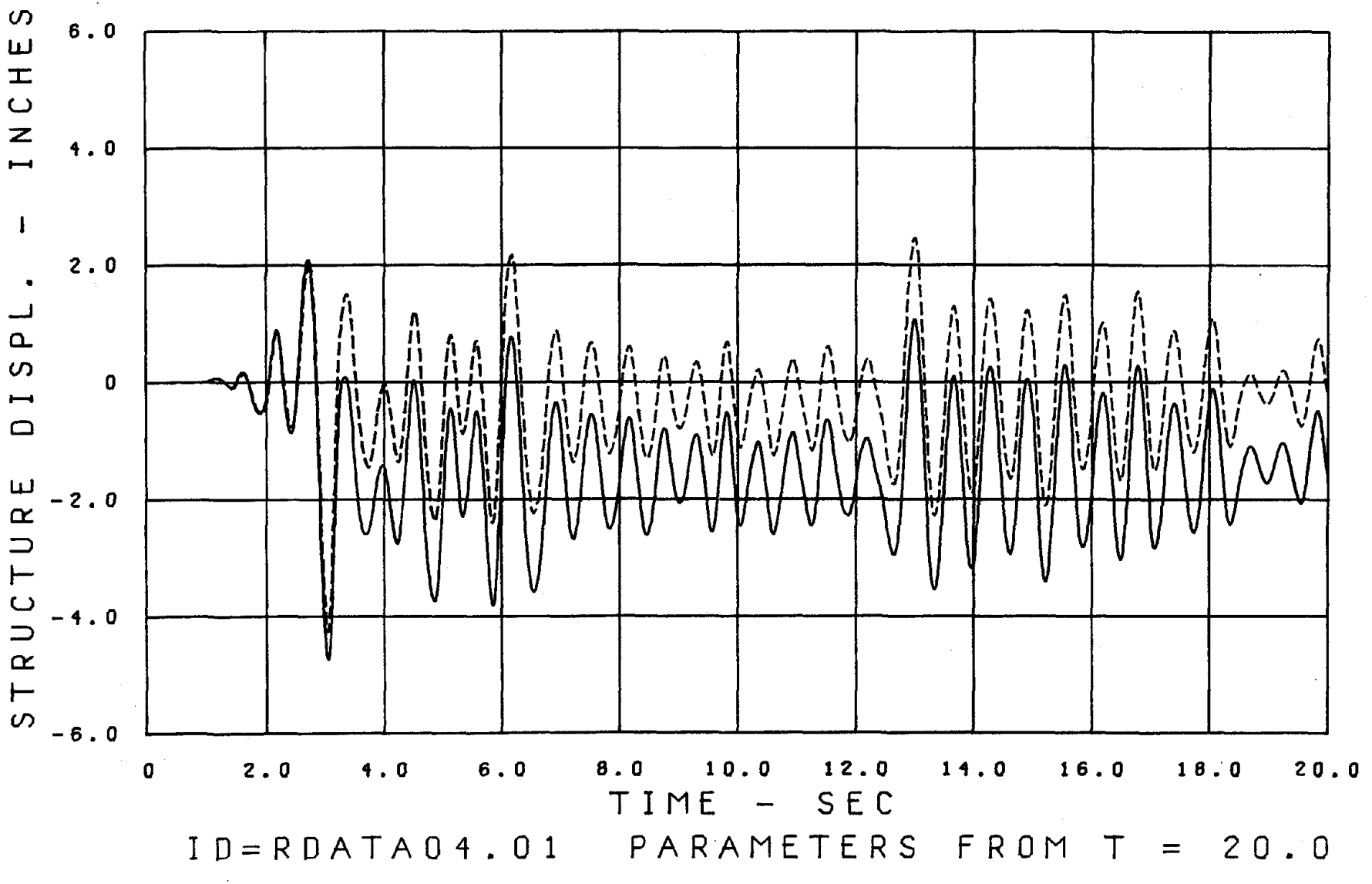

Fig. 3.4. COMPARISON OF MEASURED AND COMPUTED DISPLACEMENT RESPONSE TIME HISTORIED, EL CENTRO SPAN 950.

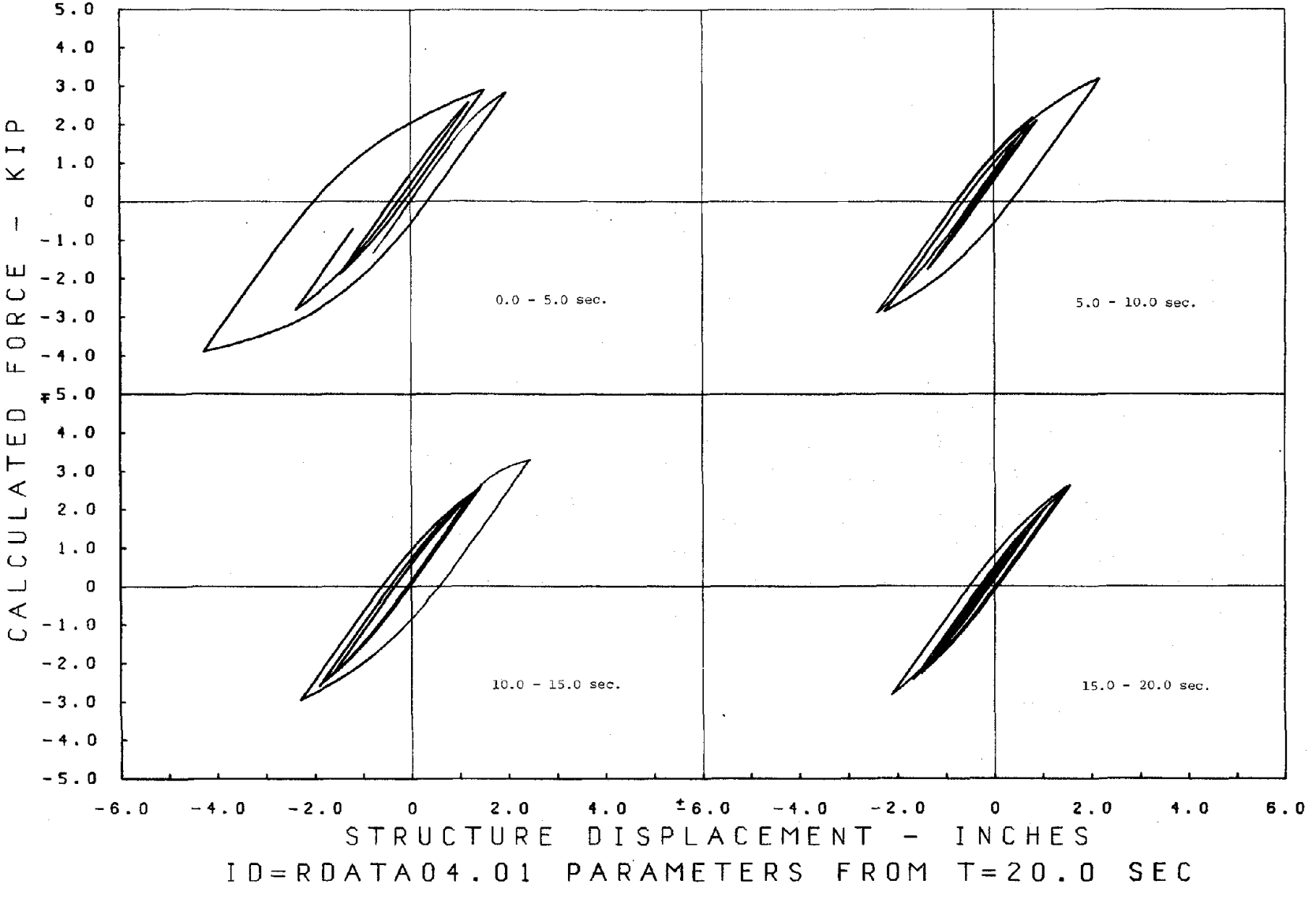

Fig. 3.5. COMPUTED HYSTERETIC LOOPS, EL CENTRO SPAN 950.

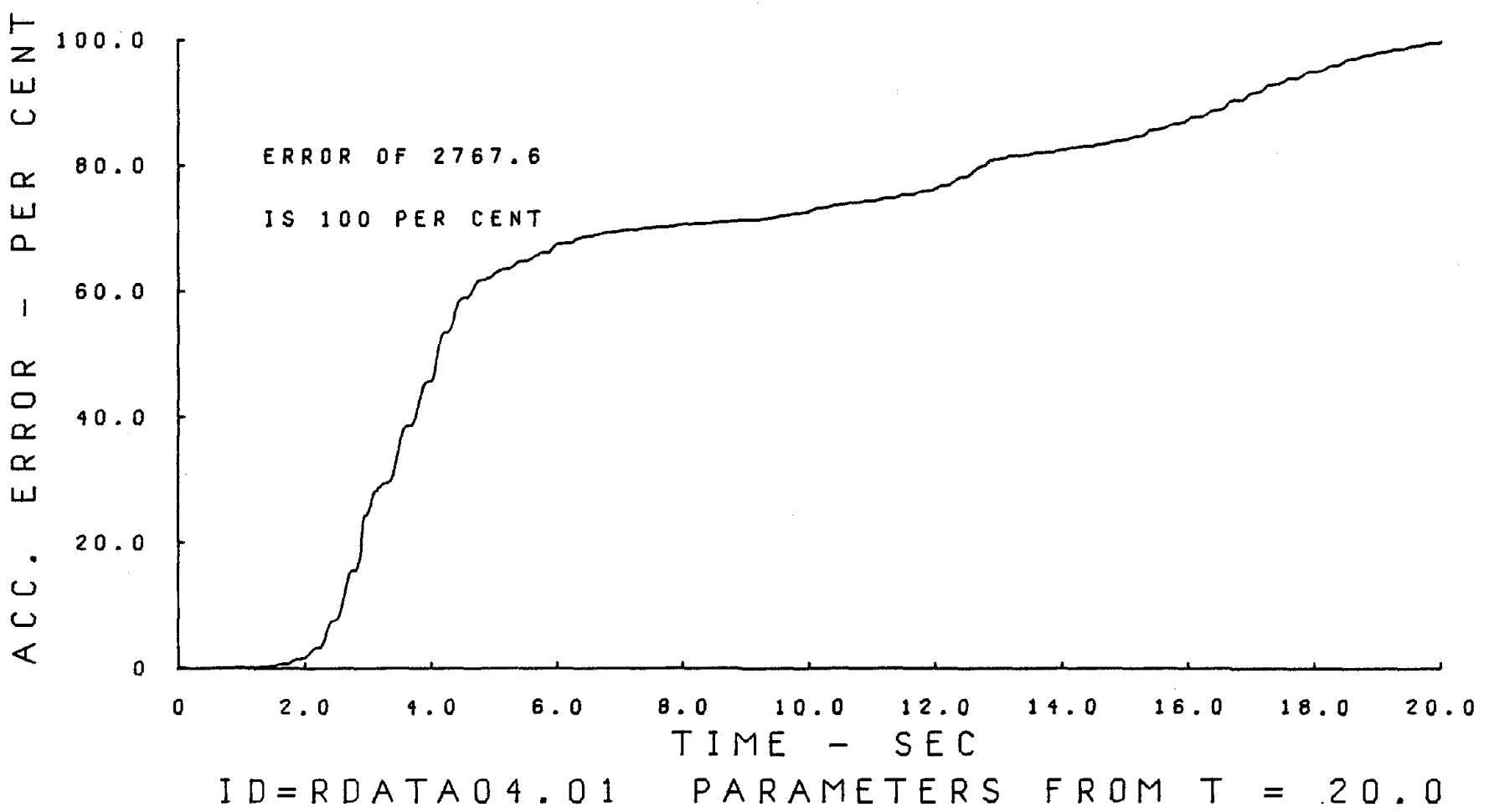

Fig. 3.6. ACCELERATION ERROR TIME HISTORY, EL CENTRO SPAN 950.

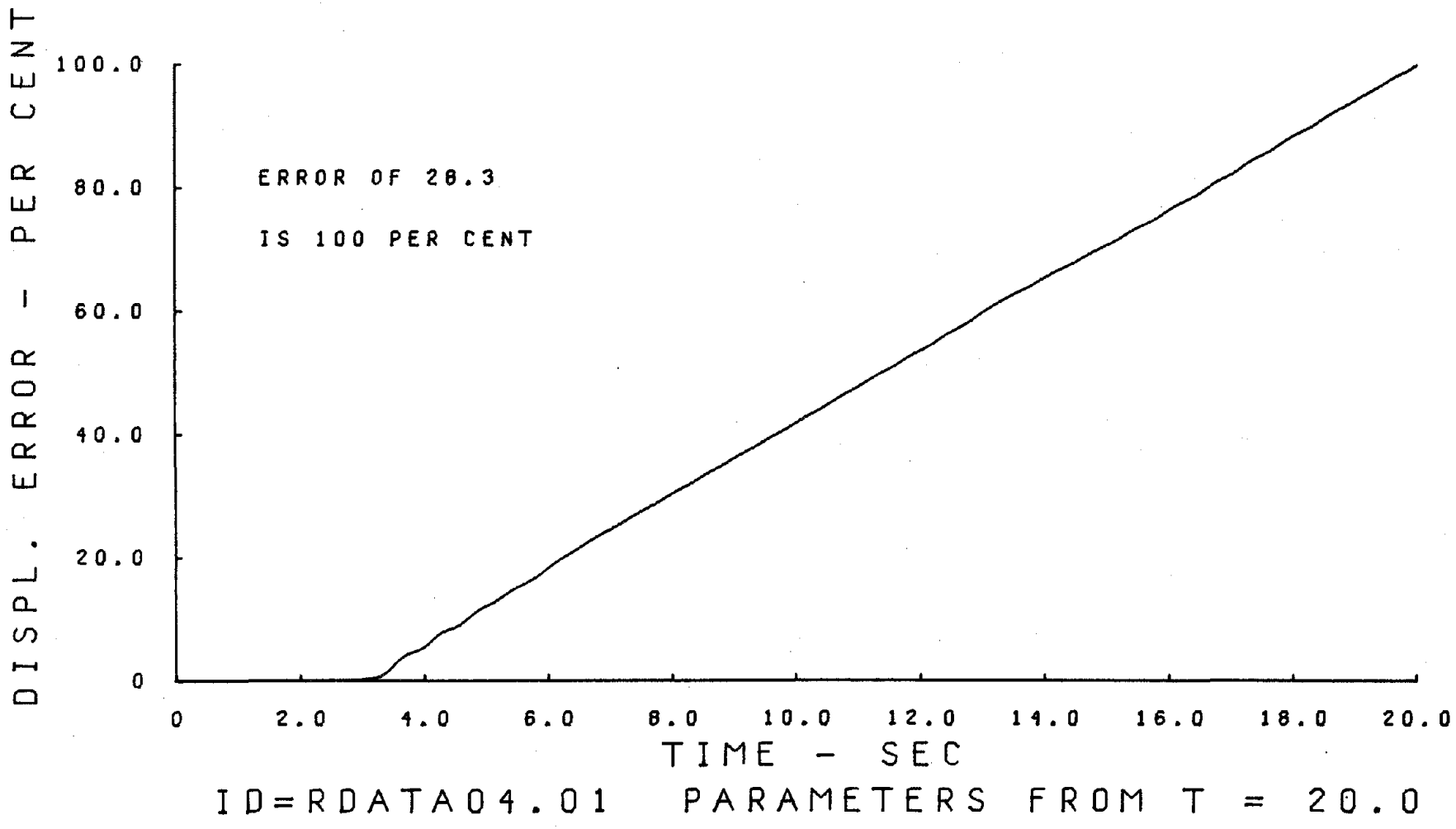

Fig. 3.7. DISPLACEMENT ERROR TIME HISTORY, EL CENTRO SPAN 950.

4. ASSESSMENT OF THE MODEL

We now have a complete nonlinear model of a one-story steel frame. Having constructed the model (Chapter 3) using a particular excitation, we now wish to ascertain how well the model can predict the response of the same structure to other excitations. It is in this sense that we make our assessment.

4.1 Test Series B - Pacoima Span 950

The model obtained in Section 3.3 for the full duration of motion has the parameters:

$$M = 15.47 \quad \frac{\#\text{-sec}^2}{\text{in.}}$$

$$C = 3.671 \quad \frac{\#\text{-sec.}}{\text{in.}}$$

$$K = 1787.7 \quad \#/\text{in.}$$

$$A = 0.0292$$

$$R = 5.462$$

This model is now subjected to the measured table acceleration of Pacoima Span 750, shown in Fig. 2.7. The duration of table motion is only about 13.3 sec. (counted from zero time), whereas the response is calculated for full 18.0 sec. The calculated and measured (dashed and solid lines, respectively) acceleration and displacement time histories, calculated hysteretic loops and the error time histories are shown in Figs. 4.1 to 4.5.

We see that the model predicts the acceleration response accurately for the full duration of motion. The free vibration phase between times t = 13.3 to t = 18.0 sec. shows matching amplitudes, but the calculated response oscillates with a shorter period than the measured free vibra-

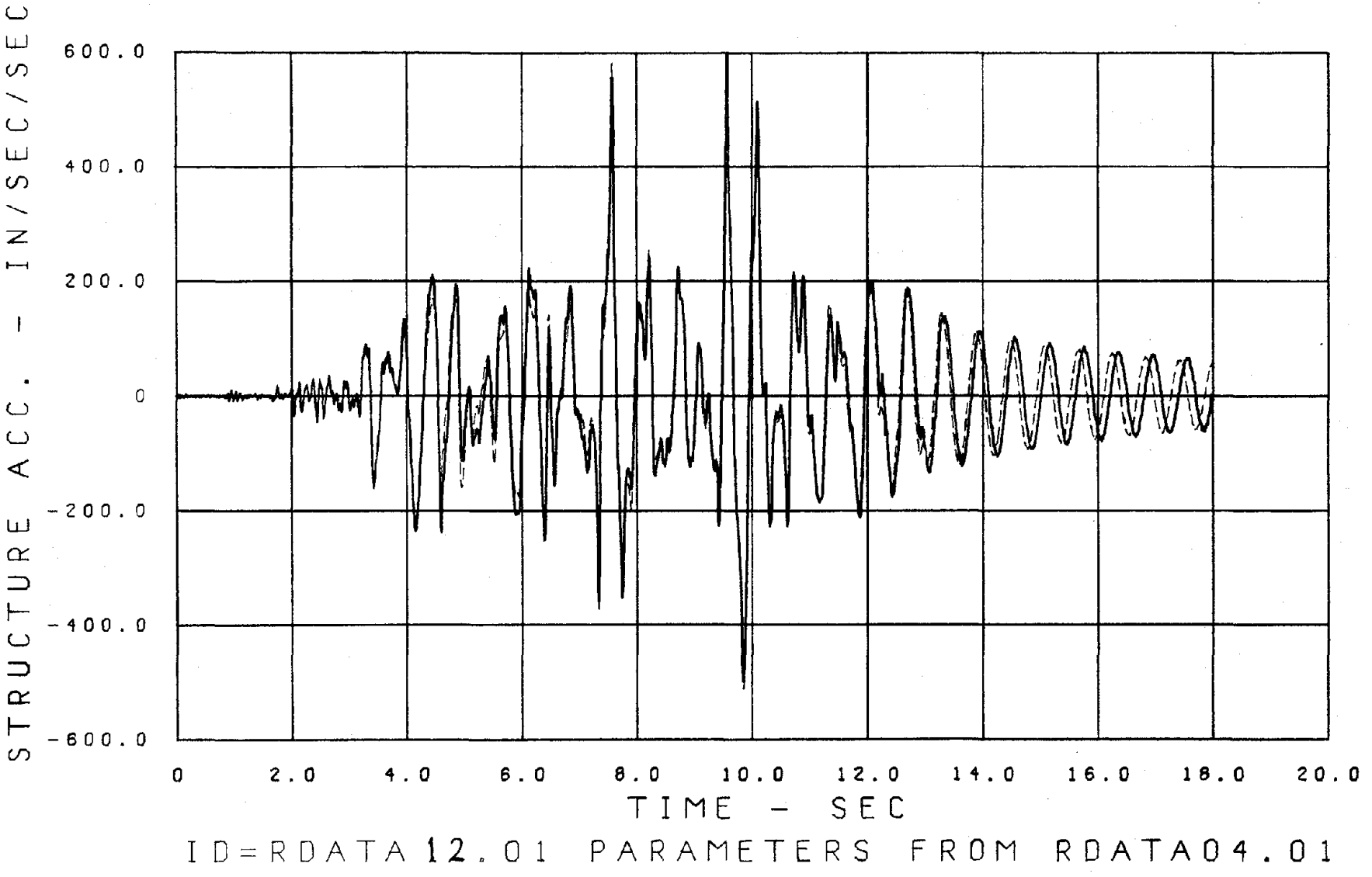

Fig. 4.1. COMPARISON OF MEASURED AND COMPUTED ACCELERATION RESPONSE TIME HISTORIES, PACOIMA SPAN 750.

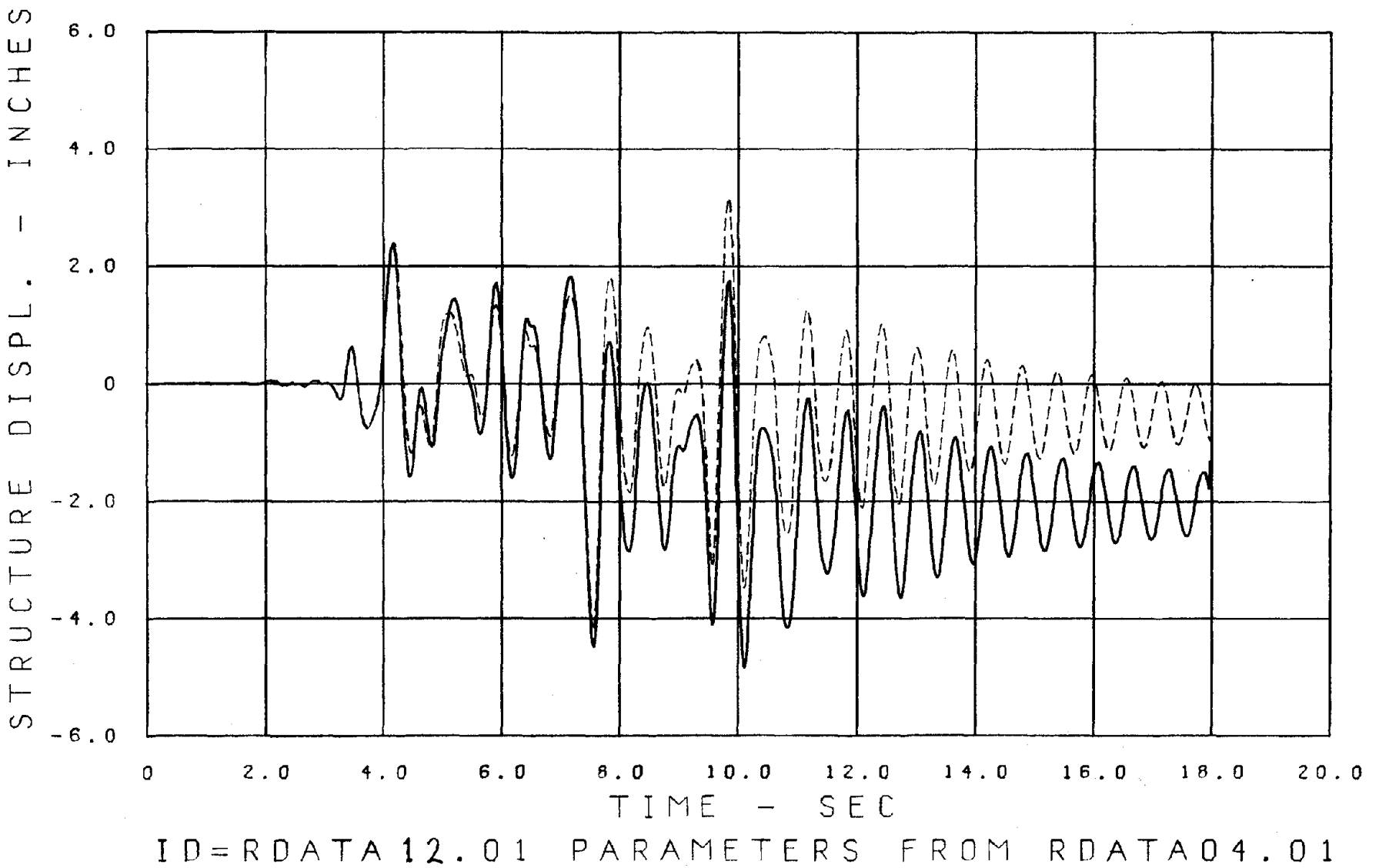

Fig. 4.2. COMPARISON OF MEASURED AND COMPUTED DISPLACEMENT RESPONSE TIME HISTORIES, PACOIMA SPAN 750.

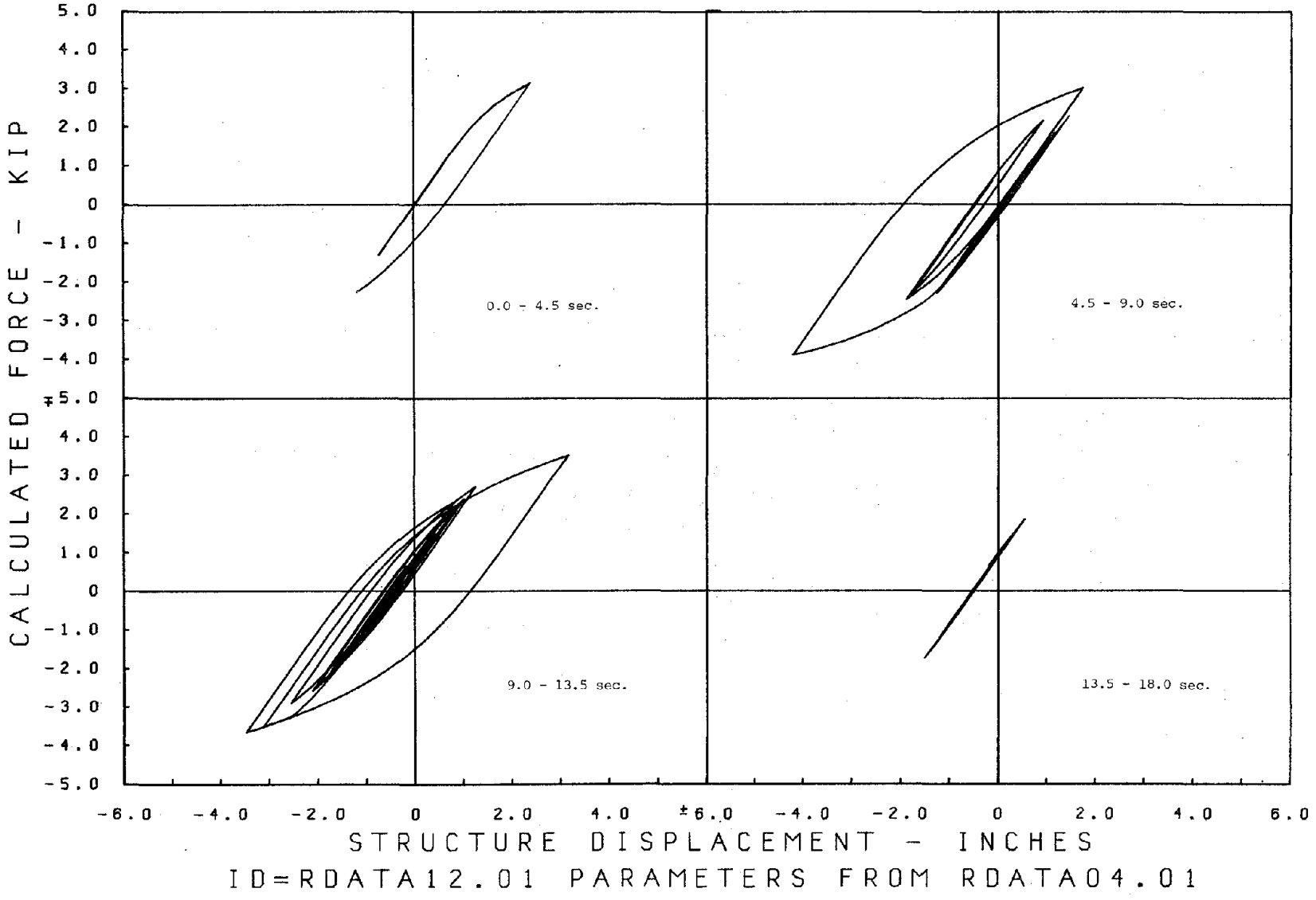

Fig. 4.3. COMPUTED HYSTERETIC LOOPS, PACOIMA SPAN 750.

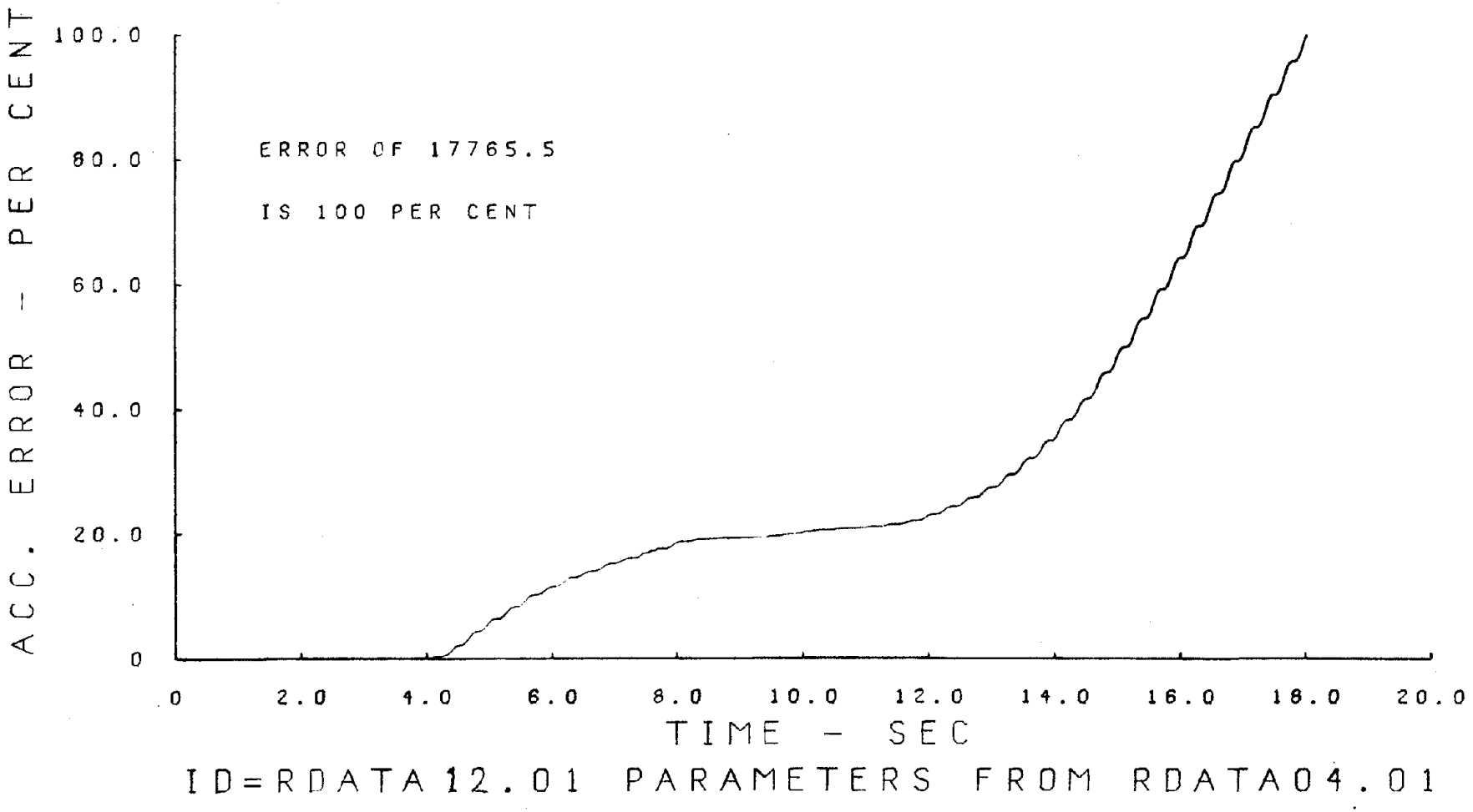

Fig. 4.4. ACCELERATION ERROR TIME HISTORY, PACOIMA SPAN 750.

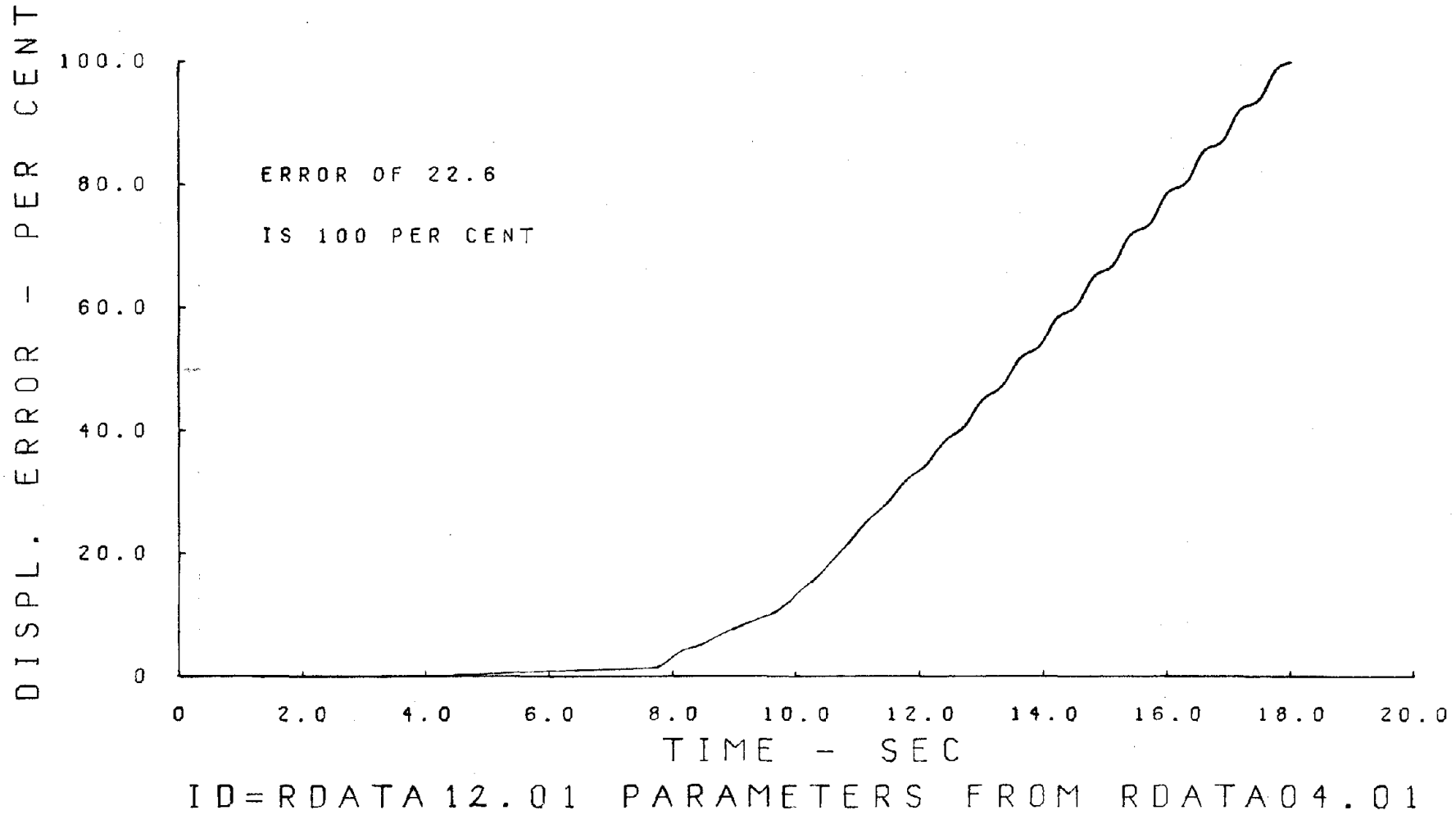

Fig. 4.5. DISPLACEMENT ERROR TIME HISTORY, PACOIMA SPAN 750.

tions of the structure. This is understood when we look at Tables 2.1 and 2.2. From the stiffness values in the tables we see that the real structure of Test Series A is a little stiffer than the structure of Test Series B, which also reflects directly on the free vibrations of the model. From the acceleration error time history we see that about 70% of the total accumulated error comes from the free vibration phase (13.3 - 18 sec.). From the displacement time history we see that the first inelastic excursion occurs at about the 4.1 sec. mark, but it is a small one and causes only minor discrepancies between the structure and model responses. The first major excursion comes at about the 7.5 sec. mark and causes a larger permanent offset. From 7.5 sec. on the model predicts the response well except for the offset. The shape of the model response is the same as the response of the structure. In the free vibration phase (13.3 - 18 sec.) we again see the difference in period between structure and model. This difference is what causes the oscillatory type of behavior in the displacement error curve.

The calculated hysteresis loops of Fig. 4.3 differ from the pseudo-hysteresis loops for reasons given at the end of Chapter 3 for Test Series A.

4.2 Test Series C - Taft Span 950

The model is now subjected to the Taft Span 950 excitation whose acceleration time history is shown in Fig. 2.11. The duration of this motion is 20.0 sec. (actually a little more, but this is what is considered here) or the same duration for which the response is calculated. Accordingly we do not have any free vibration phase included after the shaking has ceased. This, combined with the fact that shaking was not intense enough to cause serious inelastic excursions, leads us to expect

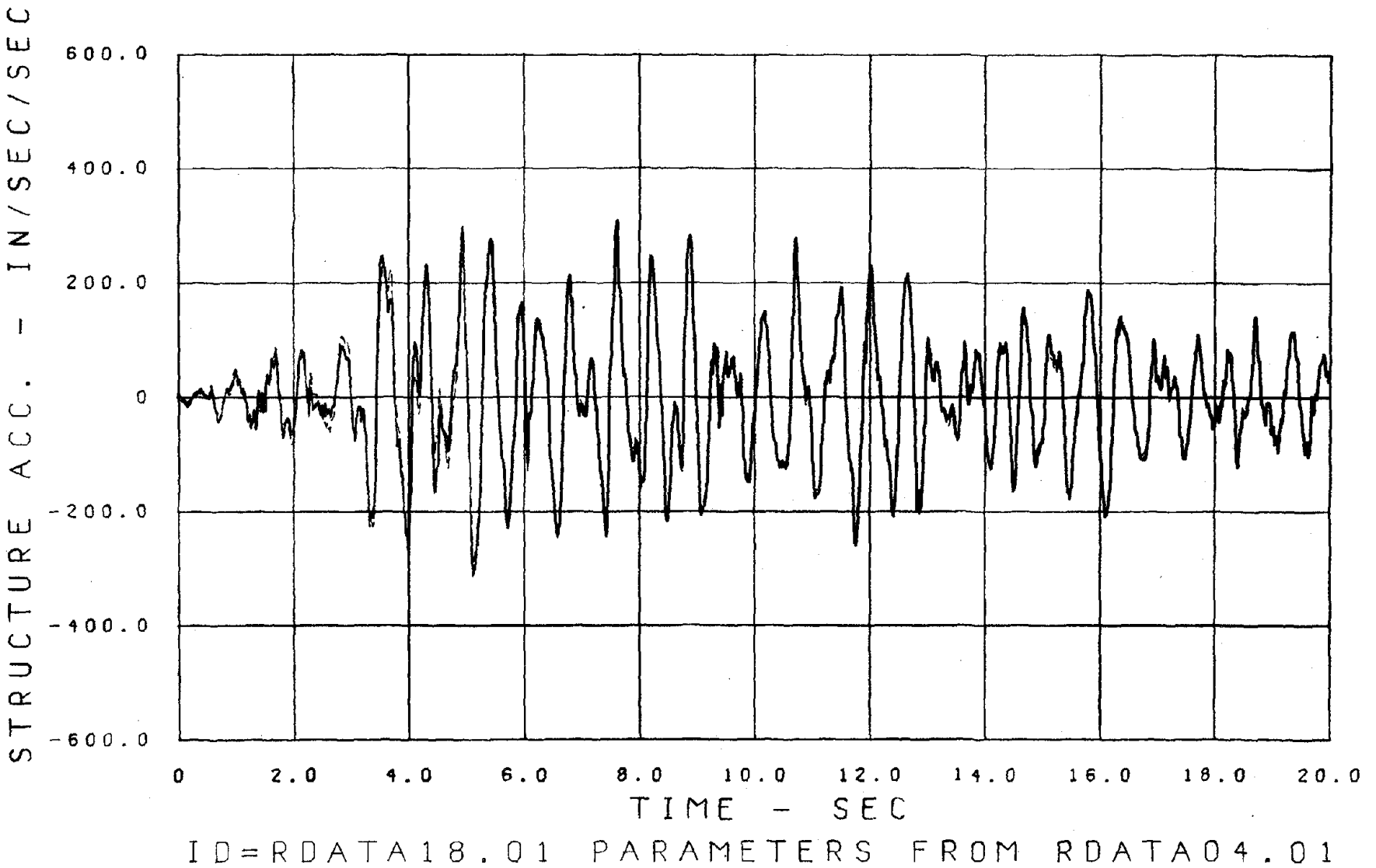

Fig. 4.6. COMPARISON OF MEASURED AND COMPUTED ACCELERATION RESPONSE TIME HISTORIES, TAFT SPAN 950.

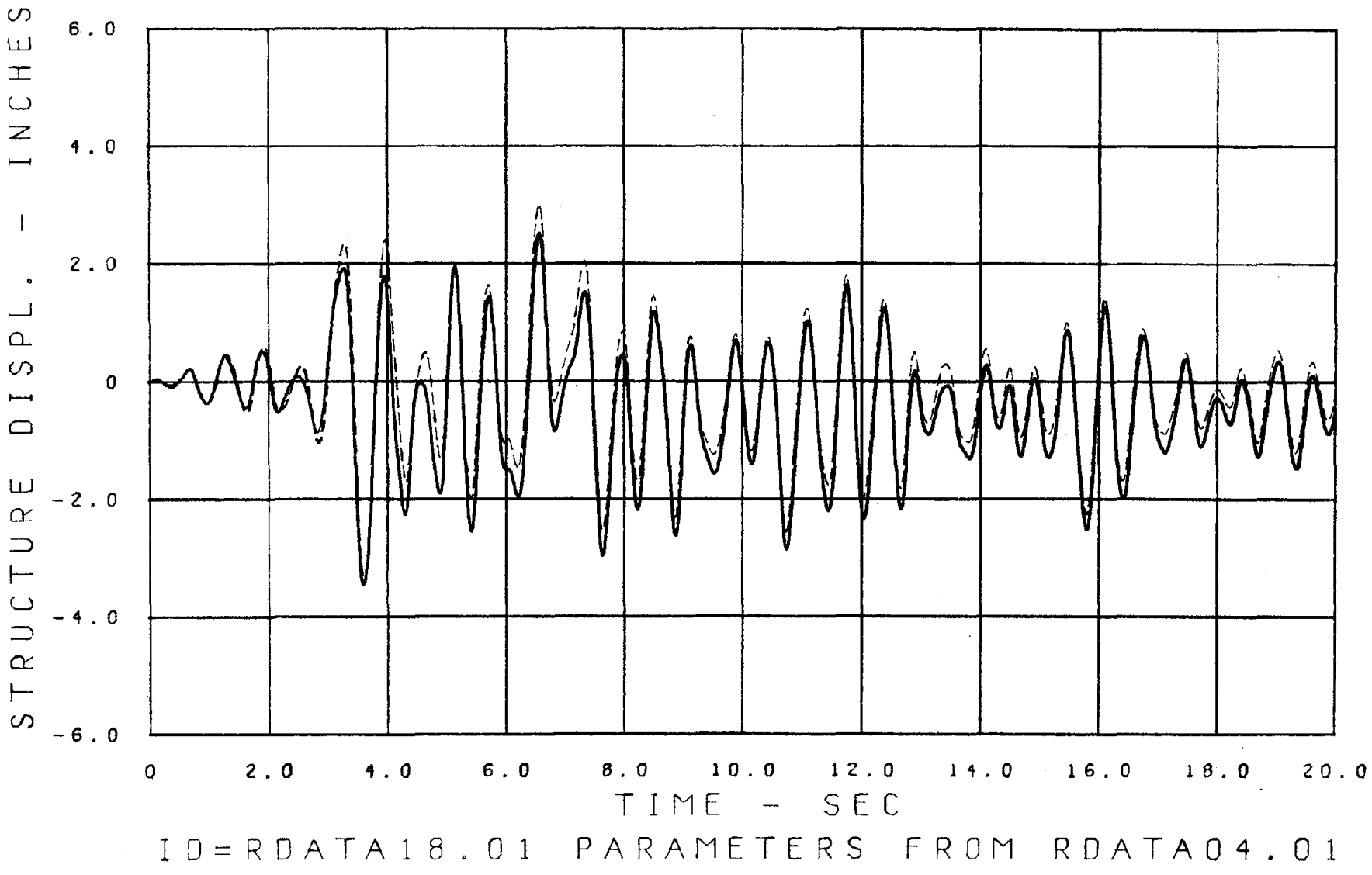

Fig. 4.7. COMPARISON OF MEASURED AND COMPUTED DISPLACEMENT RESPONSE TIME HISTORIES, TAFT SPAN 950.

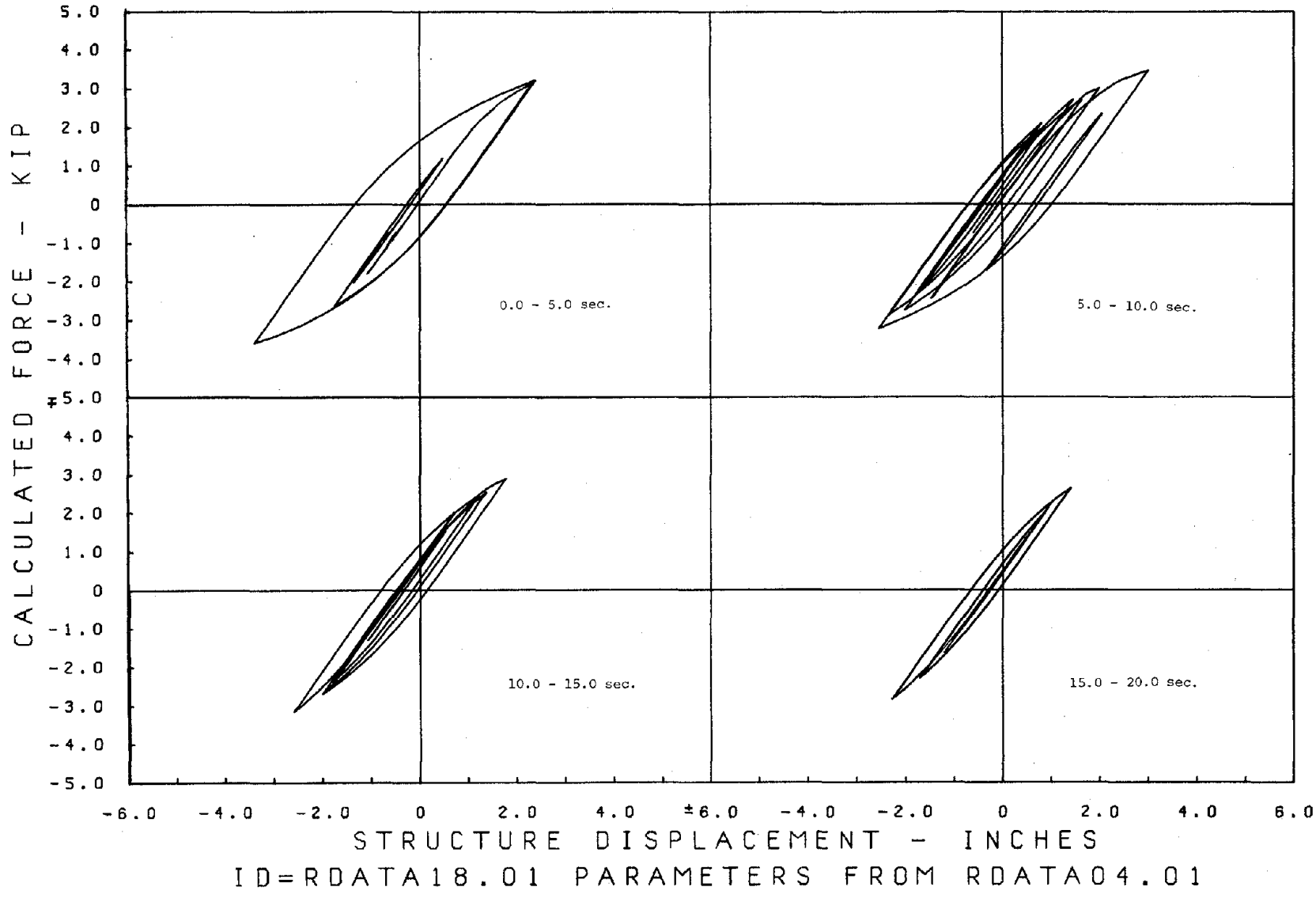

Fig. 4.8. COMPUTED HYSTERETIC LOOPS, TAFT SPAN 950.

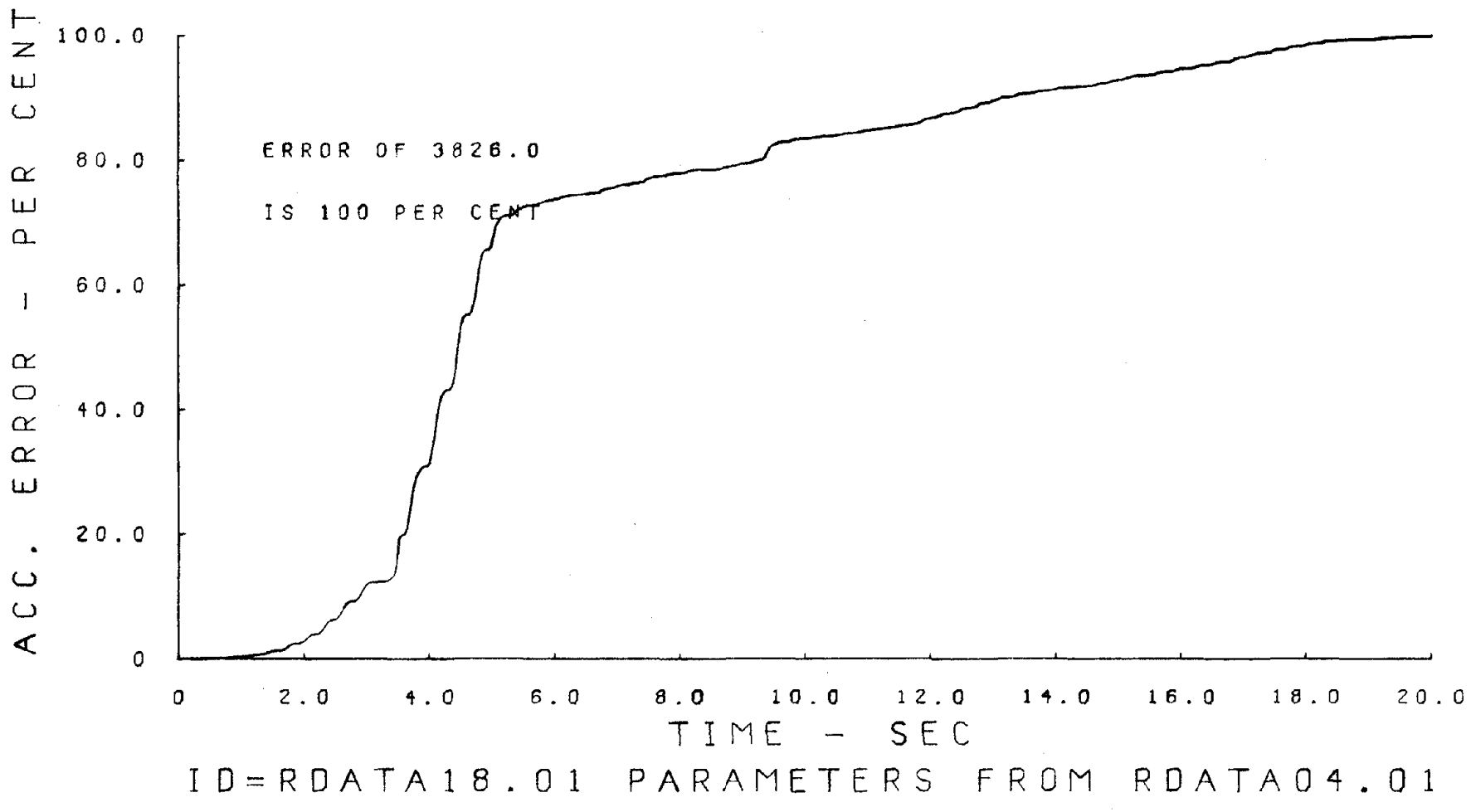

Fig. 4.9. ACCELERATION ERROR TIME HISTORY, TAFT SPAN 950.

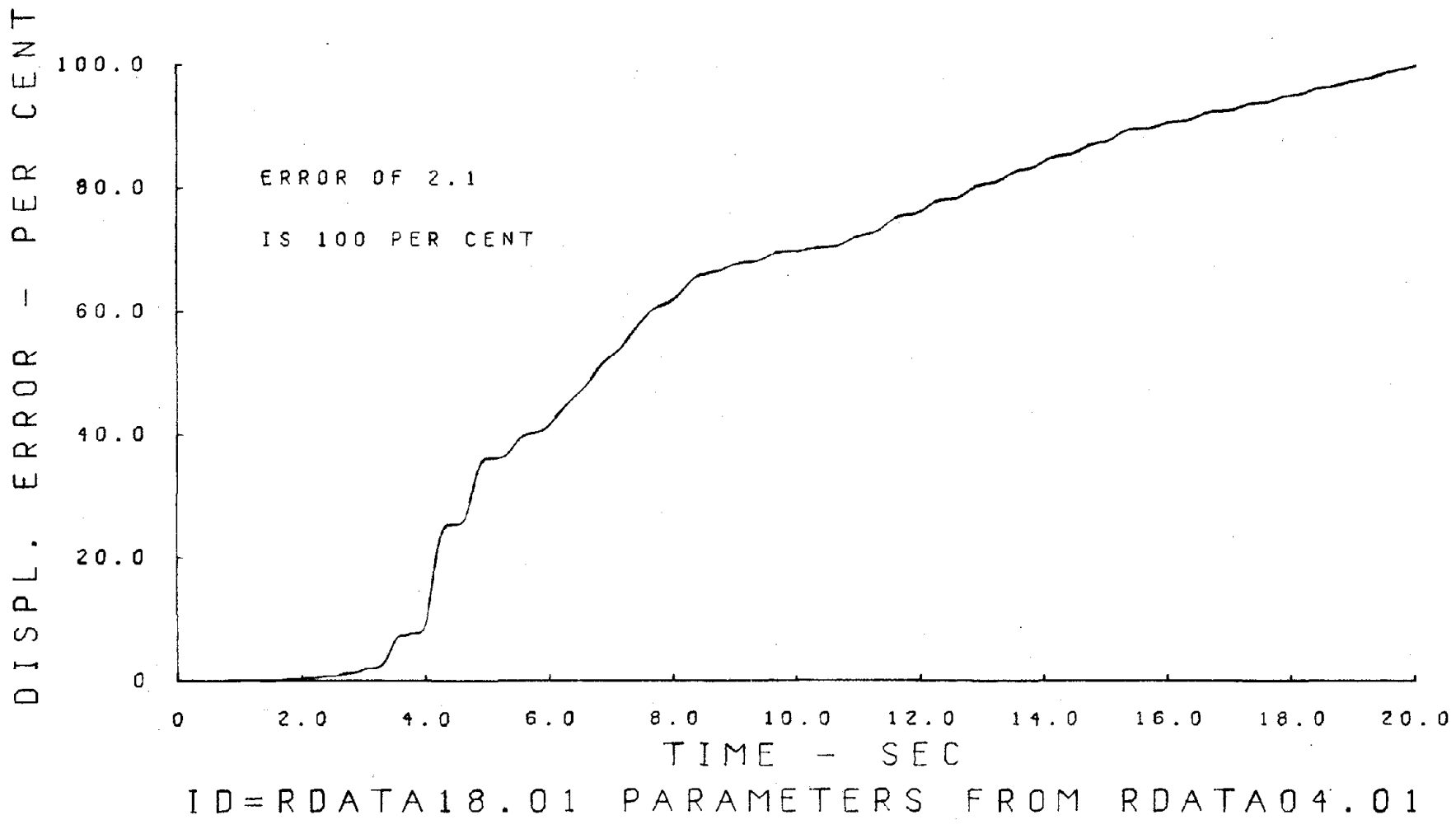

Fig. 4.10. DISPLACEMENT ERROR TIME HISTORY, TAFT SPAN 950.

good reproduction of the structure response. The results are shown in Figs. 4.6 to 4.10. As can be seen, the accelerations are reproduced very well - the major discrepancy coming about the time of first yield, 3.25 sec., but well accounted for by the model. This can also be seen from the error time history of Fig. 4.9. The displacements are more accurately reproduced by the model for this excitation than for the El Centro and Pacoima excitations. The reason is because of the lack of a major inelastic excursion. The error function of the displacements shows this also clearly, as the error now obtained is only about 7.5% of the error obtained for Test Series A from which the model was identified. This is also reflected in a fairly good matching of the hysteresis loops of Fig. 4.8 and the pseudo loops of Fig. 2.12.

4.3 Test Series D - Parkfield Span 1000

Lastly, the model is subjected to the Parkfield Earthquake Span 1000, whose acceleration time history is shown in Fig. 2.15. The duration of this motion is 15.5 sec., but the strong motion is mainly between the times 2.0 sec. and 5.0 sec. The calculated and measured (dashed and solid lines, respectively) acceleration and displacement time histories are plotted in Figs. 4.11 and 4.12. The calculated hysteresis loops are shown in Fig. 4.13 and the error functions in Figs. 4.14 and 4.15. As can be seen from the calculated and the pseudo-hysteresis loops, the response is purely elastic about the permanent displacement of about 0.6 in. after the time t = 5.0 in. This low amplitude response is therefore characterized by the natural frequency of the structure which, as can be seen from Table 2.4, is different from the "natural frequency" of the model as it simulates best the properties of the structure of Table 2.1. This is what causes the calculated response to have a shorter

period of vibration, seen in Figs. 4.11 and 4.12. Ignoring this, the model reproduces the acceleration time history well and the displacement time history is also well matched for the final offset which is created at t = 4.6 sec. and is constant from there on as is reflected in the linear error function in Fig. 4.15. The raggedness of the line is due to the difference in natural frequency. The acceleration error plot of Fig. 4.14 also shows that the strong motion response is well matched. At t = 10.0 sec. only about 16% of the final error has been produced.

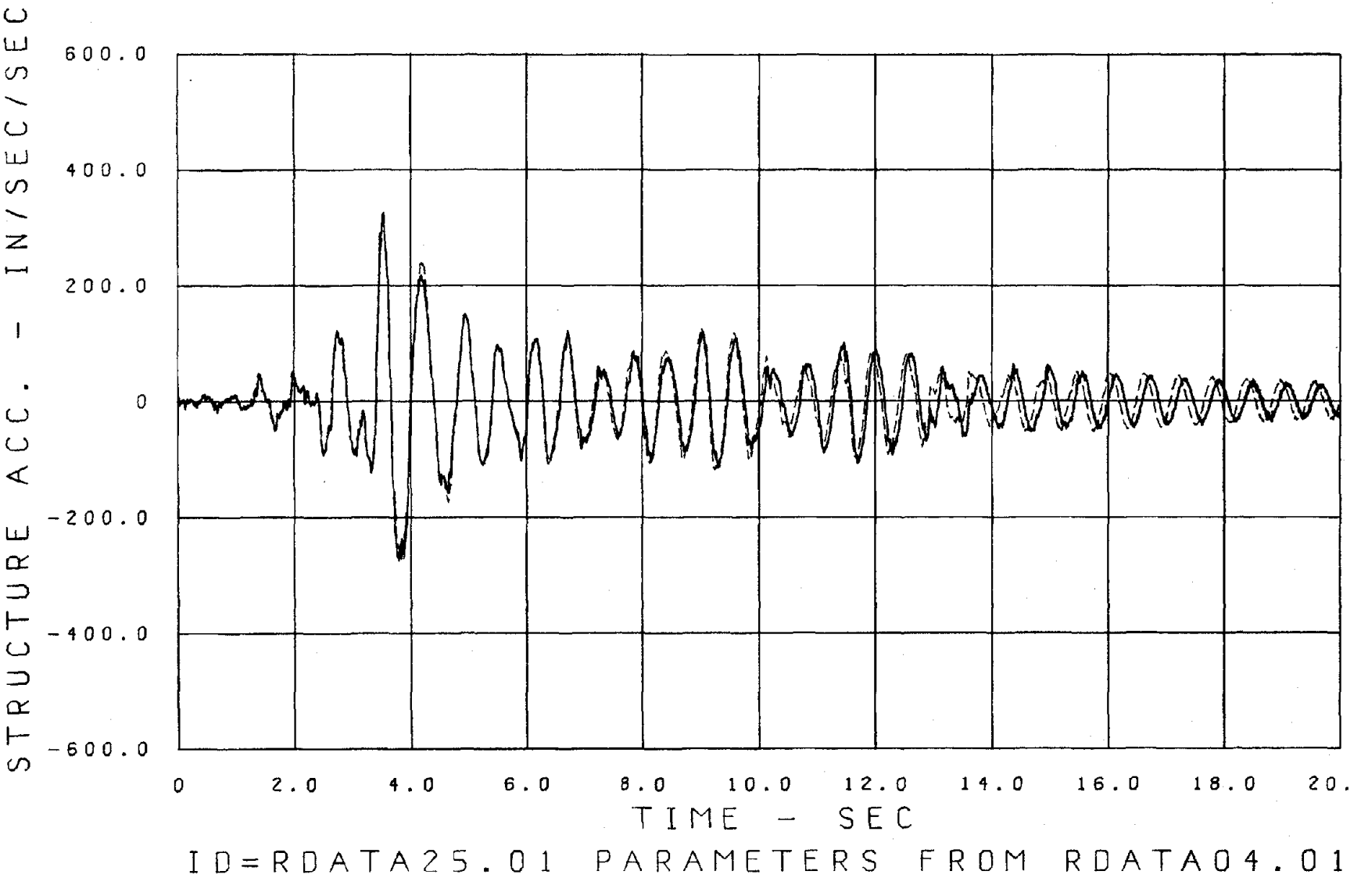

Fig. 4.11. COMPARISON OF MEASURED AND COMPUTED ACCELERATION RESPONSE TIME HISTORIES, PARKFIELD SPAN 1000.

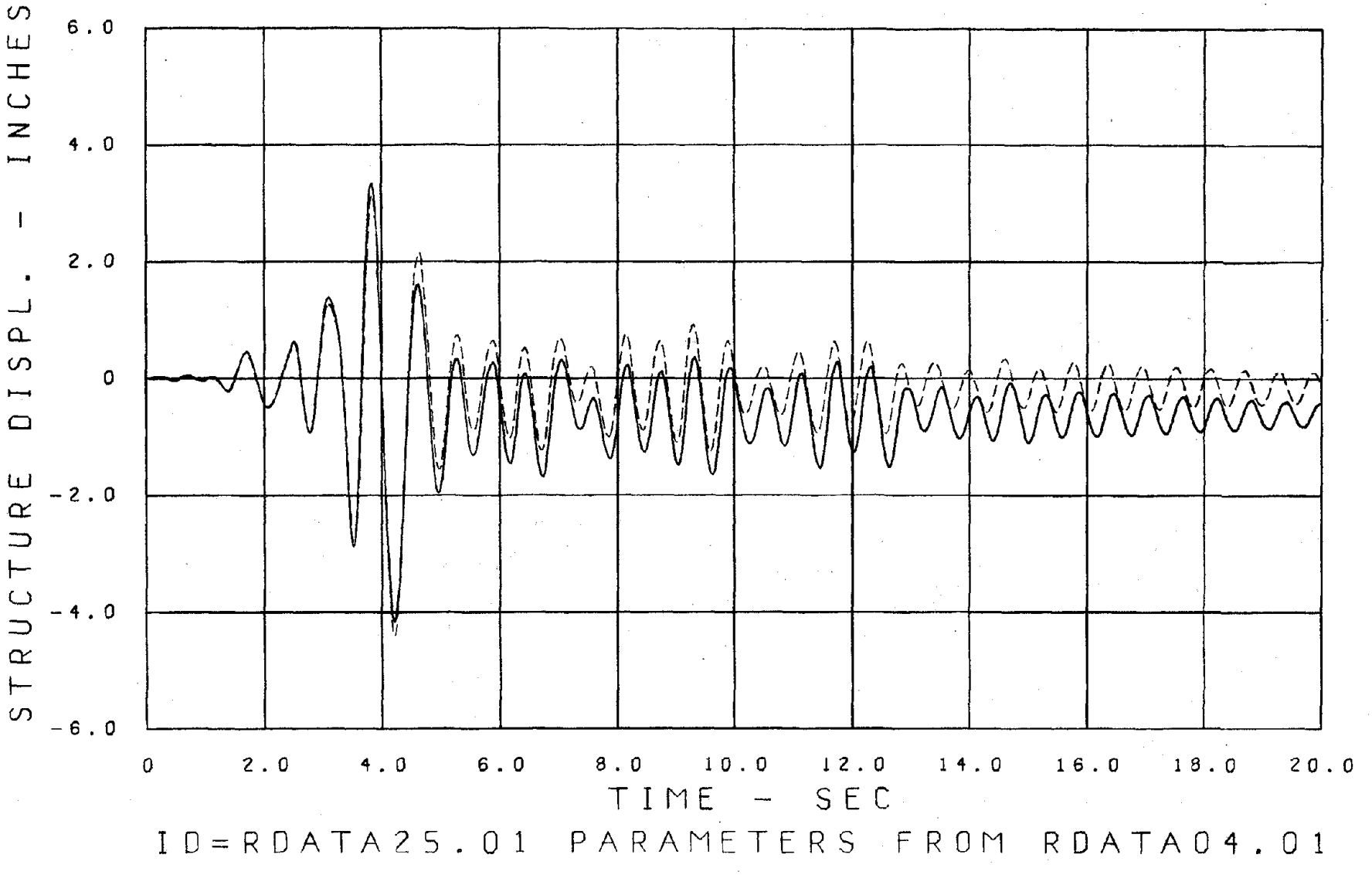

Fig. 4.12. COMPARISON OF MEASURED AND COMPUTED DISPLACEMENT RESPONSE TIME HISTORIES, PARKFIELD SPAN 1000.

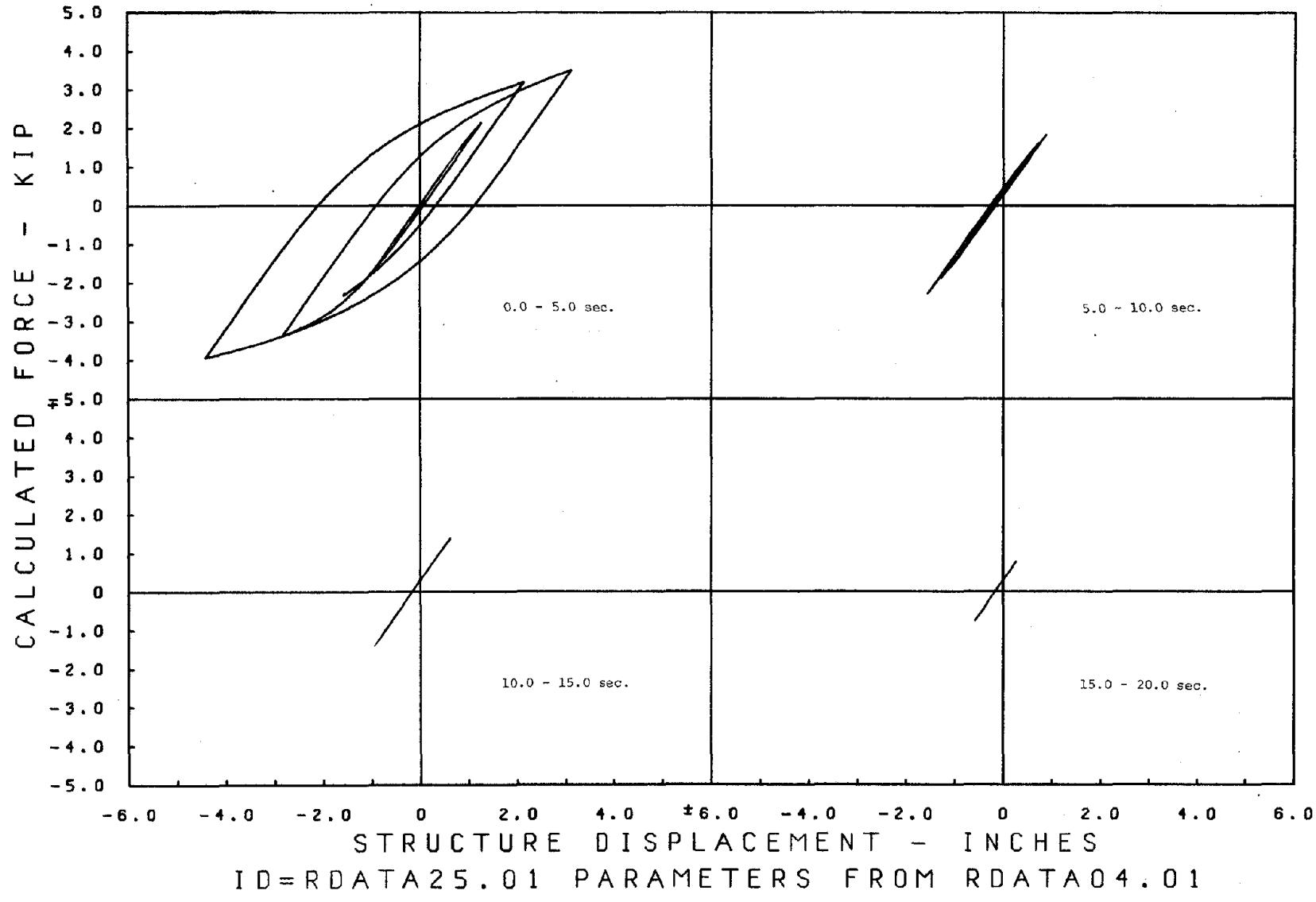

Fig. 4.13. COMPUTED HYSTERETIC LOOPS, PARKFIELD SPAN 1000.

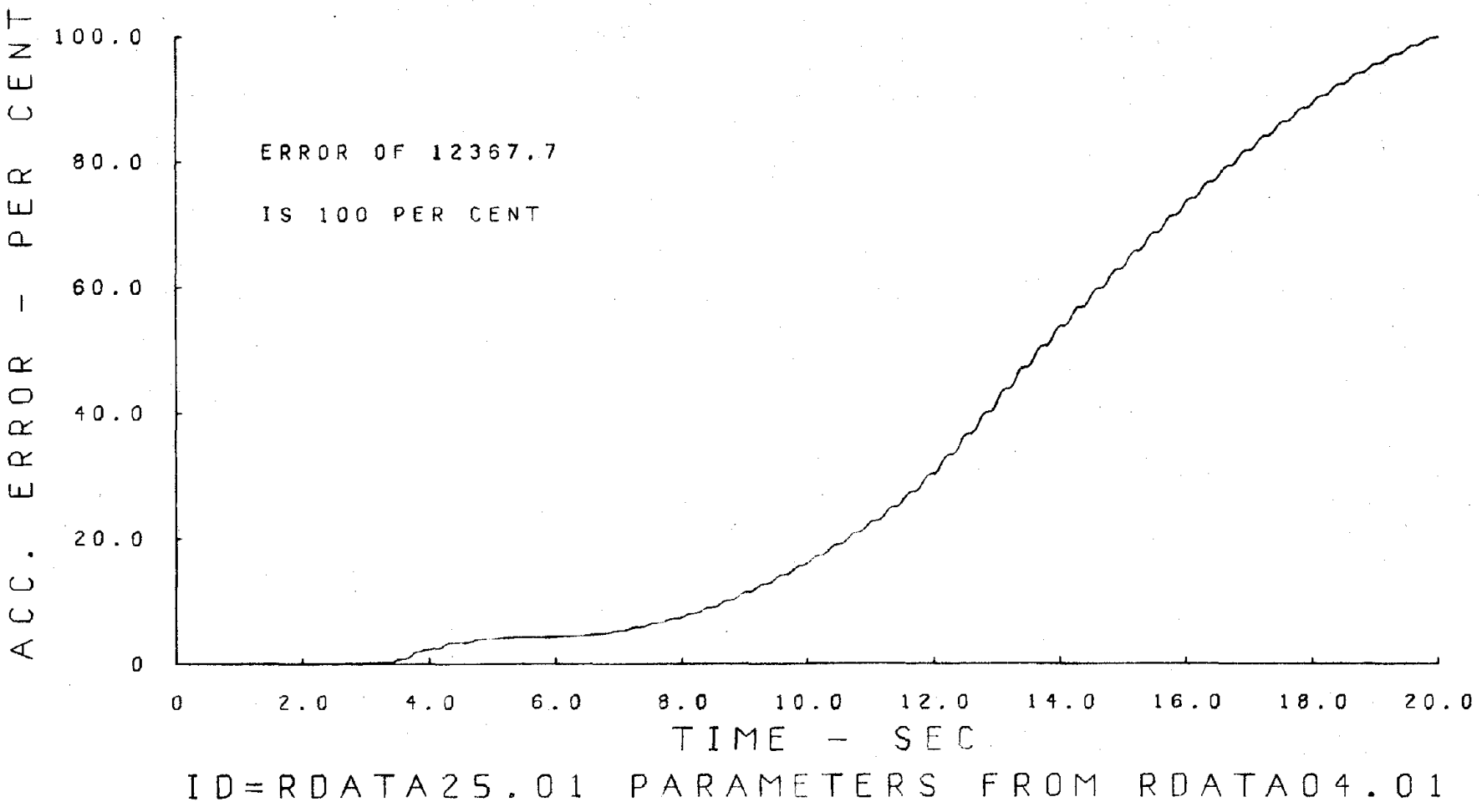

Fig. 4.14. ACCELERATION ERROR TIME HISTORY, PARKFIELD SPAN 1000.

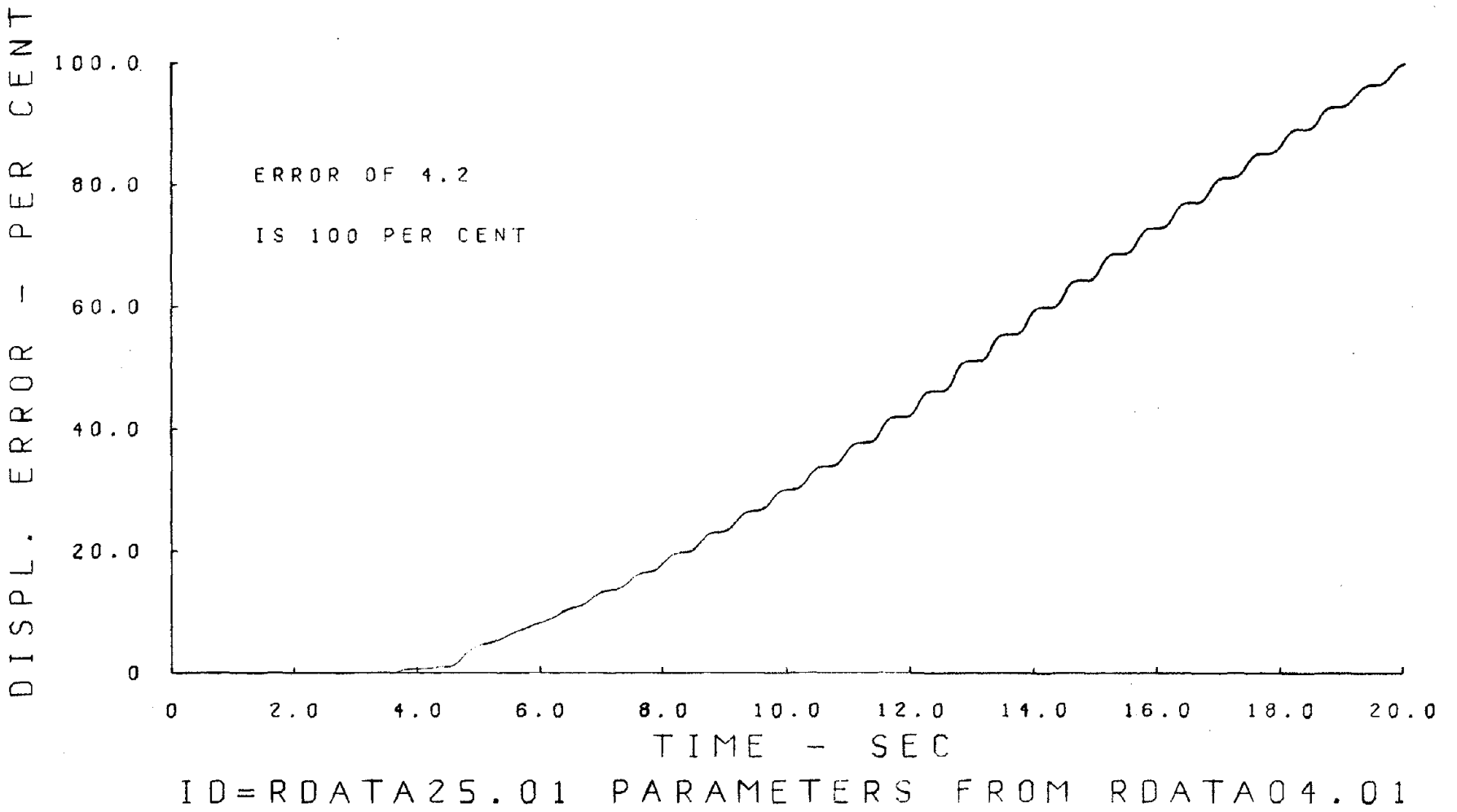

Fig. 4.15. DISPLACEMENT ERROR TIME HISTORY, PARKFIELD SPAN 1000.

5. CONCLUSIONS

Even though we follow with conclusions about the ways of improving the model, the major conclusion from the study is that the nonlinear model constructed from one earthquake excitation predicts the responses of a single-story steel frame to a variety of other earthquake excitations accurately, and as well as it does the responses used for its construction.

The acceleration response is much more accurately predicted by the model than the displacements. This is perhaps due to the fact that the accelerations and not the displacements were included in the criterion function, but much more likely due to the peculiar stress-strain behavior of mild steel and the inability of the Ramberg-Osgood model to predict elastic-plastic material behavior.

Mild structural steel, in the context of its stress-strain relationship, behaves as if it were two different materials when it is subjected to strains beyond the yield strain. During the first major excursion into the plastic zone the material behaves elasto-plastically, but subsequently it becomes a strain hardened material. The same dual properties are exhibited in the steel's global behavior, the load-displacement relationship, and are displayed in the shapes of the hysteretic loops exhibited in the body of the paper. Since the parameters of the model are derived from matching the hysteretic behavior, accurate matching for the whole duration of excitation can be attained only if the model is represented by the two sets of parameters. One set would be applicable to the response history up to the end of the first major excursion into the plastic zone, and the other set for all subsequent responses.

The form of the mathematical model also contributes to the inability of the model to predict the displacement response accurately for the full duration. The hysteretic cyclic behavior in our model is accommodated by the Ramberg-Osgood equations. These equations cannot reproduce an elastic-plastic behavior. The stress-strain (or load-displacement) relationships produced by these equations always exhibit some strain hardening. When the equations are asked to reproduce the elastic-plastic behavior of the first major excursion into the plastic zone, they cannot. The equations find a point on the hysteresis curve which matches the resisting force developed in the structure correctly, but at a smaller displacement than the actual. The model then rebounds following a slightly more curved path than the structure, resulting in an increase in the difference between the calculated and measured displacements at the next reversal point (Fig. 3.2). Thereafter the model predicts the shape of the displacement response quite well, but the offset, Δ_2, that originated from the first major inelastic excursion, continues to exist without change throughout the remainder of the predicted displacement response history.

The mathematical model would predict displacement time histories accurately if the Ramberg-Osgood material model were replaced by a bilinear one or, better still, a modified Menegotto and Pinto model[4] as used by Stanton and McNiven[5], and if the model incorporated two sets of parameters, each applicable to its own domain of strain behavior.

APPENDIX A: RAMBERG-OSGOOD MODEL

The hysteretic model used here is based on the Ramberg-Osgood equations:

$$x(P) = \frac{P}{K}\left(1 + A\left|\frac{P}{K}\right|^{R-1}\right) \tag{A1}$$

for skeletal curves, and

$$x(P) = x_{re} + \frac{P-P_{re}}{K}\left(1 + A\left|\frac{P-P_{re}}{2K}\right|^{R-1}\right) \tag{A2}$$

for branch curves. To complete the model a set of rules are established to specify the way in which branch curves are linked together to represent arbitrary loading patterns. These rules are based in part on four properties that can be derived from Eqs. (A1) and (A2). These properties, which are described in detail by Jennings (1963)[6], are given below:

1. If (x,P) is a point on the skeletal curve, then so is the point (-x, -P).
2. A branch curve originating from (x,P) [or (-x, -P)] on the skeletal curve will intersect the skeletal curve at (-x, -P) [or (x,P)] and will have at that point the same slope as the skeletal curve.
3. The initial slopes of ascending and descending branch curves are the same as the slope of the skeletal curves at the origin.
4. A branch curve originating from another branch curve will intersect that first branch at its origin.

Since these properties are covered by the Ramberg-Osgood equations, they are not left open to interpretation. There are two

more properties required to complete the model, and these are open to interpretation. The first concerns a bounding curve. Jennings (1963)[3] states that a branch curve qualifies as a new bounding curve only if both its origin (the point of reversal) and its intercept on the deflection axis (the zero-force crossing) have larger absolute values of deflection than those from the previously established bounding curve. We subscribe to this interpretation.

The second matter concerns the fate of an interior curve as the magnitude of the load is increased. Apparently there are two schools of thought regarding the interpretation. The first is described by Newmark and Rosenblueth (1971)[7], "if an (interior) curve crosses a curve described in a previous load cycle, the load-deformation curve follows that of the previous cycle". The second is due to Jennings, "force-deflection values are given by a hysteretic curve orginating from the point of most recent loading reversal until either the upper or lower boundary is contacted. Thereafter the force-deflection values are given by that boundary until the direction of loading is again reversed". In our hysteretic model we have adopted the Jenning's interpretation.

Before giving the rules for the hysteretic model, it is necessary to define the following terms:

Skeletal Curve. A curve passing through the origin and having the form:

$$x(P) = \frac{P}{K}\left(1 + A\left|\frac{P}{K}\right|^{R-1}\right)$$

Branch Curve. A curve originating from a coordinate (x_{re}, P_{re}) and having the form:

$$x(P) = x_{re} + \frac{P-P_{re}}{K}\left(1 + A\left|\frac{P-P_{re}}{2K}\right|^{R-1}\right)$$

Maximum Bounding Curve. A descending branch curve that, along with portions of the descending skeletal curve, limits the descent of subsequent branch curves. The coordinates of its origin and zero-force crossing are maximum values, that is they are greater than those of all previous descending branch curves.

Minimum Bounding Curve. An ascending branch that, along with portions of the ascending skeletal curve, limits the ascent of subsequent branch curves. The coordinates of its origin and zero-force crossing are minimum values, that is they are less than those of all previous ascending branch curves.

Interior Curve. A branch curve that is not a bounding curve.

(x,P). Current coordinates.

(xZ,0). Coordinates of zero-force crossing of a curve that is a candidate for a bounding curve.

(xMINL, PMINL). Coordinates of the origin of the minimum bounding curve.

(xMINU, PMINU). Coordinates of the terminus of the minimum bounding curve.

(xMINZ,0). Coordinates of the zero-force crossing of the minimum bounding curve.

(xMAXU, PMAXU). Coordinates of the origin of the maximum bounding curve.

(xMAXL, PMAXL). Coordinates of the terminus of the maximum bounding curve.

(xMAXZ,0). Coordinates of the zero-force crossing of the maximum bounding curve.

(xBC, PBC). Coordinates of the most recent reversal from a bounding or skeletal curve.

(x3,P). Coordinates of the 3 curve corresponding to the load, P, of the

current point.

(XIC, PIC). Coordinates of the most recent reversal from an interior curve.

(x5,P). Coordinates of the 5 curve corresponding to the load, P, of the current point.

(xSKEL,P). Coordinates of the skeletal curve corresponding to the load, P, of the current point.

The rules that define the hysteretic model use the following numbering system for the two types of skeletal curves and the eleven types of branch curves (the numbers are referred to as IBS numbers):

1. The ascending skeletal curve.
2. The descending skeletal curve.
3. The minimum bounding curve.
4. The interior ascending branch curve originating from the 2 curve.
5. The maximum bounding curve.
6. An interior descending branch curve originating from the 1 curve.
7. An interior ascending branch curve originating from a 6 curve.
8. An interior descending branch curve originating from a 4 curve.
9. An interior ascending branch curve originating from an 11 curve.
10. An interior descending branch curve originating from a 12 curve.
11. An interior descending branch curve originating from a 3 curve.

12. An interior ascending branch curve originating from a 5 curve.
13. An arbitrary interior branch curve that may originate from curves 7, 8, 9, 10 or another 13 curve.

The rules governing the hysteretic model are contained in Table A1 for ascending curves, and in Table A2 for descending curves. These tables give for each curve its identification (IBS) number, its type, the curves from which it may originate, the fate of the loading path after a reversal, and two pieces of information about intersections: whether a bounding curve has been intersected; and, if it has, the IBS number of the new curve.

To illustrate the use of these rules, a sample hysteretic response is given in Fig. A1. The initial loading in this example is negative, and proceeds from A along the negative skeletal curve (IBS=2) to point B where unloading begins. By referring to the row of information for IBS=2, and noting that the load at B is less than PMINL (which, along with all other reference points, is set to zero initially), it is seen that the new curve is a minimum bounding curve (IBS=3). Since the reversal is from a skeletal curve, it is not necessary to check the zero-force crossing before declaring the new curve to be a boundary. After the reversal point is established for the new minimum bounding curve, the following reference points are computed and stored for future use:

xMINL = x

PMINL = P

xMINZ

xMINU = -x

PMINU = -P

The new ascending curve proceeds uneventfully to C where it again reverses. The load at C is less than PMAXU (which is still zero), so the new curve is merely an interior descending curve (IBS=11). The path proceeds to D, then up to E on a 9 curve, and then reverses to a 13 curve. This descending 13 curve intersects the skeletal curve at F and then proceeds to G. This path from E to F illustrates the consequence of continuing an interior curve until it intersects a boundary. It may be that this path is not particularly realistic; but in the measured results considered here, this type of behavior (two reversals very close together) never occurred.

The path continues from G to H to I and on to J, where it reverses into a 5 curve. This new descending curve, even though it reverses almost immediately, establishes a new maximum bounding curve, and the following are computed and stored:

xMAXU = x

PMAXU = P

xMAXZ

xMAXL = xBC (at G)

PMAXL = PBC (at G)

The path then moves down to K, up to L on a 12 curve, along a 3 curve to M where it impinges upon the positive skeletal curve. It then proceeds to N, where it reverses to a new maximum bounding curve, and then down to 0 where the path terminates.

TABLE A1: RULES GOVERNING THE BEHAVIOR OF ASCENDING CURVES IN THE RAMBERG-OSGOOD MODEL

IBS Number	Type	Originating Curves	Reversal Rules	Intersection Rules
1	Skeletal	---	P>PMAXU? Y:IBS=5 N:IBS=6	---
3	Minimum Bounding	2,5,6,13	P>PMAXU? Y:xZ>xMAXZ? Y:IBS=5 N:IBS=11 N:IBS=11	P>PMINU? Y:IBS=1 N:IBS=3
4	Interior	2	P>PMAXU? Y:xZ>xMAXZ? Y:IBS=5 N:IBS=8 N:IBS=8	P>-PBC? Y:IBS=1 N:IBS=4
7	Interior	6	IBS = 13	P>PBC? Y:IBS=1 N:IBS=7
9	Interior	11	IBS = 13	P>PBC? Y:IBS=3 N:IBS=9
12	Interior	5	IBS = 10	P>PMAXU? Y:PMAXU>PMINU? Y:IBS=1 Y:IBS=3 N:IBS=12 N:x<x3? N:IBS=12
13	Interior	8,10,13	P>PMAXU? Y:xZ>xMAXZ? Y:IBS=5 N:IBS=13 N:IBS=13	P<PMINU? Y:x<x3? Y:IBS=3 N:IBS=13 N:x<xSKEL? Y:IBS=1 N:IBS=13

TABLE A2: RULES GOVERNING THE BEHAVIOR OF DESCENDING CURVES IN THE RAMBERG-OSGOOD MODEL

IBS Number	Type	Originating Curves	Reversal Rules	Intersection Rules
2	Skeletal	---	P<PMINL? Y:IBS=3 N:IBS=4	---
5	Maximum Bounding	1,3,4,13	P<PMINL? Y:xZ<xMINZ? Y:IBS=3 N:IBS=12 N:IBS=12	P<PMAXL? Y:IBS=2 N:IBS=5
6	Interior	1	P<PMINL? Y:xZ<xMINZ? Y:IBS=3 N:IBS=7 N:IBS=7	P<-PBC? Y:IBS=2 N:IBS=6
8	Interior	4	IBS = 13	P<PBC? Y:IBS=2 N:IBS=8
10	Interior	12	IBS = 13	P<PBC? Y:IBS=5 N:IBS=10
11	Interior	3	IBS = 9	P<PMINL? Y:PMINL<PMAXL? Y:IBS=2 N:x>x5? Y:IBS=5 N:IBS=11 N:IBS=11
13	Interior	7,9,13	P<PMINL? Y:xZ<xMINZ? Y:IBS=3 N:IBS=13 N:IBS=13	P>PMAXL? Y:x>x5? Y:IBS=5 N:IBS=13 N:x>xSKEL? Y:IBS=2 N:IBS=13

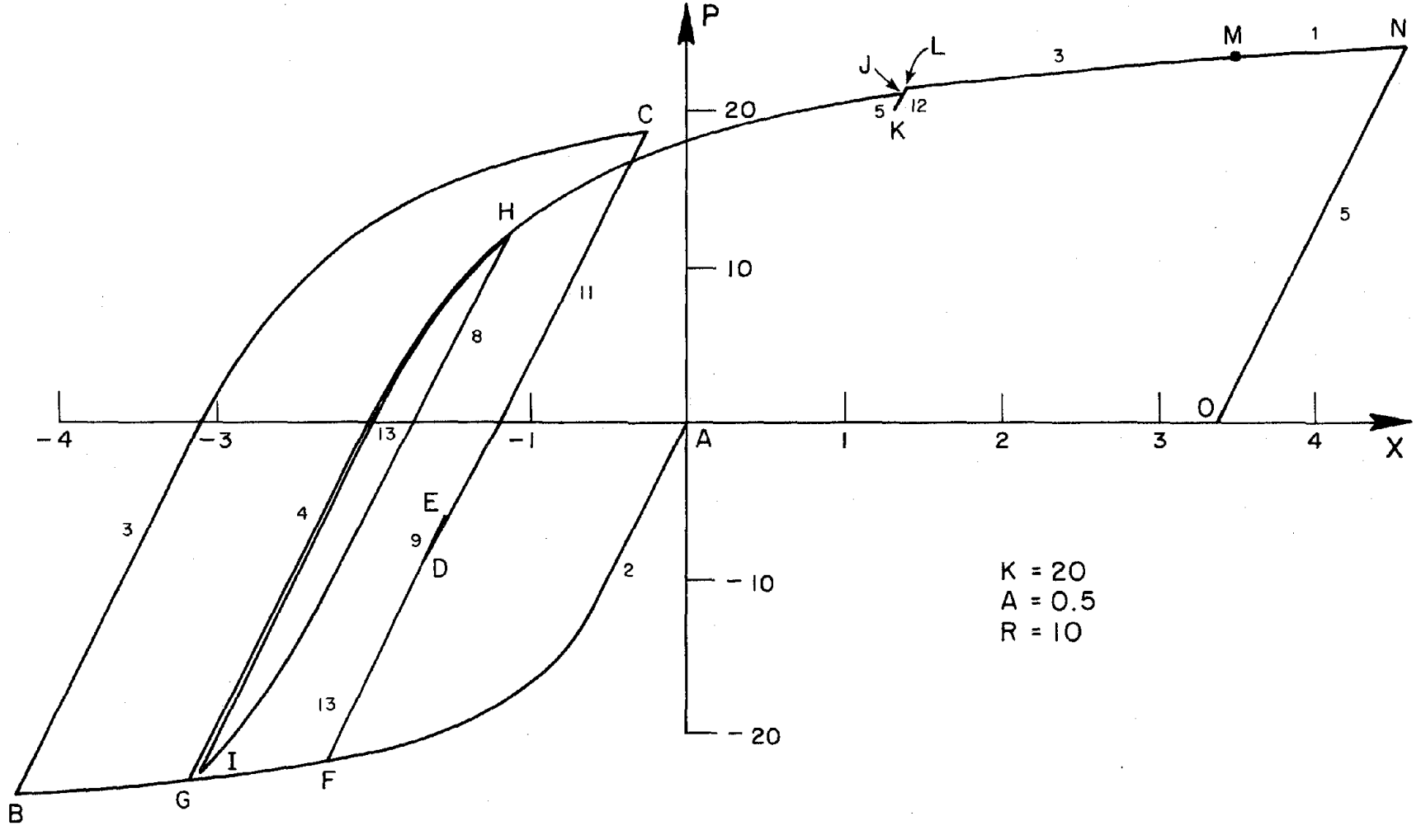

Fig. A1 Sample Hysteretic Loops from Ramberg-Osgood Model

APPENDIX B: INTEGRATION OF THE MATHEMATICAL MODEL

The differential Eq. (3.2) is solved numerically, so it is written at the i^{-th} time step as,

$$M\ddot{v}_i + C\dot{v}_i + P_i(v) = -M\ddot{v}_{gi} \tag{B1}$$

a step by step solution technique is used so that the equation is put in incremental form. Using the definition:

$$\Delta(\quad)_i = (\quad)_{i+1} - (\quad)_i \tag{B2}$$

we can write for the i^{-th} increment of time,

$$M\Delta\ddot{v}_i + C\Delta\dot{v}_i + \Delta P_i(v) = -M\Delta\ddot{v}_{gi} \tag{B3}$$

the nonlinearity of Eq. (B1) is a consequence of the term $P_i(v)$ which is given by:

$$v(P_i) = \frac{P_i}{K}\left(1 + A\left|\frac{P_i}{K}\right|^{R-1}\right) \tag{B4a}$$

$$v(P_i) = v_{re} + \frac{P_i - P_{re}}{2K}\left(1 + A\left(\frac{P_i - P_{re}}{2K}\right)^{R-1}\right) \tag{B4b}$$

depending on whether the current point is on a skeletal or a branch curve.

Assuming that the time step used is small enough, we will use within each time step, not the nonlinear Eq's (B4) but their linearized counterpart. First P_i is expanded into a Taylor series about the current point v_i:

$$P(v_{i+1}) = P(v_i) + \frac{dP(v_i)}{dv}(v_{i+1} - v_i) + H.O.T. \tag{B5}$$

The linear relationship is now obtained by neglecting the higher order terms:

$$\Delta P_i = \frac{dP(v_i)}{dv} \Delta v_i \tag{B6}$$

deriving an expression for $\frac{dP(v_i)}{dv}$ is complicated by the fact that Eqs. (B4) do not specify P as a function of v, but rather v as a function of P. The appropriate expression can be obtained by first writing Eq. (B4a) as a homogeneous function of two variables.

$$(v,P) = v - \frac{P}{K}\left(1 + A\left|\frac{P}{K}\right|^{R-1}\right) = 0 \tag{B7}$$

equating the total difference to zero gives

$$df = \frac{\partial f}{\partial v} dv + \frac{\partial f}{\partial P} dP = 0 \tag{B8}$$

Further, if $\frac{\partial f}{\partial P}$ is never zero

$$\frac{dP}{dv} = \frac{\partial f/\partial v}{\partial f/\partial P} = \frac{1}{\frac{1}{K}\left(1 + AR\left|\frac{P}{K}\right|^{R-1}\right)} \tag{B9}$$

Substituting this in Eq. (B6) we get:

$$\Delta P(v_i) = \frac{1}{\frac{1}{K}\left(1 + AR\left|\frac{P}{K}\right|^{R-1}\right)} \Delta v_i \tag{B10}$$

The same procedure can be applied to Eq. (B4b) giving:

$$\Delta P(v_i) = \frac{1}{\frac{1}{K}\left(1 + AR\left|\frac{P_i - P_{re}}{2K}\right|^{K-1}\right)} \Delta v_i \tag{B11}$$

recognizing that $dP(v_i)/dv$ is the tangent stiffness to the Ramberg-Osgood curve at v_i we denote,

$$\frac{dP(v_i)}{dv} = TS_i \tag{B12}$$

Now Eq. (B3) can be written as:

$$M\Delta\ddot{v}_i + C\Delta\dot{v}_i + TS_i\,\Delta v_i = -M\Delta\ddot{v}_{gi} \tag{B13}$$

The choice of method for solving Eq. (B13) is linear acceleration which is one of the family of Newmark methods (the one with $\beta = 1/6$). This method gives the conversion formulas:

$$\Delta\ddot{v}_i = \ddot{v}_{i+1} - \ddot{v}_i \tag{B14a}$$

$$\Delta\dot{v}_i = \Delta t(\ddot{v}_i + \frac{1}{2}\,\Delta\ddot{v}_i) \tag{B14b}$$

$$\Delta v_i = \Delta t\dot{v}_i + \frac{1}{2}\,(\Delta t)^2\,(\ddot{v}_i + \frac{1}{3}\,\Delta\ddot{v}_i) \tag{B14c}$$

The method assuming linear acceleration allows flexibility about how Eqs. (B14) are used, and experience in solving Eq. (B13) has shown us that the method appears to be more stable when all the incremental quantities are converted to acceleration rather than displacement as is usually done.

Substitution of Eqs. (B14b) and (B14c) into Eq. (B13) and algebraic manipulation gives

$$\Delta\ddot{v}_i = \frac{-M\Delta\ddot{v}_{gi} - C\Delta t\dot{v}_i - TS_i[\Delta t\dot{v}_i + \frac{1}{2}(\Delta t)^2\,\ddot{v}_i]}{M + \frac{1}{2}\,C\Delta t + \frac{1}{6}\,TS_i\,(\Delta t)^2} \tag{B15}$$

noting that $-M\Delta\ddot{v}_{gi}$ is fixed, Eq. (B15) is solved for $\Delta\ddot{v}_i$ and the result is substituted into Eqs. (B14) to give Δv_i and consequently, v_{i+1}. Eq. (B1), however, calls for P_{i+1} not v_{i+1} and therefore, an acceptable P_{i+1} is found by going to Eq. (B3) and using an iterative scheme to get

a P_{i+1} corresponding to v_{i+1}. For this purpose we chose to use an algorithm based on the Newton-Raphson method. Since the method demands a starting point we use for the first iteration a point $\bar{P}_{i+1}$ found from

$$\bar{P}_{i+1} = P_i + TS_i \, \Delta v_i \tag{B16}$$

and which is a point not on the Ramberg-Osgood curve.

We now find that when the set $\ddot{v}_{i+1}$, $\dot{v}_{i+1}$ and P_{i+1} is substituted into Eq. (B1), the equation is not satisfied. This is understandable when we realize that the evaluation of the set began with the use of Eq. (B15). This equation embraces two approximations. It represents the approximation that the acceleration is linear for an individual time step and, perhaps more important, it represents the solution to Eq. (B13) the incremental equation resulting from the linearization of the original differential equation.

Before proceeding to the next time step it is necessary to get a set $\ddot{v}_{i+1}$, $\dot{v}_{i+1}$ and P_{i+1} that will satisfy Eq. (B1), at least within an acceptable residue, here thought of as a residual force. Because the model used here consists of a single differential equation, our decision is to iterate the solution until the residual force is quite small before proceeding to the next. Each set of values obtained at a step in this process is identified in what follows by a superscript. Eq. (B1) is satisfied therefore when we write it in the form

$$M\ddot{v}^{(n)}_{i+1} + C\dot{v}^{(n)}_{i+1} + P^{(n)}_{i+1} = - M\ddot{v}_{gi+1} - RF^{(n)}_{i+1} \tag{B17}$$

where $RF^{(n)}_{i+1}$ denotes the residual force necessary to satisfy Eq. (B17) at the n^{th} iteration.

Within the method we now have $\ddot{v}_{i+1}$, $\dot{v}_{i+1}$, P_{i+1} and RF_{i+1} which satisfy Eq. (B17) with n = 0, that is

$$M\ddot{v}_{i+1}^{(0)} + C\dot{v}_{i+1}^{(0)} + P_{i+1}^{(0)} + RF_{i+1}^{(0)} = - M\ddot{v}_{gi+1} \tag{B18}$$

The sum of the first three terms in the left side of Eq. (B18) is too small by an amount $RF_{i+1}^{(0)}$ to satisfy the equation, so the first iteration begins by adding this force to the right side of Eq. (B13).

The equation to be solved now is

$$M\Delta\ddot{v}_i^{(1)} + C\Delta\dot{v}_i^{(1)} + TS_i\Delta v_i^{(1)} = RHS_i^{(1)} \tag{B19}$$

where

$$RHS_i^{(1)} = RHS_i^{(0)} + RF_{i+1}^{(0)} = - M\Delta\ddot{v}_{gi} + RF_{i+1}^{(0)} \tag{B20}$$

The solution begins with Eq. (B15) in which $RHS^{(1)}$ replaces $RHS_i^{(0)}$ in the solution for $\Delta\ddot{v}_i^{(1)}$. Having $\Delta\ddot{v}_i^{(0)}$, one obtains $\Delta\dot{v}_i^{(1)}$ and $\Delta v_i^{(1)}$ from Eqs. (B14b & c) and using Newton-Raphson with $P_{i+1}^{(0)}$ as a starting value one obtains $P_{i+1}^{(1)}$ from Eq. (B4).

Eq. (B1) will be satisfied with this set and a new residual force $RF_{i+1}^{(1)}$:

$$M\ddot{v}_{i+1}^{(1)} + C\dot{v}_{i+1}^{(1)} + P_{i+1}^{(1)} + RF_{i+1}^{(1)} = - M\ddot{v}_{gi+1} \tag{B21}$$

The differential equation to be solved now is

$$M\Delta\ddot{v}_i^{(2)} + C\Delta\dot{v}_i^{(2)} + TS_i\Delta v_i^{(2)} = RHS_i^{(2)} \tag{B22}$$

where

$$RHS_i^{(2)} = RHS_i^{(1)} + RF_{i+1}^{(1)} = - M\Delta\ddot{v}_{gi} + RF_{i+1}^{(0)} + RF_{i+1}^{(1)} \tag{B23}$$

The iterative procedure is repeated until the residual force is less in magnitude than some preassigned number.

An interesting insight into why this iterative procedure is effective in compensating for the linearization of the incremental equation is gained when we write Eq. (B22) for the n^{th} interation. The equation can be written

$$M\Delta\ddot{v}_i^{(n)} + C\Delta\dot{v}_i^{(n)} + TS_i\Delta v_i^{(n)} - \sum_{r=0}^{n-1} RF_{i+1}^{(r)} = - M\Delta\ddot{v}_{gi} \tag{B24}$$

If we consider the academic case where n is infinitely large, the set $\Delta\ddot{v}_i^{(n)}$, $\Delta\dot{v}_i^{(n)}$ and $\Delta P_i^{(n)}$ would satisfy Eq. (B5) giving

$$M\Delta\ddot{v}_i^{(n)} + C\Delta\dot{v}_i^{(n)} + \Delta P_i^{(n)} = - M\Delta\ddot{v}_{gi} \tag{B25}$$

For the value of n, we can equate Eqs. (B24) and (B25). This gives

$$\Delta P_i^{(n)} = TS_i\Delta v_i^{(n)} = \sum_{r=0}^{n-1} RF_{i+1}^{(r)} \quad (n\to\infty)$$

from which

$$P_{i+1} = P_i + \frac{dP_i}{dv}\,\Delta v_i - \sum_{r=0}^{\infty} RF_{i+1}^{(r)} \tag{B26}$$

We can see from comparing Eqs. (B26) and (B6) that the residual forces compensate for the higher order terms (which are forces) that were severed from Eq. (B6) to achieve a linear equation. Our experience is that the series $\sum_{r=0}^{n-1} RF_{i+1}^{(r)}$ is convergent.

With the satisfaction of Eq. (B1) within a prescribed tolerance, one moves on to the next time step and the next without incident until a point is reached on the Ramberg-Osgood curve that is either a reversal point or an intersection.

A point of reversal is identified in the following way. When moving along a curve, not only are the coordinates established for the ends of each time step, but so is the sign of the velocity found for

each point. A positive velocity indicates ascension, a negative velocity descension. If the velocity changes sign within a time step a reversal point exists within that step. Our method requires the establishment of a reversal point with more accuracy than is provided by its location somewhere within the ordinary time step. Accordingly, we return to the beginning point of the time step, divide the time interval by five, interpolate the forcing function linearly, and proceed with the new smaller time step until a change in velocity is again recorded. We then treat the point at the beginning of the final time step as the point of reversal and proceed with the smaller time step in the opposite direction until the substeps are completed, and then revert to the original time steps.

The check for intersections is somewhat more complicated. When an intersection is imminent, as indicated by the rules for the Ramberg-Osgood model, each new force-displacement pair is checked to determine whether or not a bounding curve has been violated. If it has, the step is retaken in subdivided increments as before. When the boundary is crossed with these subdivided steps, the path is switched over to bounding curve.

APPENDIX C: GENERALIZED MASS OF THE COLUMNS

The structure had two types of columns supporting the platform. One type was fixed at bottom and pinned on top. The other was pinned both at top and bottom and furthermore, had concentrated masses of about 1/8 M at distance L/6 from each end where M is the mass of one column and L is its length. The generalized mass of the columns and acting at the platform level is now obtained from

$$M^* = \int_0^L m(x) \left[\phi(x)\right]^2 dx + \Sigma M_i \left[\phi(x_i)\right]^2 \tag{C1}$$

where $m(x)$ is the mass variation over the column length.

M_i is the concentrated mass at x_i

ϕ is the assumed elastic column deflection curve.

For the fixed-pinned column we have:

$$\phi_1(x) = 1 = \frac{3}{2}\left(\frac{x}{L}\right) + \frac{1}{2}\left(\frac{x}{L}\right)^3 \tag{C2}$$

where x is measured from the fixed end. Furthermore, we have:

$$m_1(x) = \bar{m}_1 = \text{constant} \tag{C3}$$

Substituting Eqs. (C2) and (C3) into Eq. (C1) and integrating gives:

$$M_1^* = 0.236\ M_1 \tag{C4}$$

For the pinned-pinned columns we have only a rigid body rotation or:

$$\phi_2(x) = \frac{x}{L} \tag{C5}$$

and also

$$m_2(x) = \bar{m}_2 = \bar{m}_1 \tag{C6}$$

which by substituting into Eq. (C1) along with the concentrated masses gives:

$$M_2^* = 0.424\ M_2 = 0.424\ M_1 \tag{C7}$$

Now for the four columns of the structure we have:

$$M^* = 2(0.236 + 0.424)\ M_1 = 1.32\ M_1 \tag{C8}$$

where M_1 is the weight of one fixed-pinned column. Hence, M^* is equal to 1/3 of the sum of the column weights.

REFERENCES

1. Matzen, C. M., and McNiven, H. D., "Investigation of the Inelastic Characteristics of a Single Story Steel Structure Using System Identification and Shaking Table Experiments", Report No. UCB/EERC-76-20, Earthquake Engineering Research Center, University of California, Berkeley, August 1976.

2. Rea, D., Clough, R. W., and Bouwkamp, J. G., "Damping Capacity of a Model Steel Structure", Report No. UCB/EERC-69-14, Earthquake Engineering Research Center, University of California, Berkeley, December 1969.

3. Rea, D., and Penzien, J., "Dynamic Response of a 20 ft x 20 ft Shaking Table", Proceedings of the Fifth World Conference on Earthquake Engineering, Rome, Italy, 1972, pp. 1447-1456.

4. Menegotto, M., and Pinto, P., "Method of Analysis for Cyclically Loaded Reinforced Concrete Plane Frames Including Changes in Geometry and Nonelastic Behavior of Elements Under Combined Normal Force and Bending", IABSE Symposium on the Resistance and Ultimate Deformability of Structures Acted on by Well-Defined Repeated Loads, Lisbon, 1973.

5. Stanton, J. F., and McNiven, H. D., "The Development of a Mathematical Model to Predict the Flexural Response of Reinforced Concrete Beams to Cyclic Loads, Using System Identification", Report No. UCB/EERC-79-02, Earthquake Engineering Research Center, University of California, Berkeley, January 1979.

6. Jennings, P. C., "Response of Simple Yielding Structures to Earthquake Excitation", Ph.D. Dissertation, California Institute of Technology, Pasadena, 1963.

7. Newmark, N. M., and Rosenblueth, E., Fundamentals of Earthquake Engineering, Prentice Hall, Englewood Cliffs, N.J., 1971.

EARTHQUAKE ENGINEERING RESEARCH CENTER REPORTS

NOTE: Numbers in parenthesis are Accession Numbers assigned by the National Technical Information Service; these are followed by a price code. Copies of the reports may be ordered from the National Technical Information Service, 5285 Port Royal Road, Springfield, Virginia, 22161. Accession Numbers should be quoted on orders for reports (PB --- ---) and remittance must accompany each order. Reports without this information were not available at time of printing. Upon request, EERC will mail inquirers this information when it becomes available.

EERC 67-1 "Feasibility Study Large-Scale Earthquake Simulator Facility," by J. Penzien, J.G. Bouwkamp, R.W. Clough and D. Rea - 1967 (PB 187 905)A07

EERC 68-1 Unassigned

EERC 68-2 "Inelastic Behavior of Beam-to-Column Subassemblages Under Repeated Loading," by V.V. Bertero - 1968 (PB 184 888)A05

EERC 68-3 "A Graphical Method for Solving the Wave Reflection-Refraction Problem," by H.D. McNiven and Y. Mengi - 1968 (PB 187 943)A03

EERC 68-4 "Dynamic Properties of McKinley School Buildings," by D. Rea, J.G. Bouwkamp and R.W. Clough - 1968 (PB 187 902)A07

EERC 68-5 "Characteristics of Rock Motions During Earthquakes," by H.B. Seed, I.M. Idriss and F.W. Kiefer - 1968 (PB 188 338)A03

EERC 69-1 "Earthquake Engineering Research at Berkeley," - 1969 (PB 187 906)A11

EERC 69-2 "Nonlinear Seismic Response of Earth Structures," by M. Dibaj and J. Penzien - 1969 (PB 187 904)A08

EERC 69-3 "Probabilistic Study of the Behavior of Structures During Earthquakes," by R. Ruiz and J. Penzien - 1969 (PB 187 886)A06

EERC 69-4 "Numerical Solution of Boundary Value Problems in Structural Mechanics by Reduction to an Initial Value Formulation," by N. Distefano and J. Schujman - 1969 (PB 187 942)A02

EERC 69-5 "Dynamic Programming and the Solution of the Biharmonic Equation," by N. Distefano - 1969 (PB 187 941)A03

EERC 69-6 "Stochastic Analysis of Offshore Tower Structures," by A.K. Malhotra and J. Penzien - 1969 (PB 187 903)A09

EERC 69-7 "Rock Motion Accelerograms for High Magnitude Earthquakes," by H.B. Seed and I.M. Idriss - 1969 (PB 187 940)A02

EERC 69-8 "Structural Dynamics Testing Facilities at the University of California, Berkeley," by R.M. Stephen, J.G. Bouwkamp, R.W. Clough and J. Penzien - 1969 (PB 189 111)A04

EERC 69-9 "Seismic Response of Soil Deposits Underlain by Sloping Rock Boundaries," by H. Dezfulian and H.B. Seed 1969 (PB 189 114)A03

EERC 69-10 "Dynamic Stress Analysis of Axisymmetric Structures Under Arbitrary Loading," by S. Ghosh and E.L. Wilson 1969 (PB 189 026)A10

EERC 69-11 "Seismic Behavior of Multistory Frames Designed by Different Philosophies," by J.C. Anderson and V. V. Bertero - 1969 (PB 190 662)A10

EERC 69-12 "Stiffness Degradation of Reinforcing Concrete Members Subjected to Cyclic Flexural Moments," by V.V. Bertero, B. Bresler and H. Ming Liao - 1969 (PB 202 942)A07

EERC 69-13 "Response of Non-Uniform Soil Deposits to Travelling Seismic Waves," by H. Dezfulian and H.B. Seed - 1969 (PB 191 023)A03

EERC 69-14 "Damping Capacity of a Model Steel Structure," by D. Rea, R.W. Clough and J.G. Bouwkamp - 1969 (PB 190 663)A06

EERC 69-15 "Influence of Local Soil Conditions on Building Damage Potential during Earthquakes," by H.B. Seed and I.M. Idriss - 1969 (PB 191 036)A03

EERC 69-16 "The Behavior of Sands Under Seismic Loading Conditions," by M.L. Silver and H.B. Seed - 1969 (AD 714 982)A07

EERC 70-1 "Earthquake Response of Gravity Dams," by A.K. Chopra - 1970 (AD 709 640)A03

EERC 70-2 "Relationships between Soil Conditions and Building Damage in the Caracas Earthquake of July 29, 1967," by H.B. Seed, I.M. Idriss and H. Dezfulian - 1970 (PB 195 762)A05

EERC 70-3 "Cyclic Loading of Full Size Steel Connections," by E.P. Popov and R.M. Stephen - 1970 (PB 213 545)A04

EERC 70-4 "Seismic Analysis of the Charaima Building, Caraballeda, Venezuela," by Subcommittee of the SEAONC Research Committee: V.V. Bertero, P.F. Fratessa, S.A. Mahin, J.H. Sexton, A.C. Scordelis, E.L. Wilson, L.A. Wyllie, H.B. Seed and J. Penzien, Chairman - 1970 (PB 201 455)A06

EERC 70-5 "A Computer Program for Earthquake Analysis of Dams," by A.K. Chopra and P. Chakrabarti - 1970 (AD 723 994)A05

EERC 70-6 "The Propagation of Love Waves Across Non-Horizontally Layered Structures," by J. Lysmer and L.A. Drake 1970 (PB 197 896)A03

EERC 70-7 "Influence of Base Rock Characteristics on Ground Response," by J. Lysmer, H.B. Seed and P.B. Schnabel 1970 (PB 197 897)A03

EERC 70-8 "Applicability of Laboratory Test Procedures for Measuring Soil Liquefaction Characteristics under Cyclic Loading," by H.B. Seed and W.H. Peacock - 1970 (PB 198 016)A03

EERC 70-9 "A Simplified Procedure for Evaluating Soil Liquefaction Potential," by H.B. Seed and I.M. Idriss - 1970 (PB 198 009)A03

EERC 70-10 "Soil Moduli and Damping Factors for Dynamic Response Analysis," by H.B. Seed and I.M. Idriss - 1970 (PB 197 869)A03

EERC 71-1 "Koyna Earthquake of December 11, 1967 and the Performance of Koyna Dam," by A.K. Chopra and P. Chakrabarti 1971 (AD 731 496)A06

EERC 71-2 "Preliminary In-Situ Measurements of Anelastic Absorption in Soils Using a Prototype Earthquake Simulator," by R.D. Borcherdt and P.W. Rodgers - 1971 (PB 201 454)A03

EERC 71-3 "Static and Dynamic Analysis of Inelastic Frame Structures," by F.L. Porter and G.H. Powell - 1971 (PB 210 135)A06

EERC 71-4 "Research Needs in Limit Design of Reinforced Concrete Structures," by V.V. Bertero - 1971 (PB 202 943)A04

EERC 71-5 "Dynamic Behavior of a High-Rise Diagonally Braced Steel Building," by D. Rea, A.A. Shah and J.G. Bouwkamp 1971 (PB 203 584)A06

EERC 71-6 "Dynamic Stress Analysis of Porous Elastic Solids Saturated with Compressible Fluids," by J. Ghaboussi and E. L. Wilson - 1971 (PB 211 396)A06

EERC 71-7 "Inelastic Behavior of Steel Beam-to-Column Subassemblages," by H. Krawinkler, V.V. Bertero and E.P. Popov 1971 (PB 211 335)A14

EERC 71-8 "Modification of Seismograph Records for Effects of Local Soil Conditions," by P. Schnabel, H.B. Seed and J. Lysmer - 1971 (PB 214 450)A03

EERC 72-1 "Static and Earthquake Analysis of Three Dimensional Frame and Shear Wall Buildings," by E.L. Wilson and H.H. Dovey - 1972 (PB 212 904)A05

EERC 72-2 "Accelerations in Rock for Earthquakes in the Western United States," by P.B. Schnabel and H.B. Seed - 1972 (PB 213 100)A03

EERC 72-3 "Elastic-Plastic Earthquake Response of Soil-Building Systems," by T. Minami - 1972 (PB 214 868)A08

EERC 72-4 "Stochastic Inelastic Response of Offshore Towers to Strong Motion Earthquakes," by M.K. Kaul - 1972 (PB 215 713)A05

EERC 72-5 "Cyclic Behavior of Three Reinforced Concrete Flexural Members with High Shear," by E.P. Popov, V.V. Bertero and H. Krawinkler - 1972 (PB 214 555)A05

EERC 72-6 "Earthquake Response of Gravity Dams Including Reservoir Interaction Effects," by P. Chakrabarti and A.K. Chopra - 1972 (AD 762 330)A08

EERC 72-7 "Dynamic Properties of Pine Flat Dam," by D. Rea, C.Y. Liaw and A.K. Chopra - 1972 (AD 763 928)A05

EERC 72-8 "Three Dimensional Analysis of Building Systems," by E.L. Wilson and H.H. Dovey - 1972 (PB 222 438)A06

EERC 72-9 "Rate of Loading Effects on Uncracked and Repaired Reinforced Concrete Members," by S. Mahin, V.V. Bertero, D. Rea and M. Atalay - 1972 (PB 224 520)A08

EERC 72-10 "Computer Program for Static and Dynamic Analysis of Linear Structural Systems," by E.L. Wilson, K.-J. Bathe, J.E. Peterson and H.H.Dovey - 1972 (PB 220 437)A04

EERC 72-11 "Literature Survey - Seismic Effects on Highway Bridges," by T. Iwasaki, J. Penzien and R.W. Clough - 1972 (PB 215 613)A19

EERC 72-12 "SHAKE-A Computer Program for Earthquake Response Analysis of Horizontally Layered Sites," by P.B. Schnabel and J. Lysmer - 1972 (PB 220 207)A06

EERC 73-1 "Optimal Seismic Design of Multistory Frames," by V.V. Bertero and H. Kamil - 1973

EERC 73-2 "Analysis of the Slides in the San Fernando Dams During the Earthquake of February 9, 1971," by H.B. Seed, K.L. Lee, I.M. Idriss and F. Makdisi - 1973 (PB 223 402)A14

EERC 73-3 "Computer Aided Ultimate Load Design of Unbraced Multistory Steel Frames," by M.B. El-Hafez and G.H. Powell 1973 (PB 248 315)A09

EERC 73-4 "Experimental Investigation into the Seismic Behavior of Critical Regions of Reinforced Concrete Components as Influenced by Moment and Shear," by M. Celebi and J. Penzien - 1973 (PB 215 884)A09

EERC 73-5 "Hysteretic Behavior of Epoxy-Repaired Reinforced Concrete Beams," by M. Celebi and J. Penzien - 1973 (PB 239 568)A03

EERC 73-6 "General Purpose Computer Program for Inelastic Dynamic Response of Plane Structures," by A. Kanaan and G.H. Powell - 1973 (PB 221 260)A08

EERC 73-7 "A Computer Program for Earthquake Analysis of Gravity Dams Including Reservoir Interaction," by P. Chakrabarti and A.K. Chopra - 1973 (AD 766 271)A04

EERC 73-8 "Behavior of Reinforced Concrete Deep Beam-Column Subassemblages Under Cyclic Loads," by O. Küstü and J.G. Bouwkamp - 1973 (PB 246 117)A12

EERC 73-9 "Earthquake Analysis of Structure-Foundation Systems," by A.K. Vaish and A.K. Chopra - 1973 (AD 766 272)A07

EERC 73-10 "Deconvolution of Seismic Response for Linear Systems," by R.B. Reimer - 1973 (PB 227 179)A08

EERC 73-11 "SAP IV: A Structural Analysis Program for Static and Dynamic Response of Linear Systems," by K.-J. Bathe, E.L. Wilson and F.E. Peterson - 1973 (PB 221 967)A09

EERC 73-12 "Analytical Investigations of the Seismic Response of Long, Multiple Span Highway Bridges," by W.S. Tseng and J. Penzien - 1973 (PB 227 816)A10

EERC 73-13 "Earthquake Analysis of Multi-Story Buildings Including Foundation Interaction," by A.K. Chopra and J.A. Gutierrez - 1973 (PB 222 970)A03

EERC 73-14 "ADAP: A Computer Program for Static and Dynamic Analysis of Arch Dams," by R.W. Clough, J.M. Raphael and S. Mojtahedi - 1973 (PB 223 763)A09

EERC 73-15 "Cyclic Plastic Analysis of Structural Steel Joints," by R.B. Pinkney and R.W. Clough - 1973 (PB 226 843)A08

EERC 73-16 "QUAD-4: A Computer Program for Evaluating the Seismic Response of Soil Structures by Variable Damping Finite Element Procedures," by I.M. Idriss, J. Lysmer, R. Hwang and H.B. Seed - 1973 (PB 229 424)A05

EERC 73-17 "Dynamic Behavior of a Multi-Story Pyramid Shaped Building," by R.M. Stephen, J.P. Hollings and J.G. Bouwkamp - 1973 (PB 240 718)A06

EERC 73-18 "Effect of Different Types of Reinforcing on Seismic Behavior of Short Concrete Columns," by V.V. Bertero, J. Hollings, O. Küstü, R.M. Stephen and J.G. Bouwkamp - 1973

EERC 73-19 "Olive View Medical Center Materials Studies, Phase I," by B. Bresler and V.V. Bertero - 1973 (PB 235 986)A06

EERC 73-20 "Linear and Nonlinear Seismic Analysis Computer Programs for Long Multiple-Span Highway Bridges," by W.S. Tseng and J. Penzien - 1973

EERC 73-21 "Constitutive Models for Cyclic Plastic Deformation of Engineering Materials," by J.M. Kelly and P.P. Gillis 1973 (PB 226 024)A03

EERC 73-22 "DRAIN - 2D User's Guide," by G.H. Powell - 1973 (PB 227 016)A05

EERC 73-23 "Earthquake Engineering at Berkeley - 1973," (PB 226 033)A11

EERC 73-24 Unassigned

EERC 73-25 "Earthquake Response of Axisymmetric Tower Structures Surrounded by Water," by C.Y. Liaw and A.K. Chopra 1973 (AD 773 052)A09

EERC 73-26 "Investigation of the Failures of the Olive View Stairtowers During the San Fernando Earthquake and Their Implications on Seismic Design," by V.V. Bertero and R.G. Collins - 1973 (PB 235 106)A13

EERC 73-27 "Further Studies on Seismic Behavior of Steel Beam-Column Subassemblages," by V.V. Bertero, H. Krawinkler and E.P. Popov - 1973 (PB 234 172)A06

EERC 74-1 "Seismic Risk Analysis," by C.S. Oliveira - 1974 (PB 235 920)A06

EERC 74-2 "Settlement and Liquefaction of Sands Under Multi-Directional Shaking," by R. Pyke, C.K. Chan and H.B. Seed 1974

EERC 74-3 "Optimum Design of Earthquake Resistant Shear Buildings," by D. Ray, K.S. Pister and A.K. Chopra - 1974 (PB 231 172)A06

EERC 74-4 "LUSH - A Computer Program for Complex Response Analysis of Soil-Structure Systems," by J. Lysmer, T. Udaka, H.B. Seed and R. Hwang - 1974 (PB 236 796)A05

EERC 74-5 "Sensitivity Analysis for Hysteretic Dynamic Systems: Applications to Earthquake Engineering," by D. Ray 1974 (PB 233 213)A06

EERC 74-6 "Soil Structure Interaction Analyses for Evaluating Seismic Response," by H.B. Seed, J. Lysmer and R. Hwang 1974 (PB 236 519)A04

EERC 74-7 Unassigned

EERC 74-8 "Shaking Table Tests of a Steel Frame - A Progress Report," by R.W. Clough and D. Tang - 1974 (PB 240 869)A03

EERC 74-9 "Hysteretic Behavior of Reinforced Concrete Flexural Members with Special Web Reinforcement," by V.V. Bertero, E.P. Popov and T.Y. Wang - 1974 (PB 236 797)A07

EERC 74-10 "Applications of Reliability-Based, Global Cost Optimization to Design of Earthquake Resistant Structures," by E. Vitiello and K.S. Pister - 1974 (PB 237 231)A06

EERC 74-11 "Liquefaction of Gravelly Soils Under Cyclic Loading Conditions," by R.T. Wong, H.B. Seed and C.K. Chan 1974 (PB 242 042)A03

EERC 74-12 "Site-Dependent Spectra for Earthquake-Resistant Design," by H.B. Seed, C. Ugas and J. Lysmer - 1974 (PB 240 953)A03

EERC 74-13 "Earthquake Simulator Study of a Reinforced Concrete Frame," by P. Hidalgo and R.W. Clough - 1974 (PB 241 944)A13

EERC 74-14 "Nonlinear Earthquake Response of Concrete Gravity Dams," by N. Pal - 1974 (AD/A 006 583)A06

EERC 74-15 "Modeling and Identification in Nonlinear Structural Dynamics - I. One Degree of Freedom Models," by N. Distefano and A. Rath - 1974 (PB 241 548)A06

EERC 75-1 "Determination of Seismic Design Criteria for the Dumbarton Bridge Replacement Structure, Vol. I: Description, Theory and Analytical Modeling of Bridge and Parameters," by F. Baron and S.-H. Pang - 1975 (PB 259 407)A15

EERC 75-2 "Determination of Seismic Design Criteria for the Dumbarton Bridge Replacement Structure, Vol. II: Numerical Studies and Establishment of Seismic Design Criteria," by F. Baron and S.-H. Pang - 1975 (PB 259 408)A11 (For set of EERC 75-1 and 75-2 (PB 259 406))

EERC 75-3 "Seismic Risk Analysis for a Site and a Metropolitan Area," by C.S. Oliveira - 1975 (PB 248 134)A09

EERC 75-4 "Analytical Investigations of Seismic Response of Short, Single or Multiple-Span Highway Bridges," by M.-C. Chen and J. Penzien - 1975 (PB 241 454)A09

EERC 75-5 "An Evaluation of Some Methods for Predicting Seismic Behavior of Reinforced Concrete Buildings," by S.A. Mahin and V.V. Bertero - 1975 (PB 246 306)A16

EERC 75-6 "Earthquake Simulator Study of a Steel Frame Structure, Vol. I: Experimental Results," by R.W. Clough and D.T. Tang - 1975 (PB 243 981)A13

EERC 75-7 "Dynamic Properties of San Bernardino Intake Tower," by D. Rea, C.-Y. Liaw and A.K. Chopra - 1975 (AD/A008 406) A05

EERC 75-8 "Seismic Studies of the Articulation for the Dumbarton Bridge Replacement Structure, Vol. I: Description, Theory and Analytical Modeling of Bridge Components," by F. Baron and R.E. Hamati - 1975 (PB 251 539)A07

EERC 75-9 "Seismic Studies of the Articulation for the Dumbarton Bridge Replacement Structure, Vol. 2: Numerical Studies of Steel and Concrete Girder Alternates," by F. Baron and R.E. Hamati - 1975 (PB 251 540)A10

EERC 75-10 "Static and Dynamic Analysis of Nonlinear Structures," by D.P. Mondkar and G.H. Powell - 1975 (PB 242 434)A08

EERC 75-11 "Hysteretic Behavior of Steel Columns," by E.P. Popov, V.V. Bertero and S. Chandramouli - 1975 (PB 252 365)A11

EERC 75-12 "Earthquake Engineering Research Center Library Printed Catalog," - 1975 (PB 243 711)A26

EERC 75-13 "Three Dimensional Analysis of Building Systems (Extended Version)," by E.L. Wilson, J.P. Hollings and H.H. Dovey - 1975 (PB 243 989)A07

EERC 75-14 "Determination of Soil Liquefaction Characteristics by Large-Scale Laboratory Tests," by P. De Alba, C.K. Chan and H.B. Seed - 1975 (NUREG 0027)A08

EERC 75-15 "A Literature Survey - Compressive, Tensile, Bond and Shear Strength of Masonry," by R.L. Mayes and R.W. Clough - 1975 (PB 246 292)A10

EERC 75-16 "Hysteretic Behavior of Ductile Moment Resisting Reinforced Concrete Frame Components," by V.V. Bertero and E.P. Popov - 1975 (PB 246 388)A05

EERC 75-17 "Relationships Between Maximum Acceleration, Maximum Velocity, Distance from Source, Local Site Conditions for Moderately Strong Earthquakes," by H.B. Seed, R. Murarka, J. Lysmer and I.M. Idriss - 1975 (PB 248 172)A03

EERC 75-18 "The Effects of Method of Sample Preparation on the Cyclic Stress-Strain Behavior of Sands," by J. Mulilis, C.K. Chan and H.B. Seed - 1975 (Summarized in EERC 75-28)

EERC 75-19 "The Seismic Behavior of Critical Regions of Reinforced Concrete Components as Influenced by Moment, Shear and Axial Force," by M.B. Atalay and J. Penzien - 1975 (PB 258 842)A11

EERC 75-20 "Dynamic Properties of an Eleven Story Masonry Building," by R.M. Stephen, J.P. Hollings, J.G. Bouwkamp and D. Jurukovski - 1975 (PB 246 945)A04

EERC 75-21 "State-of-the-Art in Seismic Strength of Masonry - An Evaluation and Review," by R.L. Mayes and R.W. Clough 1975 (PB 249 040)A07

EERC 75-22 "Frequency Dependent Stiffness Matrices for Viscoelastic Half-Plane Foundations," by A.K. Chopra, P. Chakrabarti and G. Dasgupta - 1975 (PB 248 121)A07

EERC 75-23 "Hysteretic Behavior of Reinforced Concrete Framed Walls," by T.Y. Wong, V.V. Bertero and E.P. Popov - 1975

EERC 75-24 "Testing Facility for Subassemblages of Frame-Wall Structural Systems," by V.V. Bertero, E.P. Popov and T. Endo - 1975

EERC 75-25 "Influence of Seismic History on the Liquefaction Characteristics of Sands," by H.B. Seed, K. Mori and C.K. Chan - 1975 (Summarized in EERC 75-28)

EERC 75-26 "The Generation and Dissipation of Pore Water Pressures during Soil Liquefaction," by H.B. Seed, P.P. Martin and J. Lysmer - 1975 (PB 252 648)A03

EERC 75-27 "Identification of Research Needs for Improving Aseismic Design of Building Structures," by V.V. Bertero 1975 (PB 248 136)A05

EERC 75-28 "Evaluation of Soil Liquefaction Potential during Earthquakes," by H.B. Seed, I. Arango and C.K. Chan - 1975 (NUREG 0026)A13

EERC 75-29 "Representation of Irregular Stress Time Histories by Equivalent Uniform Stress Series in Liquefaction Analyses," by H.B. Seed, I.M. Idriss, F. Makdisi and N. Banerjee - 1975 (PB 252 635)A03

EERC 75-30 "FLUSH - A Computer Program for Approximate 3-D Analysis of Soil-Structure Interaction Problems," by J. Lysmer, T. Udaka, C.-F. Tsai and H.B. Seed - 1975 (PB 259 332)A07

EERC 75-31 "ALUSH - A Computer Program for Seismic Response Analysis of Axisymmetric Soil-Structure Systems," by E. Berger, J. Lysmer and H.B. Seed - 1975

EERC 75-32 "TRIP and TRAVEL - Computer Programs for Soil-Structure Interaction Analysis with Horizontally Travelling Waves," by T. Udaka, J. Lysmer and H.B. Seed - 1975

EERC 75-33 "Predicting the Performance of Structures in Regions of High Seismicity," by J. Penzien - 1975 (PB 248 130)A03

EERC 75-34 "Efficient Finite Element Analysis of Seismic Structure - Soil - Direction," by J. Lysmer, H.B. Seed, T. Udaka, R.N. Hwang and C.-F. Tsai - 1975 (PB 253 570)A03

EERC 75-35 "The Dynamic Behavior of a First Story Girder of a Three-Story Steel Frame Subjected to Earthquake Loading," by R.W. Clough and L.-Y. Li - 1975 (PB 248 841)A05

EERC 75-36 "Earthquake Simulator Study of a Steel Frame Structure, Volume II - Analytical Results," by D.T. Tang - 1975 (PB 252 926)A10

EERC 75-37 "ANSR-I General Purpose Computer Program for Analysis of Non-Linear Structural Response," by D.P. Mondkar and G.H. Powell - 1975 (PB 252 386)A08

EERC 75-38 "Nonlinear Response Spectra for Probabilistic Seismic Design and Damage Assessment of Reinforced Concrete Structures," by M. Murakami and J. Penzien - 1975 (PB 259 530)A05

EERC 75-39 "Study of a Method of Feasible Directions for Optimal Elastic Design of Frame Structures Subjected to Earthquake Loading," by N.D. Walker and K.S. Pister - 1975 (PB 257 781)A06

EERC 75-40 "An Alternative Representation of the Elastic-Viscoelastic Analogy," by G. Dasgupta and J.L. Sackman - 1975 (PB 252 173)A03

EERC 75-41 "Effect of Multi-Directional Shaking on Liquefaction of Sands," by H.B. Seed, R. Pyke and G.R. Martin - 1975 (PB 258 781)A03

EERC 76-1 "Strength and Ductility Evaluation of Existing Low-Rise Reinforced Concrete Buildings - Screening Method," by T. Okada and B. Bresler - 1976 (PB 257 906)A11

EERC 76-2 "Experimental and Analytical Studies on the Hysteretic Behavior of Reinforced Concrete Rectangular and T-Beams," by S.-Y.M. Ma, E.P. Popov and V.V. Bertero - 1976 (PB 260 843)A12

EERC 76-3 "Dynamic Behavior of a Multistory Triangular-Shaped Building," by J. Petrovski, R.M. Stephen, E. Gartenbaum and J.G. Bouwkamp - 1976 (PB 273 279)A07

EERC 76-4 "Earthquake Induced Deformations of Earth Dams," by N. Serff, H.B. Seed, F.I. Makdisi & C.-Y. Chang - 1976 (PB 292 065)A08

EERC 76-5 "Analysis and Design of Tube-Type Tall Building Structures," by H. de Clercq and G.H. Powell - 1976 (PB 252 220) A10

EERC 76-6 "Time and Frequency Domain Analysis of Three-Dimensional Ground Motions, San Fernando Earthquake," by T. Kubo and J. Penzien (PB 260 556)A11

EERC 76-7 "Expected Performance of Uniform Building Code Design Masonry Structures," by R.L. Mayes, Y. Omote, S.W. Chen and R.W. Clough - 1976 (PB 270 098)A05

EERC 76-8 "Cyclic Shear Tests of Masonry Piers, Volume 1 - Test Results," by R.L. Mayes, Y. Omote, R.W. Clough - 1976 (PB 264 424)A06

EERC 76-9 "A Substructure Method for Earthquake Analysis of Structure - Soil Interaction," by J.A. Gutierrez and A.K. Chopra - 1976 (PB 257 783)A08

EERC 76-10 "Stabilization of Potentially Liquefiable Sand Deposits using Gravel Drain Systems," by H.B. Seed and J.R. Booker - 1976 (PB 258 820)A04

EERC 76-11 "Influence of Design and Analysis Assumptions on Computed Inelastic Response of Moderately Tall Frames," by G.H. Powell and D.G. Row - 1976 (PB 271 409)A06

EERC 76-12 "Sensitivity Analysis for Hysteretic Dynamic Systems: Theory and Applications," by D. Ray, K.S. Pister and E. Polak - 1976 (PB 262 859)A04

EERC 76-13 "Coupled Lateral Torsional Response of Buildings to Ground Shaking," by C.L. Kan and A.K. Chopra - 1976 (PB 257 907)A09

EERC 76-14 "Seismic Analyses of the Banco de America," by V.V. Bertero, S.A. Mahin and J.A. Hollings - 1976

EERC 76-15 "Reinforced Concrete Frame 2: Seismic Testing and Analytical Correlation," by R.W. Clough and J. Gidwani - 1976 (PB 261 323)A08

EERC 76-16 "Cyclic Shear Tests of Masonry Piers, Volume 2 - Analysis of Test Results," by R.L. Mayes, Y. Omote and R.W. Clough - 1976

EERC 76-17 "Structural Steel Bracing Systems: Behavior Under Cyclic Loading," by E.P. Popov, K. Takanashi and C.W. Roeder - 1976 (PB 260 715)A05

EERC 76-18 "Experimental Model Studies on Seismic Response of High Curved Overcrossings," by D. Williams and W.G. Godden - 1976 (PB 269 548)A08

EERC 76-19 "Effects of Non-Uniform Seismic Disturbances on the Dumbarton Bridge Replacement Structure," by F. Baron and R.E. Hamati - 1976 (PB 282 981)A16

EERC 76-20 "Investigation of the Inelastic Characteristics of a Single Story Steel Structure Using System Identification and Shaking Table Experiments," by V.C. Matzen and H.D. McNiven - 1976 (PB 258 453)A07

EERC 76-21 "Capacity of Columns with Splice Imperfections," by E.P. Popov, R.M. Stephen and R. Philbrick - 1976 (PB 260 378)A04

EERC 76-22 "Response of the Olive View Hospital Main Building during the San Fernando Earthquake," by S. A. Mahin, V.V. Bertero, A.K. Chopra and R. Collins - 1976 (PB 271 425)A14

EERC 76-23 "A Study on the Major Factors Influencing the Strength of Masonry Prisms," by N.M. Mostaghel, R.L. Mayes, R. W. Clough and S.W. Chen - 1976 (Not published)

EERC 76-24 "GADFLEA - A Computer Program for the Analysis of Pore Pressure Generation and Dissipation during Cyclic or Earthquake Loading," by J.R. Booker, M.S. Rahman and H.B. Seed - 1976 (PB 263 947)A04

EERC 76-25 "Seismic Safety Evaluation of a R/C School Building," by B. Bresler and J. Axley - 1976

EERC 76-26 "Correlative Investigations on Theoretical and Experimental Dynamic Behavior of a Model Bridge Structure," by K. Kawashima and J. Penzien - 1976 (PB 263 388)A11

EERC 76-27 "Earthquake Response of Coupled Shear Wall Buildings," by T. Srichatrapimuk - 1976 (PB 265 157)A07

EERC 76-28 "Tensile Capacity of Partial Penetration Welds," by E.P. Popov and R.M. Stephen - 1976 (PB 262 899)A03

EERC 76-29 "Analysis and Design of Numerical Integration Methods in Structural Dynamics," by H.M. Hilber - 1976 (PB 264 410)A06

EERC 76-30 "Contribution of a Floor System to the Dynamic Characteristics of Reinforced Concrete Buildings," by L.E. Malik and V.V. Bertero - 1976 (PB 272 247)A13

EERC 76-31 "The Effects of Seismic Disturbances on the Golden Gate Bridge," by F. Baron, M. Arikan and R.E. Hamati - 1976 (PB 272 279)A09

EERC 76-32 "Infilled Frames in Earthquake Resistant Construction," by R.E. Klingner and V.V. Bertero - 1976 (PB 265 892)A13

UCB/EERC-77/01 "PLUSH - A Computer Program for Probabilistic Finite Element Analysis of Seismic Soil-Structure Interaction," by M.P. Romo Organista, J. Lysmer and H.B. Seed - 1977

UCB/EERC-77/02 "Soil-Structure Interaction Effects at the Humboldt Bay Power Plant in the Ferndale Earthquake of June 7, 1975," by J.E. Valera, H.B. Seed, C.F. Tsai and J. Lysmer - 1977 (PB 265 795)A04

UCB/EERC-77/03 "Influence of Sample Disturbance on Sand Response to Cyclic Loading," by K. Mori, H.B. Seed and C.K. Chan - 1977 (PB 267 352)A04

UCB/EERC-77/04 "Seismological Studies of Strong Motion Records," by J. Shoja-Taheri - 1977 (PB 269 655)A10

UCB/EERC-77/05 "Testing Facility for Coupled-Shear Walls," by L. Li-Hyung, V.V. Bertero and E.P. Popov - 1977

UCB/EERC-77/06 "Developing Methodologies for Evaluating the Earthquake Safety of Existing Buildings," by No. 1 - B. Bresler; No. 2 - B. Bresler, T. Okada and D. Zisling; No. 3 - T. Okada and B. Bresler; No. 4 - V.V. Bertero and B. Bresler - 1977 (PB 267 354)A08

UCB/EERC-77/07 "A Literature Survey - Transverse Strength of Masonry Walls," by Y. Omote, R.L. Mayes, S.W. Chen and R.W. Clough - 1977 (PB 277 933)A07

UCB/EERC-77/08 "DRAIN-TABS: A Computer Program for Inelastic Earthquake Response of Three Dimensional Buildings," by R. Guendelman-Israel and G.H. Powell - 1977 (PB 270 693)A07

UCB/EERC-77/09 "SUBWALL: A Special Purpose Finite Element Computer Program for Practical Elastic Analysis and Design of Structural Walls with Substructure Option," by D.Q. Le, H. Peterson and E.P. Popov - 1977 (PB 270 567)A05

UCB/EERC-77/10 "Experimental Evaluation of Seismic Design Methods for Broad Cylindrical Tanks," by D.P. Clough (PB 272 280)A13

UCB/EERC-77/11 "Earthquake Engineering Research at Berkeley - 1976," - 1977 (PB 273 507)A09

UCB/EERC-77/12 "Automated Design of Earthquake Resistant Multistory Steel Building Frames," by N.D. Walker, Jr. - 1977 (PB 276 526)A09

UCB/EERC-77/13 "Concrete Confined by Rectangular Hoops Subjected to Axial Loads," by J. Vallenas, V.V. Bertero and E.P. Popov - 1977 (PB 275 165)A06

UCB/EERC-77/14 "Seismic Strain Induced in the Ground During Earthquakes," by Y. Sugimura - 1977 (PB 284 201)A04

UCB/EERC-77/15 "Bond Deterioration under Generalized Loading," by V.V. Bertero, E.P. Popov and S. Viwathanatepa - 1977

UCB/EERC-77/16 "Computer Aided Optimum Design of Ductile Reinforced Concrete Moment Resisting Frames," by S.W. Zagajeski and V.V. Bertero - 1977 (PB 280 137)A07

UCB/EERC-77/17 "Earthquake Simulation Testing of a Stepping Frame with Energy-Absorbing Devices," by J.M. Kelly and D.F. Tsztoo - 1977 (PB 273 506)A04

UCB/EERC-77/18 "Inelastic Behavior of Eccentrically Braced Steel Frames under Cyclic Loadings," by C.W. Roeder and E.P. Popov - 1977 (PB 275 526)A15

UCB/EERC-77/19 "A Simplified Procedure for Estimating Earthquake-Induced Deformations in Dams and Embankments," by F.I. Makdisi and H.B. Seed - 1977 (PB 276 820)A04

UCB/EERC-77/20 "The Performance of Earth Dams during Earthquakes," by H.B. Seed, F.I. Makdisi and P. de Alba - 1977 (PB 276 821)A04

UCB/EERC-77/21 "Dynamic Plastic Analysis Using Stress Resultant Finite Element Formulation," by P. Lukkunapvasit and J.M. Kelly - 1977 (PB 275 453)A04

UCB/EERC-77/22 "Preliminary Experimental Study of Seismic Uplift of a Steel Frame," by R.W. Clough and A.A. Huckelbridge 1977 (PB 278 769)A08

UCB/EERC-77/23 "Earthquake Simulator Tests of a Nine-Story Steel Frame with Columns Allowed to Uplift," by A.A. Huckelbridge - 1977 (PB 277 944)A09

UCB/EERC-77/24 "Nonlinear Soil-Structure Interaction of Skew Highway Bridges," by M.-C. Chen and J. Penzien - 1977 (PB 276 176)A07

UCB/EERC-77/25 "Seismic Analysis of an Offshore Structure Supported on Pile Foundations," by D.D.-N. Liou and J. Penzien 1977 (PB 283 180)A06

UCB/EERC-77/26 "Dynamic Stiffness Matrices for Homogeneous Viscoelastic Half-Planes," by G. Dasgupta and A.K. Chopra - 1977 (PB 279 654)A06

UCB/EERC-77/27 "A Practical Soft Story Earthquake Isolation System," by J.M. Kelly, J.M. Eidinger and C.J. Derham - 1977 (PB 276 814)A07

UCB/EERC-77/28 "Seismic Safety of Existing Buildings and Incentives for Hazard Mitigation in San Francisco: An Exploratory Study," by A.J. Meltsner - 1977 (PB 281 970)A05

UCB/EERC-77/29 "Dynamic Analysis of Electrohydraulic Shaking Tables," by D. Rea, S. Abedi-Hayati and Y. Takahashi 1977 (PB 282 569)A04

UCB/EERC-77/30 "An Approach for Improving Seismic - Resistant Behavior of Reinforced Concrete Interior Joints," by B. Galunic, V.V. Bertero and E.P. Popov - 1977 (PB 290 870)A06

UCB/EERC-78/01 "The Development of Energy-Absorbing Devices for Aseismic Base Isolation Systems," by J.M. Kelly and D.F. Tsztoo - 1978 (PB 284 978)A04

UCB/EERC-78/02 "Effect of Tensile Prestrain on the Cyclic Response of Structural Steel Connections, by J.G. Bouwkamp and A. Mukhopadhyay - 1978

UCB/EERC-78/03 "Experimental Results of an Earthquake Isolation System using Natural Rubber Bearings," by J.M. Eidinger and J.M. Kelly - 1978 (PB 281 686)A04

UCB/EERC-78/04 "Seismic Behavior of Tall Liquid Storage Tanks," by A. Niwa - 1978 (PB 284 017)A14

UCB/EERC-78/05 "Hysteretic Behavior of Reinforced Concrete Columns Subjected to High Axial and Cyclic Shear Forces," by S.W. Zagajeski, V.V. Bertero and J.G. Bouwkamp - 1978 (PB 283 858)A13

UCB/EERC-78/06 "Inelastic Beam-Column Elements for the ANSR-I Program," by A. Riahi, D.G. Row and G.H. Powell - 1978

UCB/EERC-78/07 "Studies of Structural Response to Earthquake Ground Motion," by O.A. Lopez and A.K. Chopra - 1978 (PB 282 790)A05

UCB/EERC-78/08 "A Laboratory Study of the Fluid-Structure Interaction of Submerged Tanks and Caissons in Earthquakes," by R.C. Byrd - 1978 (PB 284 957)A08

UCB/EERC-78/09 "Model for Evaluating Damageability of Structures," by I. Sakamoto and B. Bresler - 1978

UCB/EERC-78/10 "Seismic Performance of Nonstructural and Secondary Structural Elements," by I. Sakamoto - 1978

UCB/EERC-78/11 "Mathematical Modelling of Hysteresis Loops for Reinforced Concrete Columns," by S. Nakata, T. Sproul and J. Penzien - 1978

UCB/EERC-78/12 "Damageability in Existing Buildings," by T. Blejwas and B. Bresler - 1978

UCB/EERC-78/13 "Dynamic Behavior of a Pedestal Base Multistory Building," by R.M. Stephen, E.L. Wilson, J.G. Bouwkamp and M. Button - 1978 (PB 286 650)A08

UCB/EERC-78/14 "Seismic Response of Bridges - Case Studies," by R.A. Imbsen, V. Nutt and J. Penzien - 1978 (PB 286 503)A10

UCB/EERC-78/15 "A Substructure Technique for Nonlinear Static and Dynamic Analysis," by D.G. Row and G.H. Powell - 1978 (PB 288 077)A10

UCB/EERC-78/16 "Seismic Risk Studies for San Francisco and for the Greater San Francisco Bay Area," by C.S. Oliveira - 1978

UCB/EERC-78/17 "Strength of Timber Roof Connections Subjected to Cyclic Loads," by P. Gülkan, R.L. Mayes and R.W. Clough - 1978

UCB/EERC-78/18 "Response of K-Braced Steel Frame Models to Lateral Loads," by J.G. Bouwkamp, R.M. Stephen and E.P. Popov - 1978

UCB/EERC-78/19 "Rational Design Methods for Light Equipment in Structures Subjected to Ground Motion," by J.L. Sackman and J.M. Kelly - 1978 (PB 292 357)A04

UCB/EERC-78/20 "Testing of a Wind Restraint for Aseismic Base Isolation," by J.M. Kelly and D.E. Chitty - 1978 (PB 292 833)A03

UCB/EERC-78/21 "APOLLO - A Computer Program for the Analysis of Pore Pressure Generation and Dissipation in Horizontal Sand Layers During Cyclic or Earthquake Loading," by P.P. Martin and H.B. Seed - 1978 (PB 292 835)A04

UCB/EERC-78/22 "Optimal Design of an Earthquake Isolation System," by M.A. Bhatti, K.S. Pister and E. Polak - 1978 (PB 294 735)A06

UCB/EERC-78/23 "MASH - A Computer Program for the Non-Linear Analysis of Vertically Propagating Shear Waves in Horizontally Layered Deposits," by P.P. Martin and H.B. Seed - 1978 (PB 293 101)A05

UCB/EERC-78/24 "Investigation of the Elastic Characteristics of a Three Story Steel Frame Using System Identification," by I. Kaya and H.D. McNiven - 1978

UCB/EERC-78/25 "Investigation of the Nonlinear Characteristics of a Three-Story Steel Frame Using System Identification," by I. Kaya and H.D. McNiven - 1978

UCB/EERC-78/26 "Studies of Strong Ground Motion in Taiwan," by Y.M. Hsiung, B.A. Bolt and J. Penzien - 1978

UCB/EERC-78/27 "Cyclic Loading Tests of Masonry Single Piers: Volume 1 - Height to Width Ratio of 2," by P.A. Hidalgo, R.L. Mayes, H.D. McNiven and R.W. Clough - 1978

UCB/EERC-78/28 "Cyclic Loading Tests of Masonry Single Piers: Volume 2 - Height to Width Ratio of 1," by S.-W.J. Chen, P.A. Hidalgo, R.L. Mayes, R.W. Clough and H.D. McNiven - 1978

UCB/EERC-78/29 "Analytical Procedures in Soil Dynamics," by J. Lysmer - 1978

UCB/EERC-79/01 "Hysteretic Behavior of Lightweight Reinforced Concrete Beam-Column Subassemblages," by B. Forzani, E.P. Popov, and V.V. Bertero - 1979

UCB/EERC-79/02 "The Development of a Mathematical Model to Predict the Flexural Response of Reinforced Concrete Beams to Cyclic Loads, Using System Identification," by J.F. Stanton and H.D. McNiven - 1979

UCB/EERC-79/03 "Linear and Nonlinear Earthquake Response of Simple Torsionally Coupled Systems," by C.L. Kan and A.K. Chopra - 1979

UCB/EERC-79/04 "A Mathematical Model of Masonry for Predicting Its Linear Seismic Response Characteristics," by Y. Mengi and H.D. McNiven - 1979

UCB/EERC-79/05 "Mechanical Behavior of Lightweight Concrete Confined by Different Types of Lateral Reinforcement," by M.A. Manrique, V.V. Bertero and E.P. Popov - 1979

UCB/EERC-79/06 "Static Tilt Tests of a Tall Cylindrical Liquid Storage Tank," by R.W. Clough and A. Niwa - 1979

UCB/EERC-79/07 "The Design of Steel Energy Absorbing Restrainers and Their Incorporation Into Nuclear Power Plants for Enhanced Safety: Volume 1 - Summary Report," by P.N. Spencer, V.F. Zackay, and E.R. Parker - 1979

UCB/EERC-79/08 "The Design of Steel Energy Absorbing Restrainers and Their Incorporation Into Nuclear Power Plants for Enhanced Safety: Volume 2 - The Development of Analyses for Reactor System Piping," "Simple Systems" by M.C. Lee, J. Penzien, A.K. Chopra, and K. Suzuki "Complex Systems" by G.H. Powell, E.L. Wilson, R.W. Clough and D.G. Row - 1979

UCB/EERC-79/09 "The Design of Steel Energy Absorbing Restrainers and Their Incorporation Into Nuclear Power Plants for Enhanced Safety: Volume 3 - Evaluation of Commerical Steels," by W.S. Owen, R.M.N. Pelloux, R.O. Ritchie, M. Faral, T. Ohhashi, J. Toplosky, S.J. Hartman, V.F. Zackay, and E.R. Parker - 1979

UCB/EERC-79/10 "The Design of Steel Energy Absorbing Restrainers and Their Incorporation Into Nuclear Power Plants for Enhanced Safety: Volume 4 - A Review of Energy-Absorbing Devices," by J.M. Kelly and M.S. Skinner - 1979

UCB/EERC-79/11 "Conservatism In Summation Rules for Closely Spaced Modes," by J.M. Kelly and J.L. Sackman - 1979

UCB/EERC-79/12 "Cyclic Loading Tests of Masonry Single Piers Volume 3 - Height to Width Ratio of 0.5," by P.A. Hidalgo, R.L. Mayes, H.D. McNiven and R.W. Clough - 1979

UCB/EERC-79/13 "Cyclic Behavior of Dense Coarse-Grained Materials in Relation to the Seismic Stability of Dams," by N.G. Banerjee, H.B. Seed and C.K. Chan - 1979

UCB/EERC-79/14 "Seismic Behavior of Reinforced Concrete Interior Beam-Column Subassemblages," by S. Viwathanatepa, E.P. Popov and V.V. Bertero - 1979

UCB/EERC-79/15 "Optimal Design of Localized Nonlinear Systems with Dual Performance Criteria Under Earthquake Excitations," by M.A. Bhatti - 1979

UCB/EERC-79/16 "OPTDYN - A General Purpose Optimization Program for Problems with or without Dynamic Constraints," by M.A. Bhatti, E. Polak and K.S. Pister - 1979

UCB/EERC-79/17 "ANSR-II, Analysis of Nonlinear Structural Response, Users Manual," by D.P. Mondkar and G.H. Powell - 1979

UCB/EERC-79/18 "Soil Structure Interaction in Different Seismic Environments," A. Gomez-Masso, J. Lysmer, J.-C. Chen and H.B. Seed - 1979

UCB/EERC-79/19 "ARMA Models for Earthquake Ground Motions," by M.K. Chang, J.W. Kwiatkowski, R.F. Nau, R.M. Oliver and K.S. Pister - 1979

UCB/EERC-79/20 "Hysteretic Behavior of Reinforced Concrete Structural Walls," by J.M. Vallenas, V.V. Bertero and E.P. Popov - 1979

UCB/EERC-79/21 "Studies on High-Frequency Vibrations of Buildings I: The Column Effects," by J. Lubliner - 1979

UCB/EERC-79/22 "Effects of Generalized Loadings on Bond Reinforcing Bars Embedded in Confined Concrete Blocks," by S. Viwathanatepa, E.P. Popov and V.V. Bertero - 1979

UCB/EERC-79/23 "Shaking Table Study of Single-Story Masonry Houses, Volume 1: Test Structures 1 and 2," by P. Gülkan, R.L. Mayes and R.W. Clough - 1979

UCB/EERC-79/24 "Shaking Table Study of Single-Story Masonry Houses, Volume 2: Test Structures 3 and 4," by P. Gülkan, R.L. Mayes and R.W. Clough - 1979

UCB/EERC-79/25 "Shaking Table Study of Single-Story Masonry Houses, Volume 3: Summary, Conclusions and Recommendations," by R.W. Clough, R.L. Mayes and P. Gülkan - 1979

UCB/EERC-79/26 "Recommendations for a U.S.-Japan Cooperative Research Program Utilizing Large-Scale Testing Facilities," by U.S.-Japan Planning Group - 1979

UCB/EERC-79/27 "Earthquake-Induced Liquefaction Near Lake Amatitlan, Guatemala," by H.B. Seed, I. Arango, C.K. Chan, A. Gomez-Masso and R. Grant de Ascoli - 1979

UCB/EERC-79/28 "Infill Panels: Their Influence on Seismic Response of Buildings," by J.W. Axley and V.V. Bertero - 1979

UCB/EERC-79/29 "3D Truss Bar Element (Type 1) for the ANSR-II Program," by D.P. Mondkar and G.H. Powell - 1979

UCB/EERC-79/30 "2D Beam-Column Element (Type 5 - Parallel Element Theory) for the ANSR-II Program," by D.G. Row, G.H. Powell and D.P. Mondkar

UCB/EERC-79/31 "3D Beam-Column Element (Type 2 - Parallel Element Theory) for the ANSR-II Program," by A. Riahi, G.H. Powell and D.P. Mondkar - 1979

UCB/EERC-79/32 "On Response of Structures to Stationary Excitation," by A. Der Kiureghian - 1979

UCB/EERC-79/33 "Undisturbed Sampling and Cyclic Load Testing of Sands," by S. Singh, H.B. Seed and C.K. Chan - 1979

UCB/EERC-79/34 "Interaction Effects of Simultaneous Torsional and Compressional Cyclic Loading of Sand," by P.M. Griffin and W.N. Houston - 1979

UCB/EERC-80/01 "Earthquake Response of Concrete Gravity Dams Including Hydrodynamic and Foundation Interaction Effects," by A.K. Chopra, P. Chakrabarti and S. Gupta - 1980

UCB/EERC-80/02 "Rocking Response of Rigid Blocks to Earthquakes," by C.S. Yim, A.K. Chopra and J. Penzien - 1980

UCB/EERC-80/03 "Optimum Inelastic Design of Seismic-Resistant Reinforced Concrete Frame Structures," by S.W. Zagajeski and V.V. Bertero - 1980

UCB/EERC-80/04 "Effects of Amount and Arrangement of Wall-Panel Reinforcement on Hysteretic Behavior of Reinforced Concrete Walls," by R. Iliya and V.V. Bertero - 1980

UCB/EERC-80/05 "Shaking Table Research on Concrete Dam Models," by R.W. Clough and A. Niwa - 1980

UCB/EERC-80/06 "Piping With Energy Absorbing Restrainers: Parameter Study on Small Systems," by G.H. Powell, C. Oughourlian and J. Simons - 1980

UCB/EERC-80/07 "Inelastic Torsional Response of Structures Subjected to Earthquake Ground Motions," by Y. Yamazaki - 1980

UCB/EERC-80/08 "Study of X-Braced Steel Frame Structures Under Earthquake Simulation," by Y. Ghanaat - 1980

UCB/EERC-80/09 "Hybrid Modelling of Soil-Structure Interaction," by S. Gupta, T.W. Lin, J. Penzien and C.S. Yeh - 1980

UCB/EERC-80/10 "General Applicability of a Nonlinear Model of a One Story Steel Frame," by B.I. Sveinsson and H. McNiven - 1980